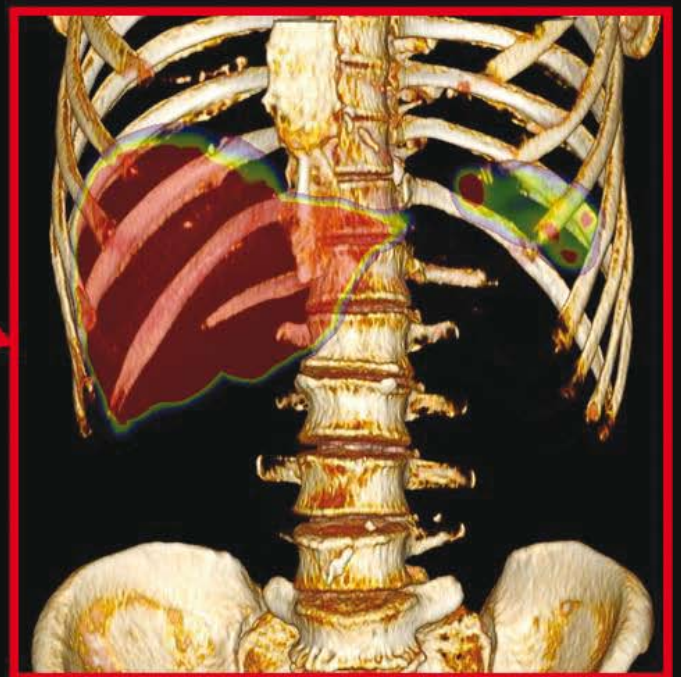
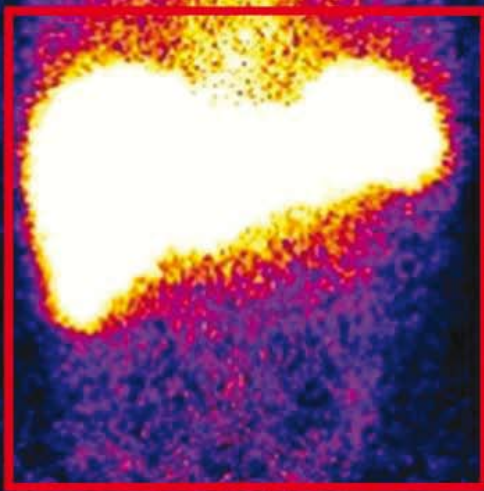
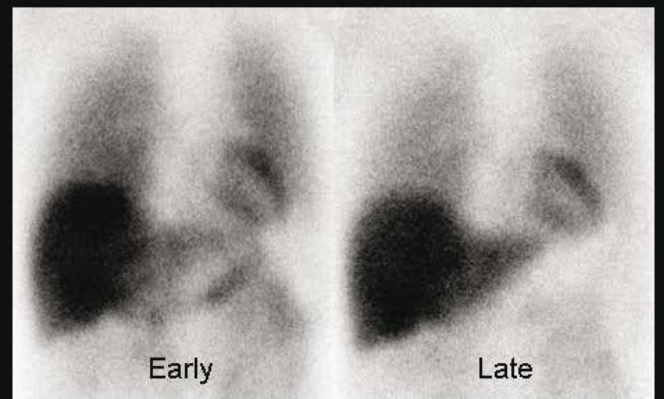


33e jaargang 2011 nummer 4 issn 1381 - 4842

TIJDSCHRIFT VOOR NUCLEAIRE GENEESKUNDE



Special issue on amyloidosis

2010

Maria reactor added to Covidien's supply chain in times of crisis

In February 2010, the **Maria reactor in Poland** was added to Covidien's global supply chain for molybdenum-99 bulk and technetium-99m generators.

In the same month the High Flux Reactor (HFR) in Petten was scheduled to begin a six-month shutdown for repairs. Canada's National Research Universal (NRU) reactor had been shut down since May 2009 and started up in August 2010 after an extensive period of repairs.

When operating, the HFR and NRU reactors have typically provided approximately 65 percent of the world's supply of medical isotopes. The restart of the HFR reactor in September 2010 marked the end of the Mo-99 supply crisis.

Covidien will continue to invest in Mo-99 supply and in the future of nuclear medicine.

We are generators



PAST > PRESENT > FUTURE

Generations of reliable supply.

For nearly fifty years we have been involved with the pioneering, discovery, realisation and development of the worlds market leading technetium generators.

We produced the first generator in 1966 and nearly half a century later are still innovating and investing to ensure a continuous supply for future generations.

Covidien. We are generators.

Visit us at www.covidien.com or call your local Covidien representative for more information.



COVIDIEN

positive results for life™

Clinical approach of patients with systemic amyloidosis	777
<i>B.P.C. Hazenberg, MD, PhD</i>	
Whole body amyloid deposition imaging by ¹²³ I-SAP scintigraphy	785
<i>R.W.J. van Rheenen, MD</i>	
Echocardiography and magnetic resonance imaging for the detection of cardiac amyloidosis	793
<i>M. Groenink, MD, PhD</i>	
Nuclear imaging in cardiac amyloidosis: the role of ¹²³ I-MIBG	799
<i>W. Noordzij, MD</i>	
Development and evaluation of agents for targeting visceral amyloid	807
<i>J.S. Wall, PhD</i>	
Amyloid Imaging in Alzheimer's Disease	816
<i>N. Tolboom, MD, PhD</i>	
Amyloid imaging with PET: what will be next?	822
<i>J. Booij, MD, PhD</i>	
COURSES & CONFERENCES	826

From the editors

Amyloidosis is the name of a group of disorders characterized by deposits of protein fibres (fibrils) in organs and tissues resulting in swelling and dysfunction. If this deposition process is not stopped in the early stages of the disease it can lead to the failure of the affected organ. Because most of the affected organs have a vital function (heart, liver, spleen and kidneys) the failure of these organs can lead to serious complications and even to death. It is therefore of great importance to identify the organs involved at the earliest possible moment. However, amyloidosis is a rare disease (estimated at 8-14 per million per year) and patients with the disease are often treated in specialized institutions (top referral care). This makes that even in a highly trained medical community (i.e. The Netherlands) amyloidosis is a relatively unknown disease.

Until thirty years ago the treatment of amyloidosis had mostly a supportive nature. In recent years however, new systemic therapies were devised and implemented with a relatively high success rate. There are indications that the response to these therapies depends on the number of organs involved. It is therefore eminent to assess which organs and to what extent these organs are involved in the disease. Non-invasive imaging techniques in general and nuclear medicine techniques in particular play a pivotal role in determining the disease and in identifying the extent of the disease. In addition, however to a lesser extent, these imaging techniques play a role in assessing the effectiveness of therapy.

In light of all these exciting developments and innovations, we felt that there was an unmet need to bring you up to date on amyloidosis and what better medium to choose than our own Journal.

To give you a better understanding of amyloidosis we have asked several national and international specialists in the field of amyloidosis to bring you up to date and to give you an idea of the future perspectives. There are contributions by clinicians, researchers and imagers. First, Dr. Hazenberg, rheumatologist and clinical immunologist at the University Medical Center Groningen (UMCG), discusses the diagnostic and therapeutic options in these patients from a clinical perspective. This is followed by a contribution from the UMCG (Drs. van Rheenen and Drs. Glaudemans) focussing on ¹²³I-serum amyloid P (SAP) scintigraphy to assess organ involvement. In a mutual effort from the nuclear medicine departments of the UMCG and the Academic Medical Center (AMC) in Amsterdam (Drs. Noordzij, Dr. Verberne and Dr. Slart), these authors highlight the possibilities of nuclear medicine techniques to assess amyloidosis in a sole organ: the heart. In addition Dr. Groenink (cardiologist) and Dr. Verberne, both from the AMC in Amsterdam, present an overview of non-nuclear medicine techniques to either demonstrate or exclude cardiac amyloidosis.

In contrast to all this amyloidosis deposition, Dr. Tolboom (nuclear medicine physician in training at the VUMC in Amsterdam) discusses the imaging possibilities of another protein deposition disorder, with a specific preference for the brains: Alzheimer's disease. Despite the promising results with PET tracers to image amyloidosis in the brain Prof. Booij (AMC, Amsterdam) emphasizes on the efforts to image amyloid in the brain with imaging techniques other than PET and to image other protein aggregates than β -amyloid which may be relevant for the neurodegenerative disorders. Last but not least there is a valuable contribution from Knoxville, USA. In this article

Prof. Wall discusses various preclinical research lines. To make full circle Prof. Wall shares the opinion of Prof. Booij that there is a need to focus on the development of new tracers for imaging of amyloidosis.

In case you have been triggered by all this exciting information and you would like to learn more on the latest developments in the field of amyloidosis, there is the opportunity to do so. In the spring of 2012 the "XIIIth International Symposium on Amyloidosis" will be held in Groningen from 6 to 10 May 2012. This Symposium with the sub-title "From misfolded proteins to well-designed treatment" is organized by GUARD (Groningen Unit for Amyloidosis Research & Development). More information and the possibility to register to attend this symposium can be found at: www.amyloidosis2012.com.

We hope this special issue of the Journal will give you a better understanding of the disease amyloidosis, the current clinical issues and the (essential) role that nuclear medicine can play in assessing disease severity and therapeutic efficacy.

As guest-editors of this special issue we hope you will enjoy reading and hopefully afterwards will share our enthusiasm on the (future) possibilities for nuclear medicine in amyloidosis.



Andor Glaudemans
Nuclear Medicine
UMC Groningen



Hein Verberne
Nuclear Medicine
AMC Amsterdam

Front page

Examples of nuclear imaging techniques in patients with amyloidosis (provided by Ronald van Rheenen, University Medical Center Groningen): whole body ^{123}I -SAP scintigraphy (left), SPECT/CT of the abdominal region of the same patient (right lower image) and ^{123}I -MIBG scintigraphy of the heart, early and late image (right upper image).

Clinical approach of patients with systemic amyloidosis

B.P.C. Hazenberg, MD, PhD

Department of Rheumatology & Clinical Immunology, University Medical Center Groningen, University of Groningen, Groningen, the Netherlands

Abstract

Hazenberg BPC. Clinical approach of patients with systemic amyloidosis

Amyloidosis is the name of diseases characterised by deposition of protein fibrils with a beta-sheet structure. This beta-sheet structure generates affinity of amyloid for Congo red dye and is resistant to proteolysis. The main three types of systemic amyloidosis are AA (related to underlying chronic inflammation), AL (related to underlying monoclonal light chain production), and ATTR amyloidosis (related to old age or underlying hereditary mutations of transthyretin). Signs and symptoms vary among the three types and the treatment is different for each type. If a patient is suspected to have systemic amyloidosis, proof of the presence of amyloid in tissue must be obtained first and systemic involvement should be unequivocal. Determination of the precise type of amyloid is extremely important and one should start to detect the particular amyloid precursor. Assessment of size and function of vital organs and tissues is essential in the clinical work-up of a patient with systemic amyloidosis. A fast and thorough clinical evaluation is necessary to obtain all relevant information for prognosis and choice of treatment. The treatment is based on the "precursor-product" concept, in which the supply of amyloid precursor is the rate limiting step for further accumulation of amyloid. Effective therapy quickly and completely stops ongoing supply of precursor. In this respect, investigations such as serum amyloid P component (SAP) scintigraphy may help not only to investigate organ involvement but also response to treatment. The effects of therapy on both underlying disease and amyloidosis should be monitored frequently during follow-up.

Tijdschr Nucl Geneesk 2011; 33(4):777-783

Introduction

Amyloidosis is the name of a group of diseases characterised by deposition of proteinaceous fibrils with a molecular β -sheet structure (1). This structure of the fibrils is responsible for its insolubility, resistance to proteolysis, and binding affinity for Congo red dye and the consequent green birefringence with polarised light. Amyloid fibrils are derived from a variety of protein precursors. The extracellular deposition of amyloid

fibrils in organs and tissues results in loss of function and often causes prominent swelling of the affected organ or tissue. Deposition of amyloid can be localised (produced in and limited to one organ or site of the body) or systemic (deposition in various organs and tissues throughout the body). The precursor protein is used for typing amyloid in the current classification of amyloidosis (2). Signs and symptoms of systemic amyloidosis differ among the various types of amyloidosis (1-3). The aim of this article is to provide a clinical overview of systemic amyloidosis: an approach to diagnosis, clinical evaluation, and background of therapy.

Systemic amyloidosis

Localised deposition of amyloid plays a still unresolved role in widespread diseases such as Alzheimer's disease (β -protein in the plaques) and diabetes mellitus type II (amylin in the islands of Langerhans). Systemic deposition of amyloid, however, is directly related to the grim prospects of systemic amyloidosis. Three major types can be distinguished (1-3). AA amyloidosis is caused by longstanding inflammation. Serum amyloid A protein (SAA), an acute phase reactant, is the precursor. Signs of kidney disease, such as proteinuria (progressing to nephrotic syndrome) and loss of renal function (progressing to renal failure), are observed most frequently (in about 90% of cases). Less frequent manifestations are autonomic neuropathy, splenomegaly, hepatomegaly, goiter, and cardiomyopathy.

AL amyloidosis is caused by a, often low-grade, plasma cell dyscrasia. Lambda or kappa immunoglobulin light chain is the precursor of this type of amyloid. Clinical manifestations are diverse, such as cardiomyopathy, hepatomegaly, splenomegaly, nephrotic syndrome, renal failure, orthostatic hypotension, diarrhea, peripheral and autonomic neuropathy, arthropathy, carpal tunnel syndrome (CTS), and glossomegaly. The diversity of disease manifestations is related to severity of deposition in the various organs and tissues.

ATTR amyloidosis is caused by many autosomal dominantly inherited point mutations of the precursor protein transthyretin (TTR). Transthyretin is the acronym of transport protein of thyroid hormone and retinol binding protein. About 100 of these TTR mutations have been described, but the so-called TTR-Met30 mutation is seen most frequently. Prominent clinical manifestations are familial peripheral and autonomic neuropathy, but cardiomyopathy, renal failure, and eye involvement (vitreous opacities) are also often observed in the course of the disease. Severe cardiomyopathy is the

presenting manifestation in some TTR mutations. In very old age, non-mutated ("wild-type") TTR can also act as amyloid precursor by a still unknown mechanism. This "wild-type" ATTR amyloidosis (formerly called senile systemic amyloidosis) is characterised by a slowly progressive cardiomyopathy. A fourth type is $A\beta_2M$ amyloidosis that is associated with renal failure and longstanding (i.e. at least 5-10 years) dialysis with decreased clearance and elevated serum levels of beta-2-microglobulin (β_2M). β_2M is the precursor of this type of amyloid. Clinical manifestations are predominantly arthropathic, such as tenosynovitis, shoulder pain, CTS, periarticular cysts, pathological fractures, and destructive spondyloarthropathy. Synovial tissue biopsy is the method to detect this type of amyloid. Kidney transplantation stops the disease (4, 5). $A\beta_2M$ amyloidosis is a disabling disease that should be recognised and treated, but can easily be distinguished from the main three types (AA, AL, and ATTR) of systemic amyloidosis because of the association with dialysis. The other three types are often difficult to diagnose, show variable involvement of many organs and tissues, and are challenging in finding the most appropriate treatment.

Histology is essential for diagnosis

The diagnosis of amyloid is based on showing its presence in tissue. Method of choice is a positive Congo red-stained tissue specimen showing the characteristic apple-green birefringence in polarised light (figure 1). Aspiration of a subcutaneous fat sample of the abdominal wall is the most elegant and least inconvenient method for this purpose, with a sensitivity ranging between 54% (6) and - in experienced

hands - 93% (7) with a corresponding specificity of 100% (7). These figures are comparable with those of the well-known rectum biopsy (7, 8). In case one of the primary biopsy sites (fat or rectum) is negative for amyloid and suspicion of amyloidosis remains strong, a biopsy of the alternate site is useful to increase the chance of detecting amyloid. A bone marrow biopsy can also be used, but has a rather low sensitivity of 50-60% (7, 8). If all screening biopsies are negative but suspicion of amyloidosis remains strong, a biopsy of the affected organ or tissue is indicated (1, 7, 9).

Localised or systemic deposition of amyloid

It is important to establish whether deposition of amyloid is localised or systemic. Some sites of the body are almost exclusively involved in systemic amyloidosis, such as kidneys, liver, nerves, abdominal fat, and spleen. If such a site is positive for amyloid, one may conclude to systemic amyloidosis. Localised amyloid can often be found in some other specific sites of the body (such as eyelid, cardiac atria, larynx, ureter, skin, etc.). If in these cases amyloid is not detected elsewhere in the body one may conclude to localised amyloidosis. Most other sites (bone marrow, heart, bowel, lung, joint, etc.) are nearly always involved in systemic amyloidosis, but can be localised occasionally. In this situation it is necessary to demonstrate histological and/or clinical presence of amyloid in two different organs or tissues. For this demonstration, however, it is sufficient to have histological proof at one site (such as bone marrow, skin, or rectum) and typical clinical involvement (such as nephrotic syndrome, hepatomegaly, macroglossia, or cardiomyopathy) at the other site (10).

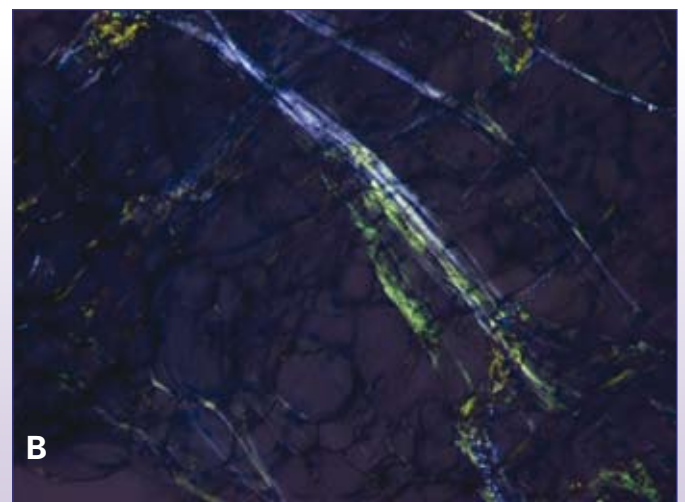
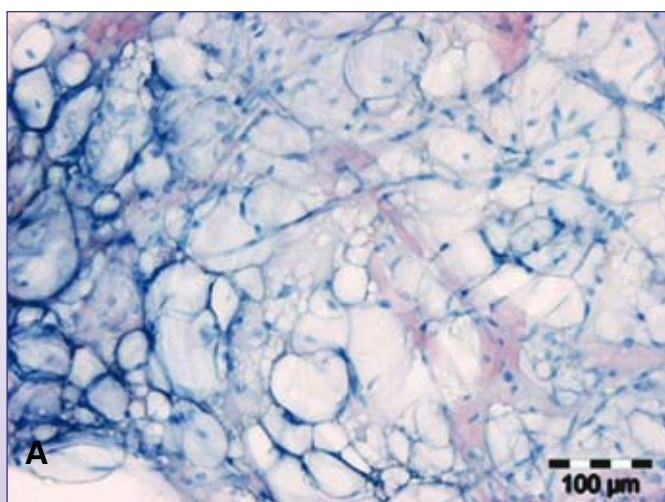


Figure 1. Example of an abdominal subcutaneous fat aspirate, stained with Congo red.

A. Viewed in normal light: amyloid is stained red. Bar length is 100 μ m.

B. The same specimen viewed in polarised light: amyloid shows apple-green birefringence (collagen is bluish-white).

Typing amyloid with confidence

Determination of the type of amyloid is very important. In the majority of cases the type of amyloid can be suspected from medical history and clinical picture. Amyloidosis in a patient with longstanding rheumatoid arthritis and nephrotic syndrome points to AA type. A patient with polyneuropathy who is member of a family with hereditary ATTR amyloidosis most probably also suffers from this disease. And for a patient with characteristic shoulder pads and glossomegaly it is hard to believe in a type different from AL amyloidosis. Nevertheless, even in patients with strong clinical evidence for a particular type of amyloid it is a good habit to search for solid confirmation of the specific type of amyloid involved. The clinical consequences of incorrect typing of amyloid can be huge, because prognosis and therapy of the three major types of systemic amyloidosis differ so much.

Immunohistochemistry of a biopsy is common practice by typing amyloid using specific antibodies. In AA amyloidosis this technique is sufficient, provided that sensitive and specific monoclonal antibodies are used, such as mc1 (10) or Reu.86.2 (11, 12). But in ATTR amyloidosis and especially in AL amyloidosis immunohistochemistry is less reliable than in AA amyloidosis (13). The false positive and false negative results may be due to heterogeneity of amyloid deposits, loss of epitopes in the fibril structure, lower sensitivity and specificity of (polyclonal) antibodies, and non-specific adherence of immunoglobulins to amyloid deposits or the background (10). One should realise that lack of a positive family history does not exclude ATTR amyloidosis as shown by a considerable number of "sporadic" cases that have been described (14). Therefore the presence of a TTR mutation must be confirmed by DNA analysis in all cases of ATTR amyloidosis. The only exclusion of this requirement is a slowly progressive amyloid cardiomyopathy at old age that is typical of "wild-type" ATTR amyloidosis.

In patients with AL amyloidosis a monoclonal plasma cell dyscrasia with overproduction of lambda or kappa light chain will be present. It can be detected in bone marrow (clonal dominance by immunophenotyping of plasma cells), urine (Bence Jones proteins, immunofixation of concentrated urine), and blood (M-protein, immunofixation, and – most important of all – by the free light chain assay). However, a monoclonal gammopathy of undetermined significance (MGUS) is frequently present in healthy older persons, about 2-4% in persons over 50 years old and even higher with advancing age (15). One should therefore realise that detection of an MGUS does not exclude other types than AL amyloidosis. It is important to notice that the clinical picture of ATTR amyloidosis and AL amyloidosis may be similar, such as in cases with polyneuropathy, autonomic neuropathy, cardiomyopathy, and carpal tunnel syndrome. In a patient with such a clinical picture it is therefore not sufficient to show the presence of a plasma cell dyscrasia but also necessary to exclude a TTR mutation before one can diagnose AL amyloidosis (14).

Immuno-electron microscopy seems to be more specific for typing all types of amyloid (16). A promising development for typing amyloid with confidence is proteomics (17). This development is especially useful to distinguish between AL and ATTR amyloid. Techniques such as two-dimensional (2D) polyacrylamide gel electrophoresis followed by matrix-assisted laser desorption/ionization mass spectrometry and peptide mass fingerprinting (18) and laser microdissection and mass spectrometry (19) have high sensitivity with corresponding high specificity. Currently these sophisticated, expensive, and time-consuming techniques are only available in highly specialised centres, so immunohistochemistry remains standard for typing amyloid in daily practice.

Amyloid precursor

After typing amyloid one should look for an amyloid precursor in the blood. Detection of such a precursor and measuring its serum concentration is important for the choice of treatment. In AA amyloidosis the precursor is SAA, an acute phase protein (20). The behaviour of SAA during inflammation is similar to C-reactive protein (CRP), a protein that is used in daily practice. In ATTR amyloidosis the precursor is mutated TTR, which protein can be detected by isoelectric focusing (21). In AL amyloidosis the free light chain assay is used to quantify serum levels of free lambda and kappa precursor proteins using specific antibodies raised against epitopes that are hidden in the complete immunoglobulin (22).

Clinical evaluation

It is useful to obtain a clinical overview of the "amyloid load", i.e. affected organs and tissues and severity of amyloid deposition in vital organs (such as heart, liver, and kidneys). One should not forget to ask for family history, impotence, orthostatic complaints, loss of sensibility, fatigue, weight loss, and bowel problems. Physical examination should also focus on signs such as orthostatic blood pressure, friability of skin, glossomegaly, arthropathy, hepatomegaly, splenomegaly, oedema, cardiac failure, and loss of sensibility and muscle strength of extremities.

A thoughtful systematic clinical approach is indicated. The heart can be examined with electrocardiography (signs of low voltage and pseudo-anteroseptal infarction), chest X-ray (normally sized heart despite signs of cardiac failure), echocardiography (thickness of septum and ventricular walls), MRI (wall thickness, delayed contrast-enhanced imaging), 24 hour Holter registration (conduction, rhythm, and heart rate variability) and a MUGA scan (left ventricle ejection fraction). NT-proBNP and troponin levels in blood are extremely useful for assessing cardiac involvement and for risk evaluation (23-25). The kidneys can be examined with serum albumin, creatinine clearance, urine sediment and proteinuria. The liver can be examined with serum albumin, liver enzymes such as alkaline phosphatase, bilirubin, coagulation tests, and cholinesterase. Thyroid stimulating hormone can be used for the thyroid and fasting cortisol for the adrenal glands.

Autonomic function tests ("Ewing battery") and heart rate variability can be used for evaluation of autonomic neuropathy (26, 27). Electromyography can be used to assess peripheral neuropathy. Abdominal ultrasound is useful to evaluate size and echogenicity of liver, spleen and kidneys. Not all of the examinations mentioned above need to be used, because often it is obvious that clinical organ involvement is not present at all. However, echocardiography should be considered in all patients, even in those without cardiac symptoms. The role of nuclear medicine techniques in diagnosis and clinical evaluation, such as serum amyloid P component (SAP) scintigraphy (28-31), will be discussed in other articles of this issue.

In 2004 at a consensus meeting in Tours, the amyloid community agreed upon guidelines for organ involvement, haematological response criteria, and organ response criteria that are currently used in AL amyloidosis (32). Table 1 shows the consensus criteria for organ involvement.

Prognosis

Prognosis is poor if the underlying precursor production remains untreated. The prognosis depends upon the type of amyloid, the severity of amyloid deposition, the number of vital organs affected, the presence of symptomatic

cardiomyopathy, the severity of the associated disease, and the response to therapy of the underlying precursor-producing process. Patients with untreated AL amyloidosis have the worst prognosis, with a median survival of less than one year (1, 9). Median survival in untreated AL amyloidosis in case of symptomatic cardiomyopathy is 4-6 months, in case of kidney involvement about 2 years, and in case of CTS more than 3-4 years. Untreated patients with AA amyloidosis have a median survival of 2-4 years (1, 9). Survival in AA strongly depends upon the activity of the underlying inflammation (33). Patients with untreated ATTR amyloidosis may survive up to 10-15 years, but median survival is between 5 and 10 years (1).

Treatment

The foundation of treatment is the so-called "precursor-product" concept (34). Central idea of this concept is that further growth of amyloid deposits will stop when the supply of necessary precursors is put to a stop. In AA amyloidosis treatment is aimed at decreasing SAA serum levels to normal basal values (below 3 mg/l). This aim can only be achieved by a complete suppression or eradication of the underlying chronic inflammation. Examples are surgical treatment of chronic osteomyelitis and antibiotic treatment of infectious diseases such as tuberculosis and leprosy. In

Organ	Criterion
Kidney	24-hr urine protein >0.5 g/day, predominantly albumin
Heart	Echo: mean wall thickness >12 mm, no other cardiac cause
Liver	Total liver span >15 cm in the absence of heart failure or alkaline phosphatase >1.5 times institutional upper limit of normal
Nerve	Peripheral: clinical; symmetric lower extremity sensorimotor peripheral neuropathy Autonomic: gastric-emptying disorder, pseudo-obstruction, voiding dysfunction not related to direct organ infiltration
Gastrointestinal tract	Direct biopsy verification with symptoms
Lung	Direct biopsy verification with symptoms Interstitial radiographic pattern
Soft tissue	Tongue enlargement, clinical Arthropathy Claudication, presumed vascular amyloid Skin Myopathy by biopsy or pseudohypertrophy Lymph node (may be localized) Carpal tunnel syndrome

Table 1. Organ involvement: biopsy of affected organ or biopsy at an alternate site*

*Alternate sites available to confirm the histologic diagnosis of amyloidosis: fine-needle abdominal fat aspirate and/or biopsy of the minor salivary glands, rectum, or gingiva. Derived from Gertz et al (32).

chronic inflammatory diseases such as rheumatoid arthritis and Crohn's disease effective suppression of inflammation (resulting in a substantial decrease of serum SAA levels below 3 mg/l) is often difficult, but should be attempted (33). To achieve this goal, cytostatic drugs can be used (such as methotrexate and azathioprine), but also biologicals such as anti-TNF (tumour necrosis factor) drugs (such as infliximab, adalimumab and etanercept). In patients with TRAPS (TNF-Receptor-Associated Periodic Syndrome), etanercept (acting as soluble TNF receptor) seems to be a rational treatment because of the abnormal function of the mutated TNF receptor. The interleukin-1-receptor antagonist anakinra is often highly effective in cryopyrin-related diseases such as familial cold urticaria and Muckle-Wells syndrome (35). Colchicine has a central place in the treatment of Familial Mediterranean Fever (FMF), not only by reducing the frequency and severity of attacks, but also by preventing the development of AA amyloidosis (36).

In AL amyloidosis the aim of treatment is to eradicate the underlying plasma cell dyscrasia by chemotherapy. High dose melphalan with autologous stem cell transplantation is favourable in a group of well-selected patients (37), but currently less toxic and less intensive regimens are studied using novel drugs such as thalidomide, lenalidomide and bortezomib, all combined with dexamethasone (38). In patients with hereditary ATTR amyloidosis liver transplantation is the only possibility to remove the source of 99% of the mutated TTR in the circulation (39). However, this approach is not always successful, because amyloid sometimes still progresses in the heart after transplantation (40, 41). Beside treatment aimed at the underlying disease, it is necessary to give supportive treatment for loss of organ function that is caused by amyloid deposition. Multisystem involvement often results in a mixture of serious problems and in such a situation it is almost impossible to realise an appropriate treatment for all symptoms (1).

Monitoring the effect of treatment

Measuring the effect of treatment is important for such an intangible disease as systemic amyloidosis. The expectation is that no further accumulation of amyloid deposits will occur after successful elimination of the precursor supply. Besides, the body itself will possibly try to remove amyloid. Repeated measurements will help to get an impression of the treatment effect. Two different processes should be monitored in this way. Firstly, the underlying precursor-producing process with the respective precursors: serum SAA, free kappa or lambda light chain, and mutated ATTR in AA, AL, and ATTR amyloidosis respectively. If treatment is successful SAA levels should fall below 3 mg/l, free kappa and lambda levels and the kappa/lambda ratio should return to the reference ranges, and mutant TTR should not be detectable in the blood anymore. Secondly, there is the process of amyloid accumulation, measuring the clinical "amyloid load". For this measurement

quantitative abnormal clinical signs should be monitored, such as serum albumin, alkaline phosphatase, bilirubin, NT-proBNP, troponin, creatinine clearance, proteinuria, ventricular wall thickness, left ventricle ejection fraction, conduction and rhythm, heart rate variability, Ewing battery results, and the sizes of enlarged organs, such as liver, spleen, and kidneys. The abdominal subcutaneous fat aspiration can be repeated at each time point to get an idea of the severity of the presence of amyloid or its disappearance from tissue (41-43). SAP scintigraphy, if abnormal at presentation, can also be used to monitor amyloid regression in the individual patient (44, 45). At the consensus meeting in Tours in 2004 also a set of response criteria in systemic AL amyloidosis has been accepted (32).

Treatment perspectives

The "precursor-product" concept focuses on stopping ongoing deposition of amyloid. Clinical research is focused on developing new drugs that interfere with amyloid deposition or stimulate removal of amyloid deposits. Currently new drugs are investigated that stabilise TTR in the circulation and hamper deposition of amyloid, such as diflunisal and tafamidis. Both drugs stabilise *in vitro* the TTR tetramer in blood and prohibit its degradation into amyloidogenic dimers and monomers (46). However, results of clinical trials have not been published yet. Doxycyclin stimulates removal of ATTR amyloid deposits in mice (47). A promising drug for patients with AA amyloidosis is eprodisate (48). This drug prohibits binding of SAA to glycosaminoglycans in tissue (49). CPHPC is a drug that leads to depletion of SAP from the circulation (50). This mechanism possibly stops accumulation of amyloid and may be useful for all types of systemic amyloidosis (51). A completely different approach is vaccination. Early research was focused on conformational epitopes present in all types of amyloid that might be used for vaccination (52). The London group recently demonstrated in mice that CPHPC followed by anti-SAP antibodies resulted in a quick removal of almost all AA amyloid from the tissues (53). If this huge effect on amyloid turns out to be valid in human beings, it might dramatically change the prospects of patients with all types of systemic amyloidosis.

Conclusion

A systematic evaluation of patients with systemic amyloidosis helps to get a grip on this intangible disease. Histological proof of amyloid, verification of systemic involvement, determination of the particular type of amyloid and its precursor form the background of a thoughtful clinical evaluation. New techniques such as ¹²³I-SAP scintigraphy may have a place in this evaluation. The "precursor-product" concept is still the current basis of treatment, but research is aimed at finding new ways to attack amyloid.

List of references

- Falk RH, Comenzo RL, Skinner M. The systemic amyloidoses. *N Engl J Med*. 1997;337: 898-909
- Sipe JD, Benson MD, Buxbaum JN et al. Amyloid fibril protein nomenclature: 2010 recommendations from the nomenclature committee of the International Society of Amyloidosis. *Amyloid*. 2010;17:101-104
- Merlini G, Bellotti V. Molecular mechanisms of amyloidosis. *N Engl J Med*. 2003;349:583-96
- Kay J. β_2 -microglobulin amyloidosis. *Amyloid*. 1997;4:187-211
- Kamphuis AG, Geerlings W, Hazenberg BP, Thijn CJ. Annual evaluation of hip joints and hands for radiographic signs of $A\beta_2M$ -amyloidosis in long-term hemodialysis patients. *Skeletal Radiol*. 1994;23:421-7
- Breedveld FC, Markusse HM, MacFarlane JD. Subcutaneous fat biopsy in the diagnosis of amyloidosis secondary to chronic arthritis. *Clin Exp Rheumatol*. 1989;7:407-10
- van Gameren II, Hazenberg BP, Bijzet J, van Rijswijk MH. Diagnostic accuracy of subcutaneous abdominal fat tissue aspiration for detecting systemic amyloidosis and its utility in clinical practice. *Arthritis Rheum*. 2006;54:2015-21
- Kyle RA, Gertz MA. Primary systemic amyloidosis: Clinical and laboratory features in 474 Cases. *Semin Hematol*. 1995;32:45-59
- Janssen S, van Rijswijk MH, Meijer S, Ruinen L, van der Hem GK. Systemic amyloidosis: a clinical survey of 144 cases. *Neth J Med*. 1986;29:376-85
- Röcken C, Sletten K. Amyloid in surgical pathology. *Virchows Arch*. 2003;443:3-16
- Hazenberg BP, Grond J, van de Top D et al. Detection of amyloid AA in rectal biopsies with a new monoclonal anti-human SAA antibody (Reu.86.2). *Kidney Int*. 1991;40:976-7
- Hazenberg BP, Limburg PC, Bijzet J, van Rijswijk MH. A quantitative method for detecting deposits of amyloid A protein in aspirated fat tissue of patients with arthritis. *Ann Rheum Dis*. 1999;58:96-102
- Kebbel A, Rocken C. Immunohistochemical classification of amyloid in surgical pathology revisited. *Am J Surg Pathol*. 2006;30:673-683
- Lachmann HJ, Booth DR, Booth SE et al. Misdiagnosis of hereditary amyloidosis as AL (primary) amyloidosis. *N Engl J Med*. 2002;346:1786-91
- Kyle RA, Therneau TM, Rajkumar SV et al. A long-term study of prognosis in monoclonal gammopathy of undetermined significance. *N Engl J Med*. 2002;346:564-9
- Arbustini E, Verga L, Concardi M et al. Electron and immunoelectron microscopy of abdominal fat identifies and characterizes amyloid fibrils in suspected cardiac amyloidosis. *Amyloid*. 2002;9:108-14
- Murphy CL, Wang S, Williams T, Weiss DT, Solomon A. Characterization of systemic amyloid deposits by mass spectrometry. *Methods Enzymol*. 2006;412:48-62
- Lavattelli F, Perlman DH, Spencer B et al. Amyloidogenic and associated proteins in systemic amyloidosis proteome of adipose tissue. *Mol Cell Proteomics*. 2008;7:1570-83
- Vrana JA, Gamez JD, Madden BJ et al. Classification of amyloidosis by laser microdissection and mass spectrometry-based proteomic analysis in clinical biopsy specimens. *Blood*. 2009;114:4957-9
- Hazenberg BP, Limburg PC, Bijzet J, van Rijswijk MH. A quantitative method for detecting deposits of amyloid A protein in aspirated fat tissue of patients with arthritis. *Ann Rheum Dis*. 1999;58:96-102
- Altland K, Benson MD, Costello CE et al. Genetic microheterogeneity of human transthyretin detected by IEF. *Electrophoresis*. 2007;28:2053-64
- Lachmann HJ, Gallimore R, Gillmore J et al. Outcome in systemic AL amyloidosis in relation to changes in concentration of circulating free immunoglobulin light chains following chemotherapy. *Br J Haematol*. 2003;122:78-84
- Palladini G, Campana C, Klersy C et al. Serum N-terminal pro-brain natriuretic peptide is a sensitive marker of myocardial dysfunction in AL amyloidosis. *Circulation*. 2003;107:2440-5
- Dispenzieri A, Gertz MA, Kyle RA et al. Prognostification of survival using cardiac troponins and N-terminal pro-brain natriuretic peptide in patients with primary systemic amyloidosis undergoing peripheral stem cell transplantation. *Blood*. 2004;104:1881-7
- Dispenzieri A, Gertz MA, Kyle RA et al. Serum cardiac troponins and N-terminal pro-brain natriuretic peptide: a staging system for primary systemic amyloidosis. *J. Clin. Oncol*. 2004;22:3751-7
- Reyners AK, Hazenberg BP, Haagsma EB et al. The assessment of autonomic function in patients with systemic amyloidosis: methodological considerations. *Amyloid Int J Exp Clin Invest*. 1998;5:193-9
- Reyners AK, Hazenberg BP, Reitsma WD, Smit AJ. Heart rate variability as a predictor of mortality in patients with AA and AL amyloidosis. *Eur Heart J*. 2002;23:157-61
- Hawkins PN, Lavender JP, Pepys MB. Evaluation of systemic amyloidosis by scintigraphy with ^{123}I -labeled serum amyloid P component. *N Engl J Med*. 1990;323:508-13
- Jager PL, Hazenberg BP, Franssen EJ et al. Kinetic studies with iodine-123-labeled serum amyloid P component in patients with systemic AA and AL amyloidosis and assessment of clinical value. *J Nucl Med*. 1998;39:699-706
- Hazenberg BP, van Rijswijk MH, Piers DA et al. Diagnostic performance of ^{123}I -labeled serum amyloid P component scintigraphy in patients with amyloidosis. *Am J Med*. 2006; 119:355.e15-24
- Hazenberg BP, van Rijswijk MH, Lub-de Hooge MN et al. Diagnostic performance and prognostic value of extravascular retention of ^{123}I -labeled serum amyloid P component in systemic amyloidosis. *J Nucl Med*. 2007;48:865-72
- Gertz MA, Comenzo R, Falk RH et al. Definition of organ involvement and treatment response in immunoglobulin light chain amyloidosis (AL): a consensus opinion from the 10th International Symposium on Amyloid and Amyloidosis, Tours, France, 18-22 April 2004. *Am J Med*. 2005;79:319-28
- Lachmann HJ, Goodman HJ, Gilbertson JA, et al. Natural history and outcome in systemic AA amyloidosis. *N Engl J Med*. 2007;356:2361-71

34. van Rijswijk MH. Amyloidosis [dissertation]. Groningen: University of Groningen, 1981
35. Hawkins PN, Lachmann HJ, McDermott MF. Interleukin-1-receptor antagonist in the Muckle-Wells syndrome. *N Engl J Med.* 2003;348:2583-4
36. Zemer D, Pras M, Sohar E et al. Colchicine in the prevention and treatment of the amyloidosis of familial Mediterranean fever. *N Engl J Med.* 1986;314:1001-5
37. Skinner M, Sanchorawala V, Seldin DC et al. High-dose melphalan and autologous stem-cell transplantation in patients with AL amyloidosis: an 8-year study. *Ann Intern Med.* 2004;140:85-93
38. van Gameren II, Vellenga E, Hazenberg BP. Novel treatments for systemic amyloidosis. *Int J Clin Rheum.* 2009;4:171-88
39. Wilczek HE, Larsson M, Ericzon BG. FAPWTR. Long-term data from the Familial Amyloidotic Polyneuropathy World Transplant Registry (FAPWTR). *Amyloid.* 2011;18 Suppl 1:193-5
40. Olofsson BO, Backman C, Karp K, Suhr OB. Progression of cardiomyopathy after liver transplantation in patients with familial amyloidotic polyneuropathy, Portugese type. *Transplantation* 2002;73:745-51
41. Haagsma EB, van Gameren II, Bijzet J, Posthumus MD, Hazenberg BP. Familial amyloidotic polyneuropathy: long-term follow-up of abdominal fat tissue aspirate in patients with and without liver transplantation. *Amyloid.* 2007;14:221-6
42. van Gameren II, van Rijswijk MH, Bijzet J, Vellenga E, Hazenberg BP. Histological regression of amyloid in AL amyloidosis is exclusively seen in patients with a complete response of serum free light chain. *Haematologica.* 2009;94:1094-100
43. van Gameren II, Hazenberg BP, Bijzet J et al. Amyloid load in fat tissue in patients with amyloidosis reflects disease severity and predicts survival. *Arthritis Care Res (Hoboken)* 2010;62:296-301
44. van Gameren II, Hazenberg BP, Jager PL, Smit JW, Vellenga E. AL amyloidosis treated with induction chemotherapy with VAD followed by high dose melphalan and autologous stem cell transplantation. *Amyloid.* 2002;9:165-74
45. Hawkins PN, Richardson S, MacSweeney JE et al. Scintigraphic quantification and serial monitoring of human visceral amyloid deposits provide evidence for turnover and regression. *Q J Med.* 1993;86:365-74
46. Hammarstrom P, Wiseman RL, Powers ET, Kelly JW. Prevention of transthyretin amyloid disease by changing protein misfolding energetics. *Science.* 2003;299:713-7
47. Cardoso I, Martins D, Ribeiro T, Merlini G, Saraiva MJ. Synergy of combined doxycycline/TUDCA treatment in lowering Transthyretin deposition and associated biomarkers: studies in FAP mouse models. *J Transl Med.* 2010;8:74
48. Dember LM, Hawkins PN, Hazenberg BP et al. Eprodisate for the treatment of AA amyloidosis. *N Engl J Med.* 2007;356:2349-60
49. Inoue S, Hultin PG, Szarek WA, Kisilevsky R. Effect of poly(vinylsulfonate) on murine AA amyloid: a high-resolution ultrastructural study. *Lab Invest.* 1996;74:1081-90
50. Pepys MB, Herbert J, Hutchinson WL et al. Targeted pharmacological depletion of serum amyloid P component for treatment of human amyloidosis. *Nature.* 2002;417:254-9
51. Gillmore JD, Tennent GA, Hutchinson WL et al. Sustained pharmacological depletion of serum amyloid P component in patients with systemic amyloidosis. *Br J Haematol.* 2010;148:760-7
52. Hrnčić R, Wall J, Wolfenbarger DA et al. Antibody-mediated resolution of light chain-associated amyloid deposits. *Am J Pathol.* 2000;157:1239-46
53. Bodin K, Ellmerich S, Kahan MC et al. Antibodies to human serum amyloid P component eliminate visceral amyloid deposits. *Nature.* 2010;468:93-7 

Quadramet[®]

Samarium (¹⁵³Sm) Lexidronam

Radio-targeted therapy

Relief of multiple osteoblastic painful bone metastases
positive on (^{99m}Tc)-bisphosphonates bone scan

**PAIN CONTROL
IN ONE INJECTION**



Protect,
enhance
and save
lives

Iba

Whole body amyloid deposition imaging by ^{123}I -SAP scintigraphy

R.W.J. van Rheenen, MD¹
A.W.J.M. Glaudemans, MD¹
B.P.C. Hazenberg, MD, PhD²

Department of Nuclear Medicine and Molecular Imaging¹, and department of Rheumatology & Clinical Immunology², University Medical Center Groningen, University of Groningen, Groningen, the Netherlands

Abstract

Van Rheenen RWJ, Glaudemans AWJM, Hazenberg BPC. Whole body amyloid deposition imaging by ^{123}I -SAP scintigraphy

Amyloidosis is the name of a group of diseases characterized by extracellular deposition of amyloid fibrils. Deposition of amyloid can be localized or systemic. The ^{123}I -SAP-scan can be used to image extent and distribution of amyloid deposition in patients with systemic AA, AL and ATTR amyloidosis. Images are assessed in a semi-quantitative way by comparing each organ directly or indirectly to the normal blood-pool distribution. Considerable variation is observed between the findings on ^{123}I -SAP-scan and clinical manifestations of organ disease. Regardless, the ^{123}I -SAP-scan still provides both an impression of specific organ involvement as well as a global view of the amyloid load of the whole body. Due to physiological uptake of iodine degradation products in the stomach or to overwhelming uptake in an enlarged liver or enlarged spleen, visualization of abdominal organs nearby is not always easy and sometimes even impossible. In these cases SPECT/CT provides additional anatomical information to enable a more reliable assessment of such an organ.

Tijdschr Nucl Geneesk 2011; 33(4):785-791

Introduction

Amyloidosis is the name of a group of diseases characterized by extracellular deposition of amyloid fibrils. This deposition can be localized (restricted to one organ or site of the body) or systemic (in various organs and tissues throughout the body). The clinical manifestations and diagnostic challenges will be described in another paper in this special issue. Several types of amyloidosis can be identified by the type of protein involved. The three most important systemic types are: Amyloid A (AA) amyloidosis, immunoglobulin light chain-associated (AL) amyloidosis and transthyretin-associated (ATTR) amyloidosis. These types all have a different underlying pathology and clinical presentation. AA amyloidosis is associated with longstanding inflammatory disorders; its predominant clinical feature is nephropathy. In AL amyloidosis

the underlying cause is a free light chains-producing monoclonal plasma cell dyscrasia; it has very diverse clinical manifestations. ATTR amyloidosis may be mutation-related (hereditary) or age-related (senile). The hereditary form is associated with mutations of the transthyretin (TTR) gene and its main manifestations are neuropathy and cardiomyopathy (1). The senile form is associated with non-mutated wild-type TTR and its main manifestation is a slowly progressive cardiomyopathy.

Histological proof remains the gold standard for the diagnosis of amyloidosis (2), but is sometimes difficult to obtain, an invasive procedure and subjected to sampling errors. Several diagnostic and laboratory tests are available to measure organ function and thus indirectly measure amyloid induced organ dysfunction. However, direct measurement of amyloid burden in the body is not available. Currently, the best whole body imaging method is the labelling of Serum amyloid P component (SAP) with radioactive ^{123}I iodine (^{123}I -SAP). This nuclear imaging technique is used to image the extent and distribution of amyloid deposition in patients with all types of amyloidosis (3-7) and has nowadays an important role in the diagnosis and follow-up of patients with (suspected) amyloidosis.

This overview article highlights the different aspects of ^{123}I -SAP scintigraphy, from the tracer characteristics and the acquisition parameters to the interpretation, patterns, prognostic value and clinical relevance.

Tracer characteristics

In the human body SAP is produced only by hepatocytes, and the plasma concentration seems to be regulated at a rather constant level, even during deposition of SAP into amyloid. This indicates that the synthesis of SAP can be increased dramatically (4). The normal function of SAP is not known. All types of amyloid bind in a calcium-dependent manner to SAP, and therefore is a suitable tool to be used for the imaging of all types of amyloidosis (8). Furthermore there does not seem to be such an interaction between SAP and normal tissue (9).

In healthy individuals SAP is mainly located in the plasma compartment, from which it is metabolized and excreted by the liver, with a half-life of about 24 hours (4). In patients with systemic amyloidosis the total amount of SAP associated with amyloid is many times higher than the total amount in the

plasma compartment of healthy individuals. During all phases of amyloid deposition and metabolism there is a constant exchange of SAP between the two compartments (figure 1) (10).

administration of potassium iodide. Scintigraphy is performed 24 hours after injection, with a dual head gamma-camera, equipped with a medium energy all-purpose collimator. Anterior and

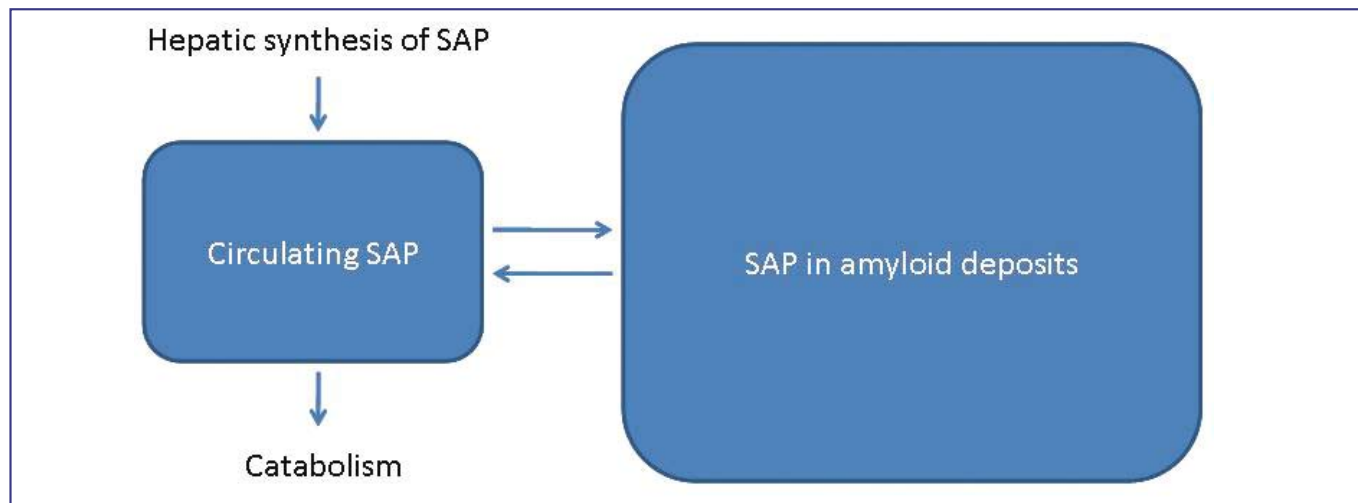


Figure 1. Schematic overview of biodistribution and metabolism of SAP in patients with systemic amyloidosis. Modified from reference 10.

For the tracer production SAP has been isolated and purified from plasma of healthy donors. N-bromosuccinimide is used to oxidatively label the SAP protein with ¹²³I, while preserving its normal function (10). The molecule characteristics and the half-life of ¹²³I (13.2 hours) make it a very suitable radionuclide for amyloid imaging and, when labeled with high affinity to SAP, it is only metabolized in the liver. Radiolabeling methods and quality controls are performed as described (2).

Scintigraphy

Patients are intravenously injected with 200 MBq ¹²³I-SAP. Uptake of free ¹²³I in the thyroid is prevented by oral

posterior total body images (in running mode;10cm/min) are acquired simultaneously, followed by detailed simultaneously acquired anterior and posterior images (10 min) of the abdomen and a single photon emission computed tomography (SPECT) of the abdomen. If necessary, a low-dose CT of the abdomen is performed additionally to obtain anatomic details.

Image assessment

The images are assessed in a semi-quantitative way by comparing each organ directly or indirectly to the normal blood-pool distribution (table 1). Organ involvement is graded

Organ	View	Visual assessment of abnormal uptake
liver	anterior	more than normal blood-pool in the heart
spleen	posterior / spect	more than the liver. if liver is positive than similar uptake is abnormal
bone marrow	posterior	visible sacral bone, pelvis, long bones or individual vertebrae
kidneys	posterior / spect	more than vertebrae. if vertebrae are positive than similar uptake is abnormal
adrenal glands	posterior / spect	one or both visible separate from kidneys, liver and spleen
joints	anterior / posterior	more than surrounding tissues

Table 1. Visual assessment of ¹²³I-SAP scintigraphy.

3 (overwhelming uptake), 2 (intense uptake), 1 (positive uptake without any doubt) and 0 (normal) (11). Examples are shown in figure 2.

The following patterns may be observed and are typical for the different types of amyloidosis (12):

- AA Amyloidosis: abnormal uptake in the spleen is common. The three most frequent uptake patterns are: (1) abnormal uptake in the spleen only, (2) abnormal uptake in the spleen and kidneys, and (3) abnormal uptake in the spleen, kidneys and adrenal glands.
- AL Amyloidosis: abnormal uptake in the spleen is common. Uptake in other organs, such as liver, kidneys, bone marrow and joints, is very diverse.
- ATTR Amyloidosis: only abnormal uptake in the spleen or kidneys is seen.

In healthy individuals there is no organ deposition of ^{123}I -SAP, and the tracer is then confined to the circulating blood pool and major blood organs (3, 13, 14).

Because of the semi-quantitative nature of the assessment, the inter-observer variety may be high, and therefore in our center the images are assessed by two experienced clinicians (rheumatologist and nuclear medicine physician) who will reach consensus.

Clinical correlation and prognostic value

Clinical studies with ^{123}I -SAP in patients with well-defined amyloidosis have shown a sensitivity of 100% in AA amyloidosis, 84% in AL amyloidosis and 95% in ATTR amyloidosis (10). The overall specificity is 93% (12).

^{123}I -SAP-scans can serve as a clinical tool for evaluation of amyloidosis patients. During life it is impossible to obtain a quantitative impression of the amount of amyloid in the body by using other procedures. Even multiple biopsies from many organs would only provide a qualitative impression of the amount of amyloidosis and serial monitoring of vital organs and tissues by biopsies is impossible (2). By using ^{123}I -SAP-scans it has become possible to obtain a (semi-) quantitative assessment of the amyloid load of specific organs, as well as

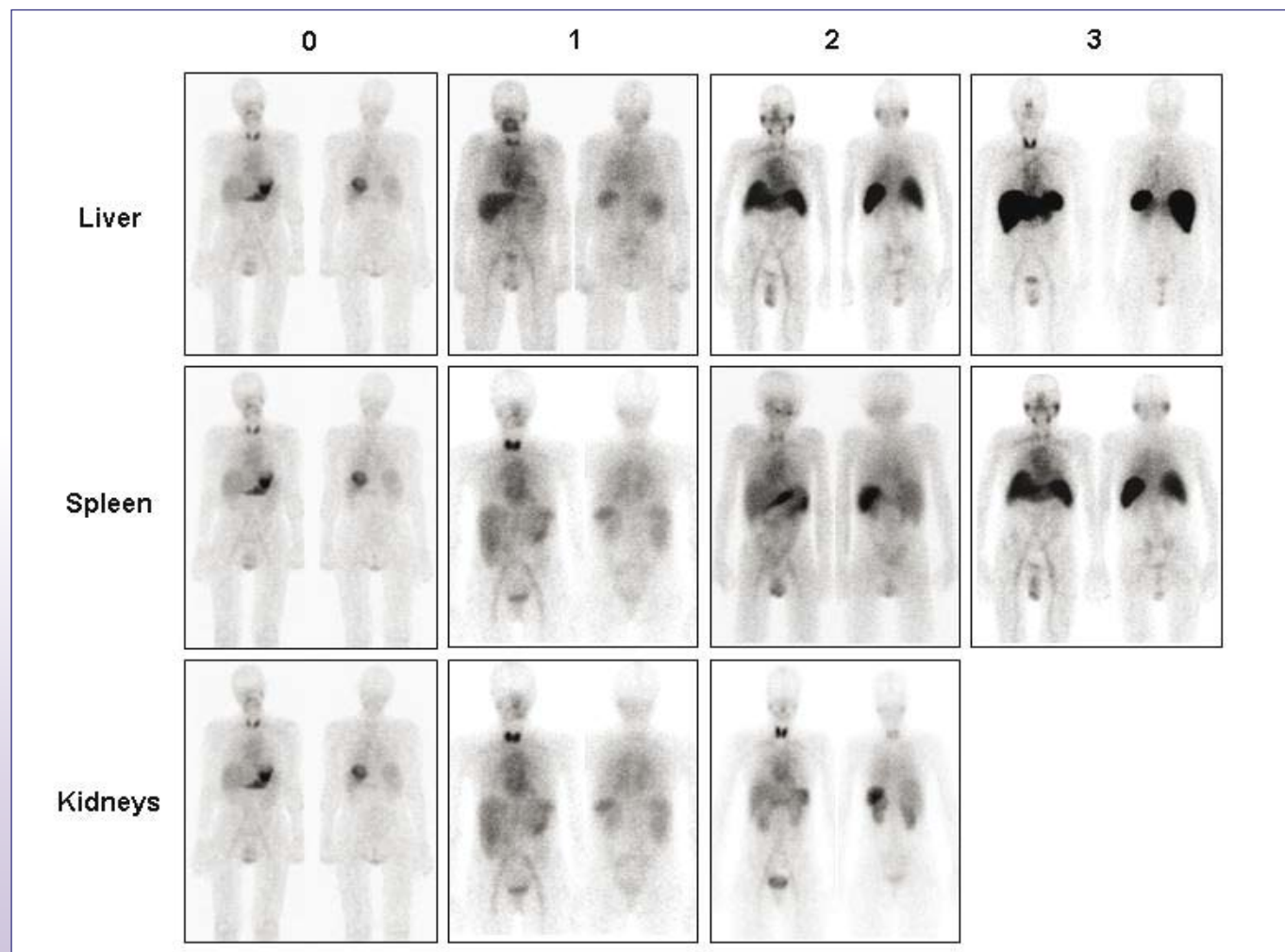


Figure 2. Clinical examples of semi-quantitative assessment of ^{123}I -SAP-scan. Grading of organ involvement: overwhelming (3), intense (2), positive without any doubt (1) and normal (0).

a general impression of the total body amyloid burden thereby providing a more complete staging of the disease and a non-invasive evaluation during and after therapy.

In clinical practice, however, the findings on a ^{123}I -SAP-scan and clinical manifestations of disease vary considerably among organs. Increased uptake of spleen and liver can be seen before clinical disease is present. On the other side, kidney involvement is detected earlier by proteinuria or loss of function than by ^{123}I -SAP-scintigraphy. Both heart and nerves are not visualized with this imaging method. Kidney uptake is concordant with severity of proteinuria (figure 3) and liver uptake in AL amyloidosis is concordant with increasing serum levels of alkaline phosphatase. One should realise that individual variation is considerable (12). Amyloid deposition is a

predictor of survival. However, in this group of patients with cardiac involvement, tissue retention of SAP helps to distinguish patients with the worst prognosis from patients in whom chemotherapy still may be beneficial (figure 4). Furthermore uptake within the joints can be challenging in the assessment of a scan because of the false positive outcome in patients with arthritis, such as rheumatoid arthritis. Uptake of SAP in these cases is non-specific because of synovial effusion in arthritic joints due to the increased blood-pool at these sites.

As already stated above, the ^{123}I -SAP-scan is not suitable for the evaluation of the heart, most likely due to lack of fenestrated endothelium in the myocardium (12). To determine amyloid burden of the heart, an indirect imaging method is available that measures the innervation of the heart (^{123}I -MIBG).

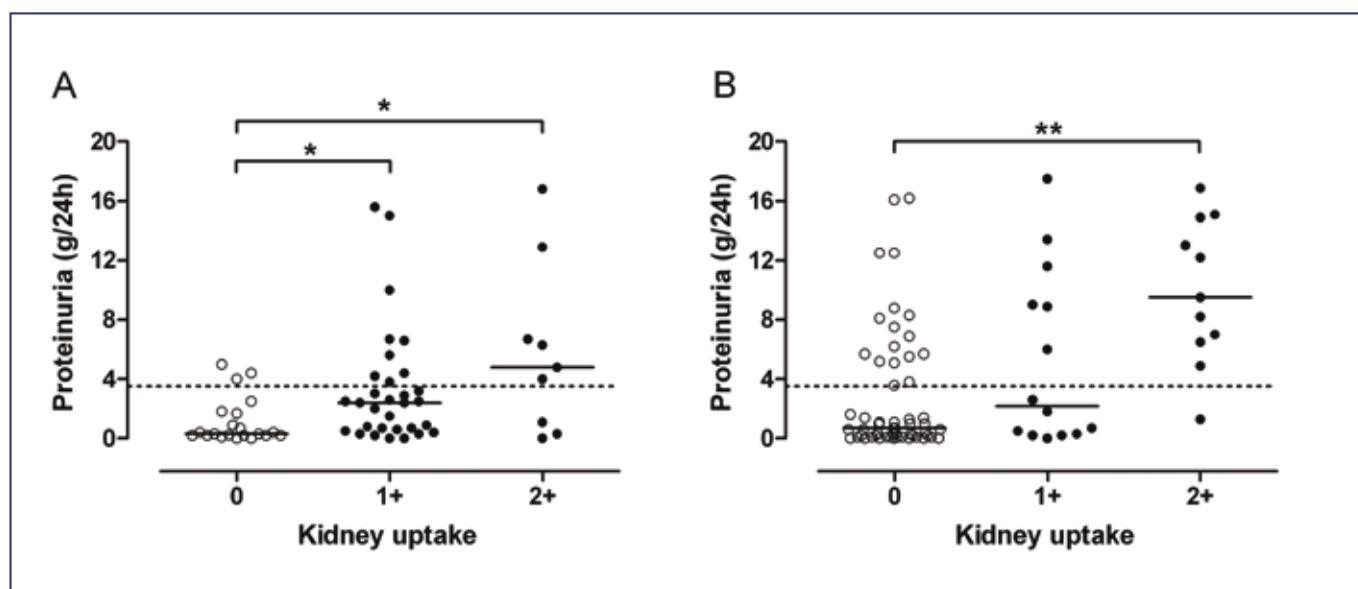


Figure 3. Proteinuria and ^{123}I -SAP kidney uptake. The dashed line indicates heavy proteinuria (>3.5 g/24h). Horizontal lines show median values. (A) AA patients. (B) AL patients. Reproduced with permission from reference 12.

more dynamic process than previously thought, with a balance of deposition and removal that also differs among various tissues and organs with even some redistribution of amyloid (15). This possible redistribution of amyloid may partly account for a sometimes unpredictable course of the disease. It puts emphasis on not only assessing individual organ uptake, but also on assessing the total body load of amyloid.

In order to obtain an impression of the total body burden, blood and urinary samples are collected after one day to calculate the tissue retention of ^{123}I -SAP. The percentage of tissue retention of SAP may sometimes help to diagnose amyloidosis. But, because of wide variation of the values, tissue retention of SAP does not reliably predict clinical stage or prognosis in the individual patient (11). In patients with AL amyloidosis, cardiac involvement is the most important

Further on, due to not crossing the blood-brain-barrier, ^{123}I -SAP is not able to visualize amyloid plaques in the brain. In this situation imaging with ^{11}C -PiB comes into sight. These two radionuclides are described elsewhere in this special issue.

Better Imaging; ^{123}I -SAP SPECT

Since the development of hybrid imaging systems, such as SPECT/CT, SPECT and CT images of the abdomen have been added to our routine imaging protocol of ^{123}I -SAP. This obviously has substantial advantages.

On planar imaging physiological stomach uptake and an enlarged liver can obscure the visualisation of the spleen. At the same time the spleen (and an enlarged liver) can obscure visualisation of the kidneys and adrenal glands (1). Inaccurate information about organ involvement may have a negative effect on diagnosis, disease staging and follow-up of a

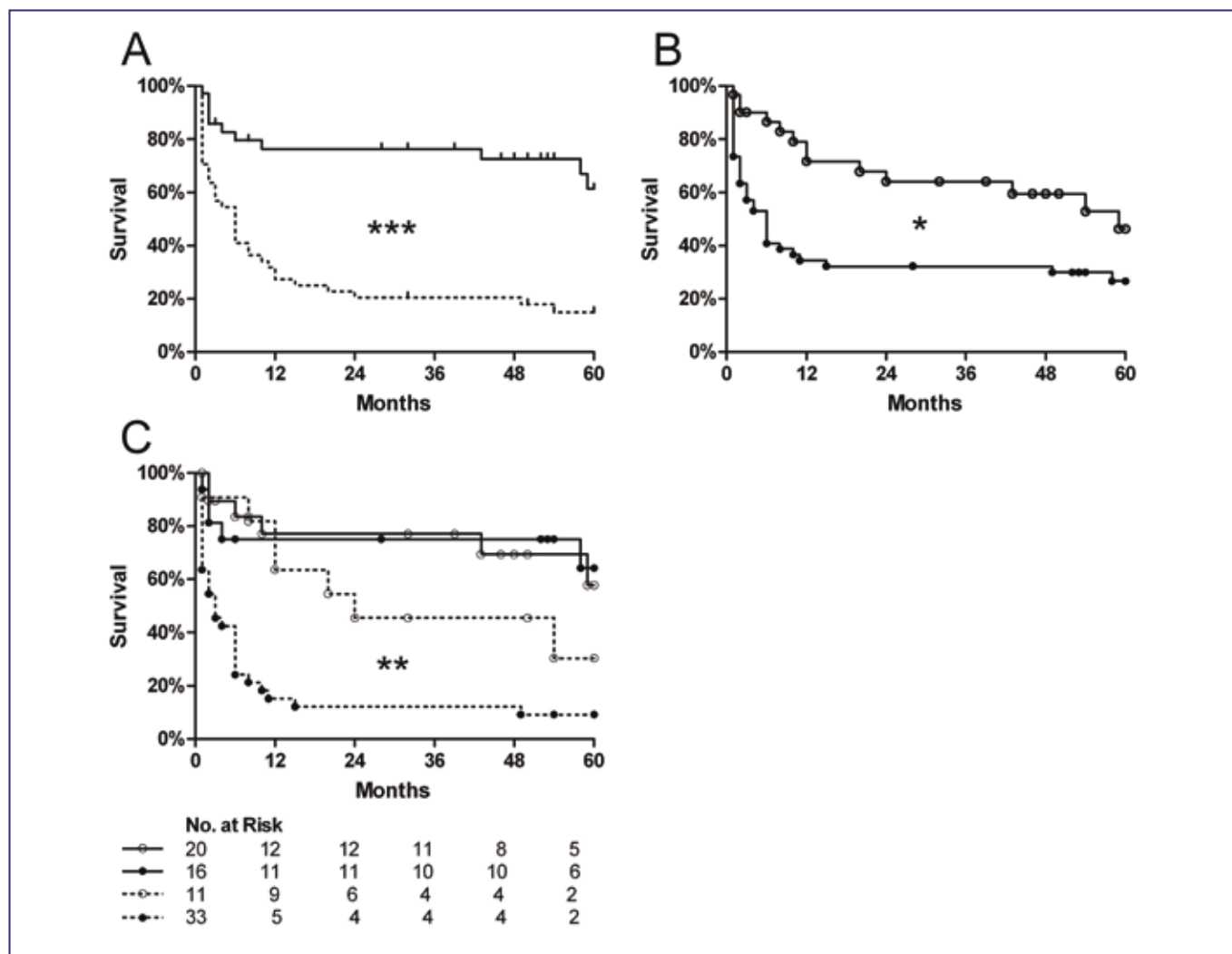


Figure 4. Survival of 80 patients with AL amyloidosis. (A) Patients with (dotted line) and without (solid line) clinical involvement of the heart. (B) Patients with high (>50%) (●) and low (<50%) (○) tissue retention of SAP after 24 hours (EVR_{24}). (C) Patients stratified according to high (>50%) (●) and low (<50%) (○) EVR_{24} and presence (dotted line) or absence (solid line) of clinical involvement of the heart. Reproduced with permission from reference 11.

patient with amyloidosis (1). Empirically it has been proposed that SPECT imaging should solve the problem of obscured visualisation of abdominal organs on a SAP scan. However, this issue has not yet been studied.

In our practice SPECT/CT has become a complementary modality next to the static planar images. Often physiological uptake in the stomach hinders accurate assessment of the spleen, but with SPECT/CT this problem can be addressed easily (figure 5). With regards to the adrenal glands it seems that SPECT/CT is the best way to assess involvement by giving accurate grading (figure 6). SPECT/CT of the abdomen is now routinely used in these patient groups and a patient study of the additional value of SPECT and CT has just been finished.

Conclusion

The ^{123}I -SAP-scan is a non-invasive sensitive imaging

modality to detect and grade amyloid deposits in most organs (except heart and brain) in patients with all types of amyloidosis. Although there is a high variety among individual patients, its use for diagnosis, disease staging and follow-up in patients with amyloidosis makes it a valuable tool in the clinical management of patients with amyloidosis. The semi-quantitative assessment and sometimes obscured nearby abdominal organs by overlap can make accurate and consistent assessment difficult and sometimes impossible. However, this problem can be addressed by collaborative assessment and the use of SPECT/CT imaging.

List of references

1. Falk RH, Comenzo RL, Skinner M. The systemic amyloidoses. *N Engl J Med.* 1997 ;337:898-909
2. Jager PL, Hazenberg BP, Franssen EJ et al. Kinetic studies with

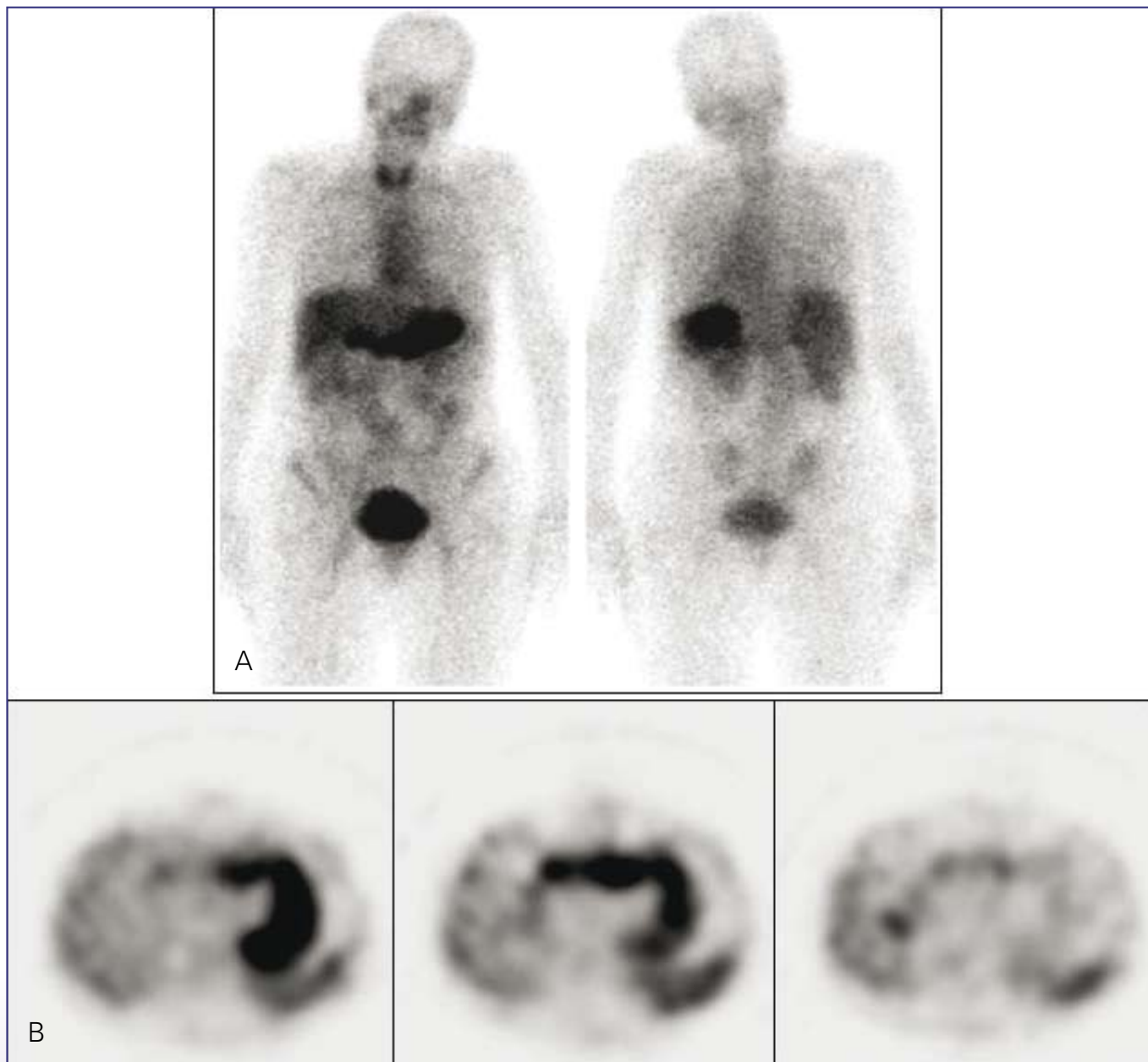


Figure 5. (A) Planar SAP scan image (anterior / posterior) of a patient with AA Amyloidosis; the spleen is difficult to assess because of uptake in the stomach. (B) SPECT/CT images conclusively show physiological uptake in the stomach and positive uptake (1+) in the spleen.

- iodine-123-labeled serum amyloid P component in patients with systemic AA and AL amyloidosis and assessment of clinical value. *J Nucl Med.* 1998;39:699-706
3. Hawkins PN, Lavender JP, Pepys MB. Evaluation of systemic amyloidosis by scintigraphy with 123I-labeled serum amyloid P component. *N Engl J Med.* 1990;323:508-13
 4. Hawkins PN, Wootton R, Pepys MB. Metabolic studies of radioiodinated serum amyloid P component in normal subjects and patients with systemic amyloidosis. *J Clin Invest.* 1990;86:1862-9
 5. Maulin L, Hachulla E, Deveaux M et al. 'Localized amyloidosis': 123I-labelled SAP component scintigraphy and labial salivary gland biopsy. *QJM.* 1997;90:45-50
 6. Rydh A, Suhr O, Hietala SO et al. Serum amyloid P component scintigraphy in familial amyloid polyneuropathy: Regression of visceral amyloid following liver transplantation. *Eur J Nucl Med.* 1998;25:709-13
 7. Hachulla E, Maulin L, Deveaux M, et al. Prospective and serial study of primary amyloidosis with serum amyloid P component scintigraphy: From diagnosis to prognosis. *Am J Med.* 1996;101:77-87
 8. Pepys MB, Dyck RF, de Beer FC et al. Binding of serum amyloid P-component (SAP) by amyloid fibrils. *Clin Exp Immunol.* 1979;38:284-93

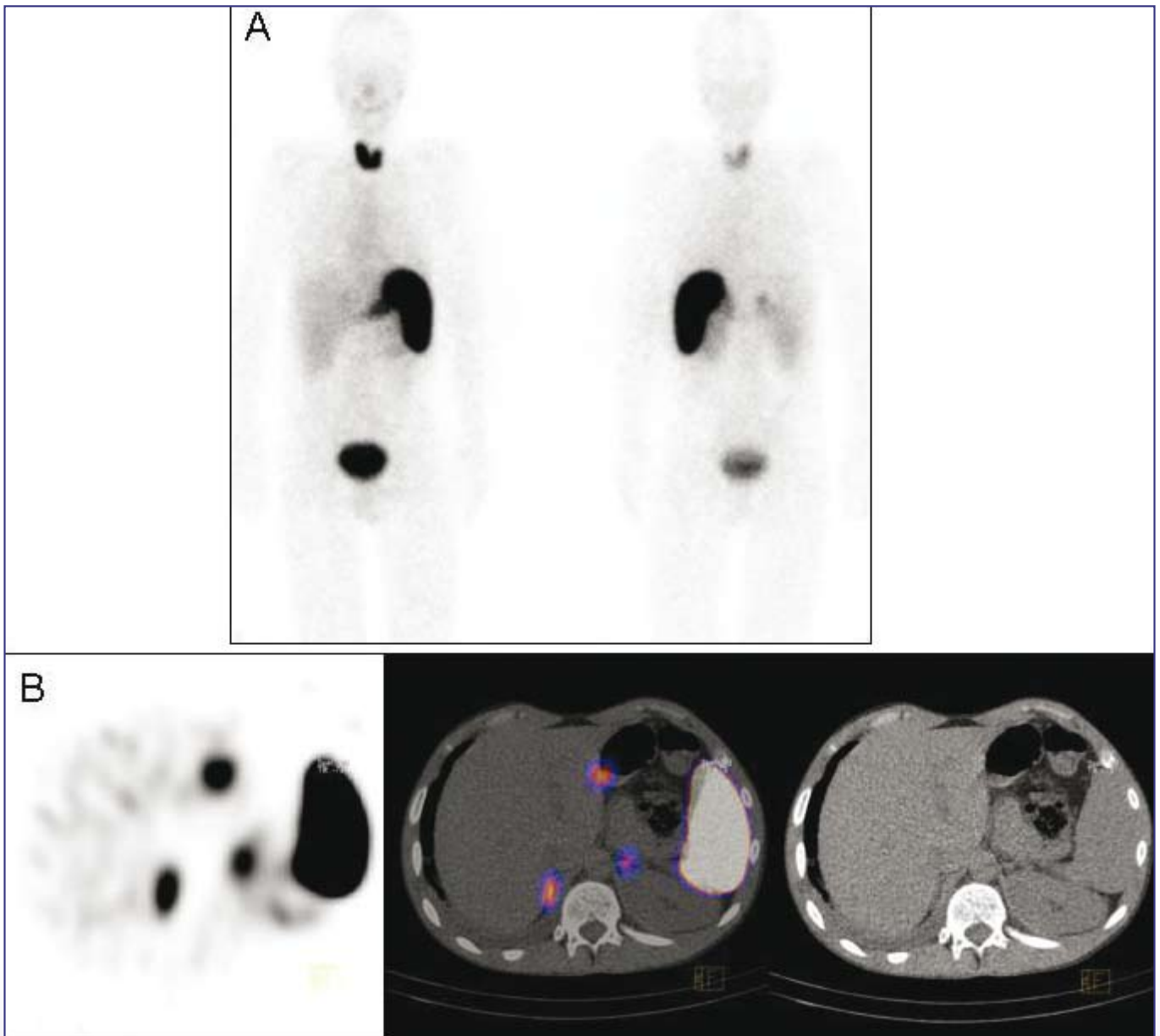


Figure 6. (A) Planar SAP scan image (anterior / posterior) of a patient with AA amyloidosis. The adrenal glands are difficult to assess. (B) SPECT/CT images show uptake in both adrenal glands.

9. Vigushin DM, Pepys MB, Hawkins PN. Metabolic and scintigraphic studies of radioiodinated human C-reactive protein in health and disease. *J Clin Invest.* 1993;91:1351-7
10. Hawkins PN. Diagnosis and monitoring of amyloidosis. *Baillieres Clin Rheumatol.* 1994;8:635-59
11. Hazenberg BP, van Rijswijk MH, Lub-de Hooge MN et al. Diagnostic performance and prognostic value of extravascular retention of ¹²³I-labeled serum amyloid P component in systemic amyloidosis. *J Nucl Med.* 2007;48:865-72
12. Hazenberg BP, van Rijswijk MH, Piers DA, et al. Diagnostic performance of ¹²³I-labeled serum amyloid P component scintigraphy in patients with amyloidosis. *Am J Med.* 2006;119:355.e15-24.
13. Hawkins PN, Myers MJ, Epenetos AA, et al. Specific localization and imaging of amyloid deposits in vivo using ¹²³I-labeled serum amyloid P component. *J Exp Med.* 1988;167:903-13
14. Hawkins PN, Myers MJ, Lavender JP, et al. Diagnostic radionuclide imaging of amyloid: Biological targeting by circulating human serum amyloid P component. *Lancet.* 1988;1:1413-8
15. Pettersson T, Konttinen YT. Amyloidosis-recent developments. *Semin Arthritis Rheum.* 2010;39:356-68

Echocardiography and magnetic resonance imaging for the detection of cardiac amyloidosis

M. Groenink, MD, PhD^{1,2}
H.J. Verberne, MD, PhD³

Departments of cardiology¹, radiology² and nuclear medicine³, Academic Medical Center, University of Amsterdam, the Netherlands.

Abstract

Groenink M, Verberne HJ. Echocardiography and magnetic resonance imaging for the detection of cardiac amyloidosis

Cardiac amyloidosis can be diagnostically challenging. The "gold standard" for the diagnosis of cardiac amyloidosis is myocardial biopsy. However this invasive method may be problematic. Thus, in practice, the diagnosis of cardiac amyloidosis is usually made by non-invasive assessment of increased left ventricular wall thickness using imaging modalities, supported by a diagnostic non-cardiac biopsy. However, diagnosis by echocardiography has some limitations, particularly if hypertrophy from other causes is present. Cardiovascular magnetic resonance (CMR) can assess abnormal myocardial interstitium and may help to overcome the limitations of echocardiography. In this review the possibilities and limitations of both echocardiography and CMR are discussed.

Tijdschr Nucl Geneesk 2011; 33(4):793-798

Introduction

Amyloidosis is a generic term that refers to the extracellular tissue deposition of fibrils composed of low molecular weight subunits of a variety of proteins, many of which circulate as constituents of plasma (1). As many as 27 different precursor proteins to the formation of amyloid have been described in man. These may deposit themselves in a fibrillar matrix within selected tissues including the heart and arteries. In the developed world, three main types of amyloidosis that affect the heart are encountered; light chain (AL) amyloidosis, senile systemic amyloidosis (SSA), and familial amyloidosis (FAP); the latter most commonly results from a mutation in transthyretin. In the developing world, secondary amyloid (AA) is more prevalent, due to chronic infections and inadequately treated inflammatory conditions. Accumulation of amyloid in cardiovascular tissue is generally accompanied by congestive heart failure, conduction abnormalities and anginal complaints in a very rapidly progressive way, with death occurring within 6 months from the development of clinically significant heart disease. Therefore, making an early diagnosis of amyloidosis is critical because delay might incapacitate patients for the most intensive forms of treatment. Here we will focus on

cardiac imaging by echocardiography and cardiovascular magnetic resonance imaging (CMR) to detect cardiac amyloidosis.

Echocardiography

In patients with a non-cardiac biopsy showing amyloid deposition, cardiac involvement has been defined by a consensus opinion from the 10th International Symposium on Amyloidosis as either a positive heart biopsy and/or increased left ventricular wall thickness (mean left ventricular wall thickness (septum and posterior wall) greater than 12 mm) in the absence of hypertension or other potential causes of true left ventricular hypertrophy in combination with a positive result of a non-cardiac biopsy (2). Other potential causes for left ventricular hypertrophy in the absence of hypertension include aortic stenosis, coarctation, hypertrophic cardiomyopathy and Fabry disease, which are often well recognized on echo. However, CMR is increasingly used to differentiate between conditions that are accompanied by cardiac hypertrophy. It is not possible to distinguish between AL, FAP, non-transthyretin FAP, senile amyloid or secondary (AA) amyloid by echocardiography (or by MRI). The LV ejection fraction and fractional shortening remain normal or nearly normal up to the late stage of the disease. Diastolic dysfunction appears early in cardiac amyloidosis and can be evaluated using standard Doppler echocardiography.

ECG and voltage-mass ratio

Typically, patients show low voltage QRS on the ECG limb leads (< 0.5 mV), which is not consistent with left ventricular hypertrophy. See figure 1 for a typical ECG. The echo in the parasternal long axis view of the same patient is shown in figure 2. Differential diagnosis should include pericardial effusion (see below), myocardial infarction and pulmonary emphysema, which may also be the cause of micro-voltage ECG. A prospective study compared the ECG voltage-to-left ventricular mass ratio to other diagnostic tests in patients with cardiac amyloidosis, predominantly due to AL amyloid (3). The ratio was more sensitive than electrocardiography, two-dimensional echocardiography alone, or nuclear scanning (^{99m}Tc-pyrophosphate and ^{99m}Tc-disphosphonate). In another report, the combination of low voltage on ECG and an interventricular septal thickness >1.98 cm detected amyloidosis with a sensitivity and specificity of 72 and 91 percent, respectively (4).

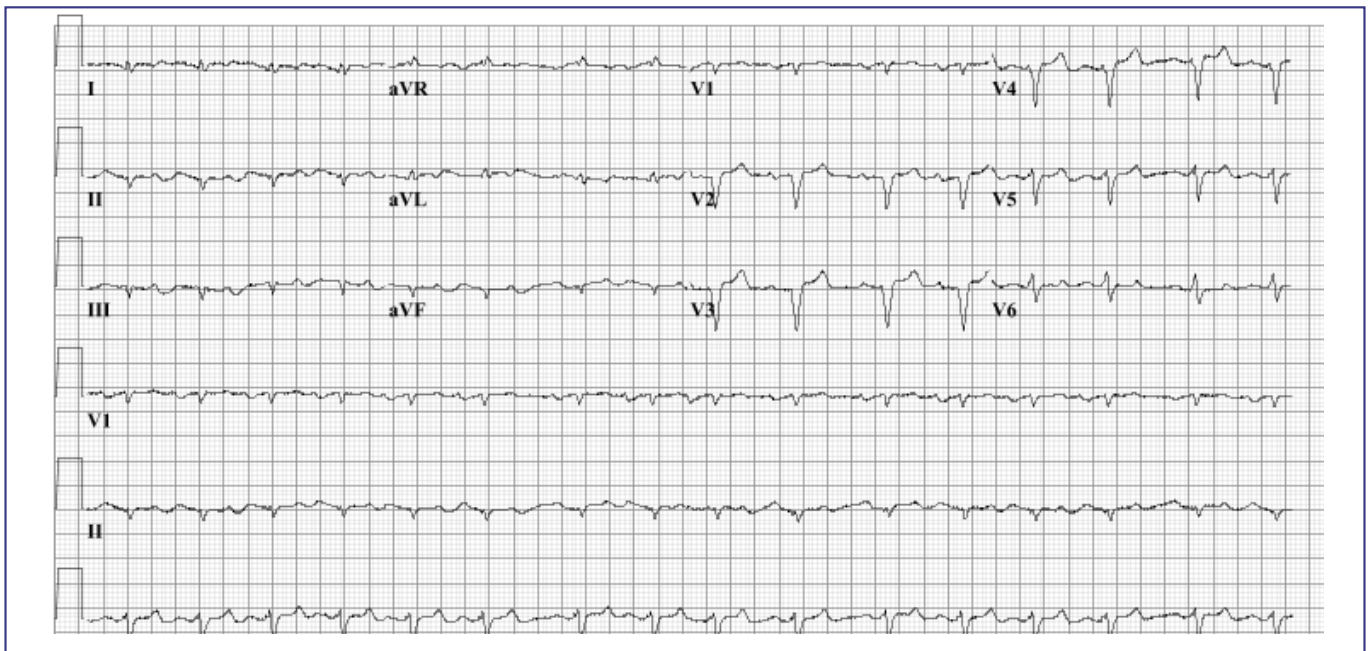


Figure 1. Typical ECG of a patient with cardiac AL-amyloidosis, showing microvoltages ($< 0.5\text{ mV}$) in the limb leads.

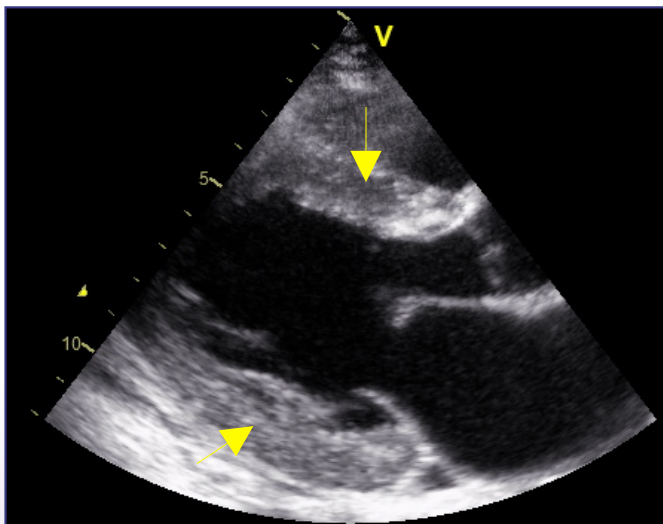


Figure 2. Echo (parasternal long axis view) from the patient whose ECG was shown in figure 1: severe concentric hypertrophy (arrows).

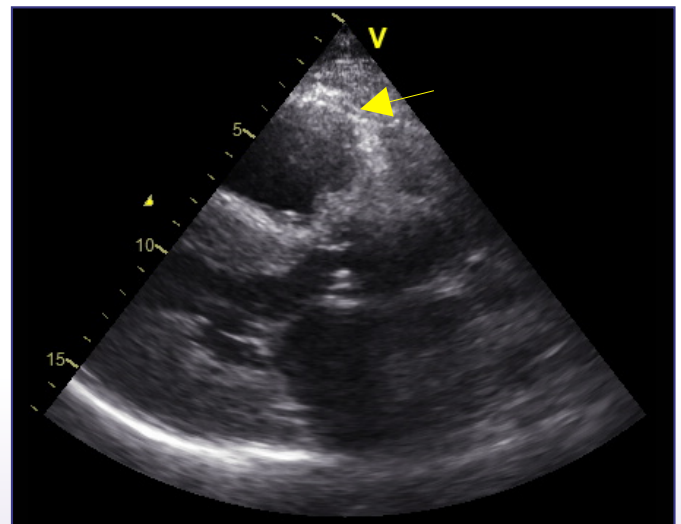


Figure 3. Echo (parasternal long axis view) showing right ventricular hypertrophy (arrow) in another patient with cardiac AL-amyloidosis.

Right ventricular dilatation or hypertrophy

Right ventricular hypertrophy is often encountered in patients with amyloidosis (figure 3). In the absence of pulmonary or systemic hypertension this strongly suggests myocardial infiltration. Right ventricular dilatation may also be present and is associated with an unfavourable prognosis (5). However, several cardiomyopathies may exhibit right ventricular dilatation (such as arrhythmogenic right ventricular cardiomyopathy [ARVC], dilated cardiomyopathy [DCM]) or hypertrophy (such as hypertrophic cardiomyopathy [HCM] or Fabry disease).

'Sparkling' myocardium

Amyloid infiltration of the heart results in increased echogenicity. This was originally described as a "granular, sparkling" appearance of the myocardium, with very high quality myocardial visualization. See figure 4 for a typical example. However, "sparkling" myocardium is not very sensitive for cardiac amyloidosis: the interpretation of this feature is highly operator dependent and advances in echotechnology make "sparkling" a more frequent finding in patients without cardiac amyloidosis. Although a recent study

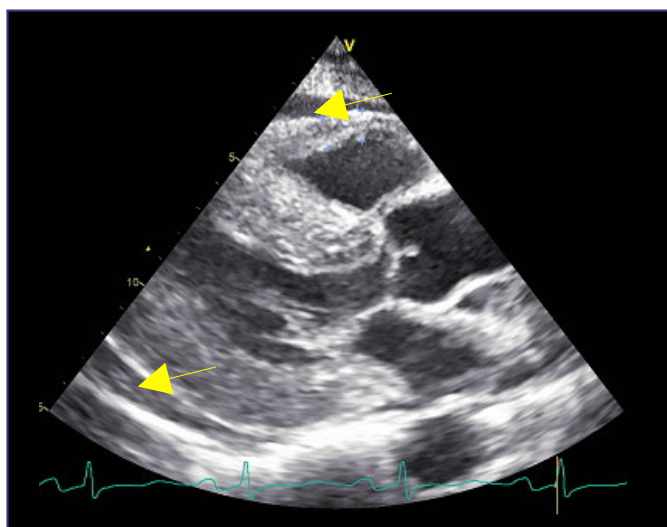


Figure 4. Echocardiographic parasternal long-axis view with a typical example of a “granular, sparkling” appearance of the myocardium. This is caused by myocardial amyloid infiltration and results in increased echogenicity. In addition there are signs of pericardial effusion (arrows).

in patients with an endomyocardial biopsy proven cardiac amyloidosis showed that these patients were more likely to have a “sparkling” myocardium, the “sparkling” myocardium could only be demonstrated in a minority of patients (approximately 25%) (4).

Bi-atrial enlargement, diastolic dysfunction and thrombi

Bi-atrial enlargement is often present with an ‘owl’s eyes’ appearance. See figure 5 (top). Diastolic dysfunction is almost always present with restrictive physiology in advanced cases (figure 5). The atria are generally less mobile which may result in intra-atrial thrombi. Thrombi may also be seen in other heart compartments.

Pericardial effusion, thickened valves and valvular (dys) function

Small pericardial effusions are often seen in cardiac amyloidosis (figure 4, 6). In addition to the thickened left ventricular wall (septum and posterior wall greater than 12 mm), the valves, papillary muscles, and intra-atrial septum can be thickened (figure 6). Mild valvular dysfunction is quite common, but severe dysfunction is rare.

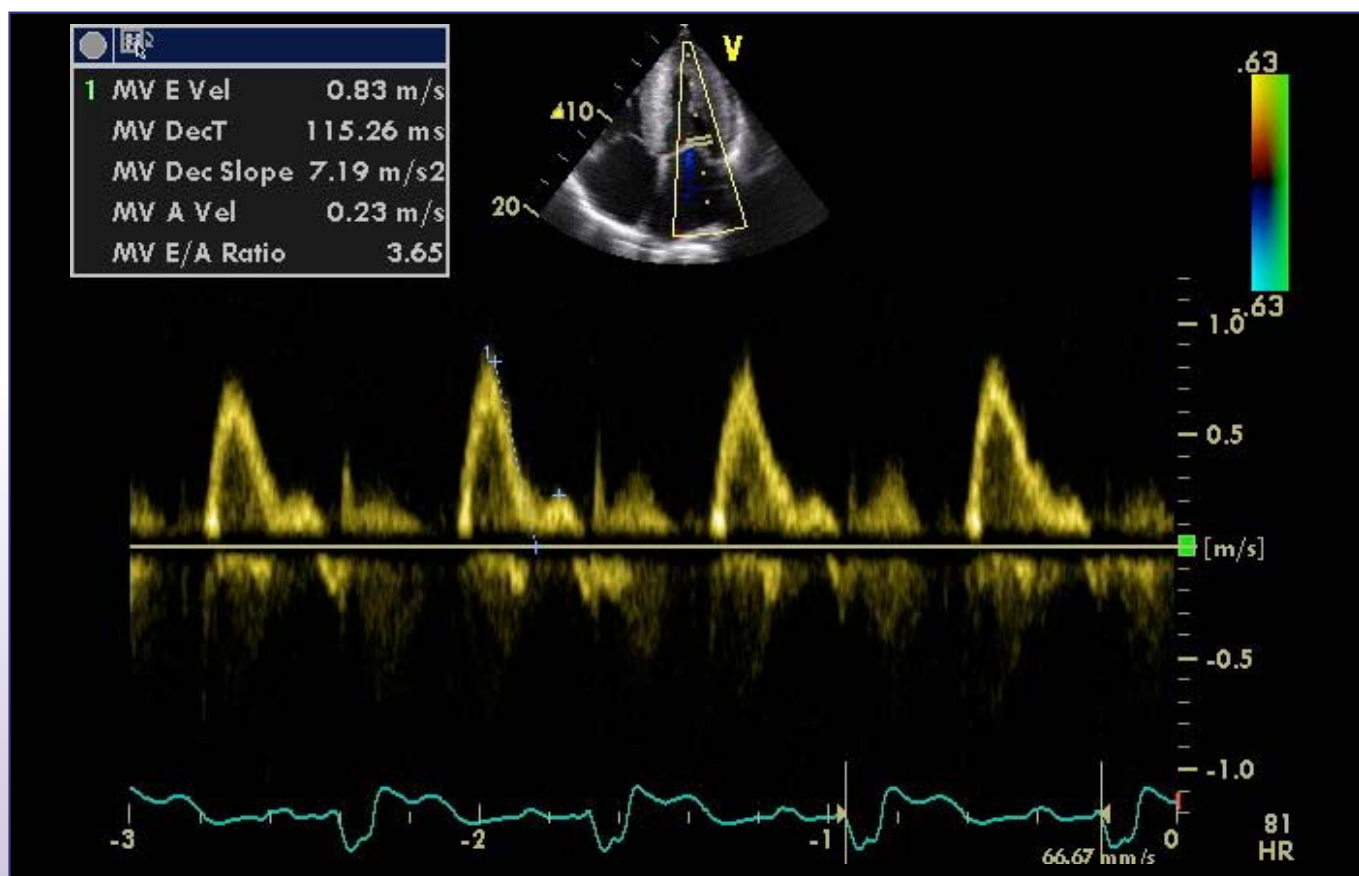


Figure 5. Echocardiographic apical long-axis view with a typical example of bi-atrial enlargement; so called “owl’s eyes” appearance (top) and pulsed Doppler evaluation of mitral inflow in the apical four chambered view showing a restrictive filling pattern in a patient with amyloidosis.

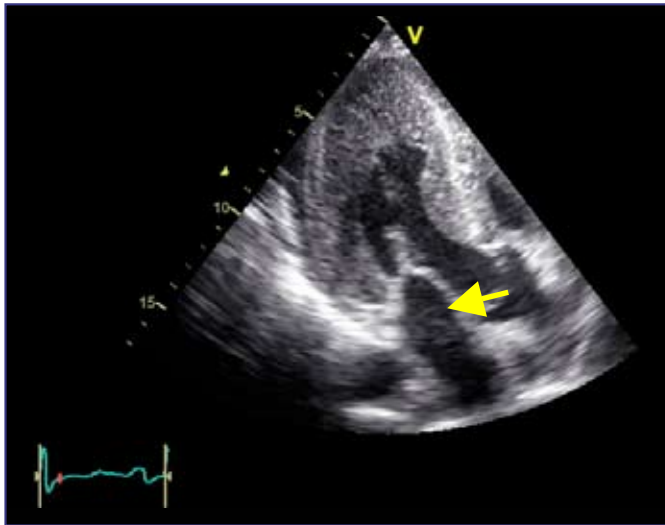


Figure 6. Echocardiographic apical three chamber view of an AL-amyloidosis patient with concentric left ventricular hypertrophy and a thickened mitral valve (arrow).

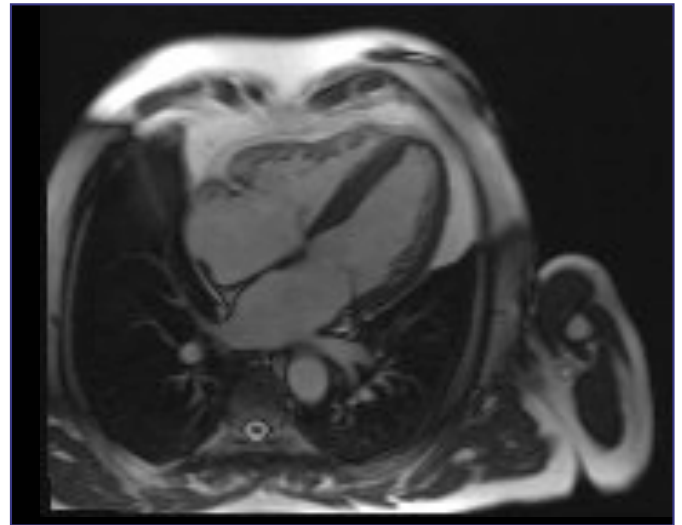


Figure 7. MR four chamber view by steady state free precession imaging in a 79 year old male with an established diagnosis of AL-amyloidosis by endocardial biopsy. No evident hypertrophy is shown although there is moderate bi-atrial enlargement.

Developments in echocardiography

Newer echocardiographic techniques are directed towards regional myocardial function assessed by tissue Doppler imaging (TDI), strain rate imaging (SRI), and 2-dimensional (2D) speckle-tracking imaging (STI), a technique based on frame-to-frame tissue tracking from 2D gray scale images (6). STI seems to be the most promising technique in patients with cardiac amyloidosis, showing reduced myocardial deformation during systole at the basal and mid-segment levels in early stages of the disease where classic echocardiographic features may not yet be apparent (7).

CMR

The above-mentioned morphological characteristics seen on echocardiography can also be assessed by CMR when a patient has poor echo windows (figure 7). In addition, CMR has now established a special role in the diagnosis of cardiac amyloidosis with the assessment of delayed hyperenhancement (DHE). With DHE imaging, differences in T1 relaxation times between diseased and normal myocardium can be used to visualize specific myocardial patterns of high and low signal intensity, a few minutes after intravenous injection of a gadolinium based T1-shortening contrast agent. In general, the time-lag between actual imaging and an inversion pre-pulse (time to inversion: TI) is tailored for optimal distinction between normal and diseased myocardium. This technique has shown to be very useful in the assessment of myocardial infarction, myocarditis and cardiomyopathies. Gadolinium-chelates are distributed in the extracellular space, and the enhancement (brighter aspect by shorter T1) depends on the imaging delay after injection (at least 5 minutes) and TI. Late gadolinium enhancement generally occurs in areas of expanded extracellular space

(e.g. fibrosis after myocardial infarction, myocarditis and in some cardiomyopathies) due to higher regional gadolinium concentration and slower distribution kinetics than in normal myocardium. In cardiac amyloidosis, however, DHE seems to be caused by accumulation of gadolinium in the areas of amyloid deposition, resulting in a sub-endocardial, diffuse and global enhancement pattern, which is different from that in infarction, myocarditis, cardiomyopathies, and especially hypertrophic cardiomyopathy. In one study in patients with cardiac amyloidosis, DHE was shown in 69% of patients with a characteristic global sub-endocardial diffuse pattern that agreed with the transmural histological distribution of amyloid protein in the myocardium and correlated with morphological markers of increased amyloid load (8). Technically, DHE imaging can be challenging due to abnormal gadolinium kinetics (fast accumulation in affected tissues and fast wash-out of the blood pool). In addition, T1 equalization of affected (amyloid infiltrated) and not affected myocardium, the latter occurring in about 8 minutes, may occur (8). Therefore, the blood pool is generally dark in these images and myocardial enhancement may be not apparent or more diffuse (figure 8). However, inability to obtain proper myocardial nulling or myocardial nulling before blood pool brightening may provide a clue (figure 9). An optimized threshold (TI: 191 ms at 4 min) between myocardium and blood has shown an 88% accuracy in the diagnosis of cardiac amyloidosis (8). In another study, diagnostic accuracy of DHE, clinical assessment, electrocardiography (ECG), and echocardiography (2-dimensional and Doppler) was assessed in 38 patients suspected of cardiac amyloidosis, with endomyocardial biopsy (EMB) as the "gold standard". Of the 38 patients, 17 had EMB-proven cardiac amyloidosis. When compared with Carroll's low-voltage criteria (defined

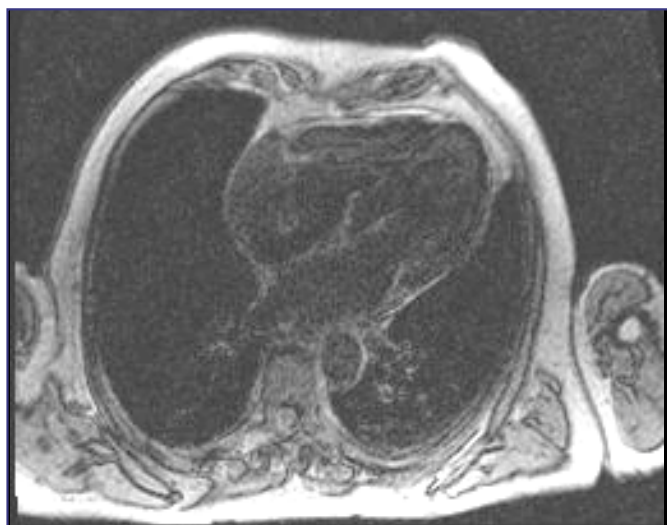


Figure 8. T1 weighted inversion recovery sequence in a similar cardiac orientation in the same patient late after gadolinium infusion. Delayed gadolinium hyperenhancement is not clearly shown and myocardial nulling ('blackening of the myocardium') occurs before blood pool enhancement.

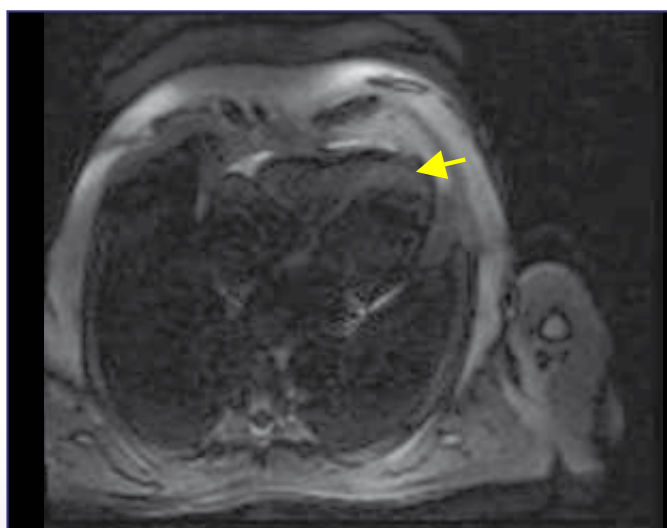


Figure 9. 'Look-locker' sequence in a similar cardiac orientation in the same patient with increasing TI lengths showing very early (short TI) nulling of the myocardium with subtle endocardial high signal intensity (arrow).

as the sum of the S-wave in lead V1 + R-wave in lead V₅ or V₆ <15 mm) (9), deceleration time <150 ms on Doppler, and New York Heart Association functional class status, DHE was the most accurate predictor of EMB-positive cardiac amyloidosis. DHE had a sensitivity, specificity, and positive and negative predictive value of 88%, 95%, 93%, and 90%, respectively. These values were within the range of previously published reports on DHE and cardiac amyloidosis but significantly higher compared to the other tests (10). Despite these good results DHE also has some pitfalls. An

early patchy sub-endocardial DHE, asymmetrical hypertrophy, or the coexistence of other conditions such as ischemic heart disease may lead to false negative and false positive results with respect to the presence of cardiac amyloidosis.

More recently, a T1 mapping technique has even shown to be of prognostic value in the assessment of patients with cardiac amyloidosis. With T1 mapping, differences in T1 relaxation time between sub-epicardium and sub-endocardium can be measured. This intramyocardial T1 gradient (sub-epicardium minus sub-endocardium) at a cut-off value of 23 ms, 2 minutes after intravenous gadolinium injection, predicted mortality with 85% accuracy in patients with cardiac amyloidosis. The intramyocardial T1 gradient was a better predictor of survival than the free light chain response to chemotherapy or diastolic function (11).

Conclusion

Longitudinal myocardial dysfunction can be documented in an early stage of patients with cardiac amyloidosis and might appear before congestive heart failure occurs and sometimes even in subjects with normal results on standard echocardiography. The detection of subclinical myocardial dysfunction in patients with cardiac amyloidosis is crucial for improving therapy efficiency as well as for prognosis. Currently, TDI and SRI seem to be the promising echocardiographic techniques in the early assessment of global and regional left ventricular and right ventricular myocardial dysfunction in patients with cardiac amyloidosis. In addition CMR shows a characteristic pattern in cardiac amyloidosis of global sub-endocardial late enhancement coupled with abnormal myocardial and blood-pool gadolinium kinetics. These findings agree with the transmural histological distribution of amyloid protein and provide information relating to risk of mortality based on gadolinium kinetics.

List of references

1. Westermark P, Benson MD, Buxbaum JN et al. A primer of amyloid nomenclature. *Amyloid*. 2007;14:179-83
2. Gertz MA, Comenzo R, Falk RH et al. Definition of organ involvement and treatment response in immunoglobulin light chain amyloidosis (AL): a consensus opinion from the 10th International Symposium on Amyloid and Amyloidosis, Tours, France, 18-22 April 2004. *Am J Hematol*. 2005;79:319-28
3. Simons M, Isner JM. Assessment of relative sensitivities of noninvasive tests for cardiac amyloidosis in documented cardiac amyloidosis. *Am J Cardiol*. 1992;69:425-27
4. Rahman JE, Helou EF, Gelzer-Bell R et al. Noninvasive diagnosis of biopsy-proven cardiac amyloidosis. *J Am Coll Cardiol*. 2004;43:410-15
5. Patel AR, Dubrey SW, Mendes LA et al. Right ventricular dilation in primary amyloidosis: an independent predictor of survival. *Am J Cardiol*. 1997;80:486-92
6. Teske AJ, De Boeck BW, Melman PG, et al. Echocardiographic quantification of myocardial function using tissue deformation imaging, a guide to image acquisition and analysis using tissue

- Doppler and speckle tracking. Cardiovasc Ultrasound. 2007;5:27
7. Liu D, Niemann M, Hu K et al. Echocardiographic evaluation of systolic and diastolic function in patients with cardiac amyloidosis. Am J Cardiol. 2011;108:591-8
 8. Maceira AM, Joshi J, Prasad SK et al. Cardiovascular magnetic resonance in cardiac amyloidosis. Circulation. 2005;111:186-93
 9. Austin BA, Tang WH, Rodriguez ER et al. Delayed hyper-enhancement magnetic resonance imaging provides incremental diagnostic and prognostic utility in suspected cardiac amyloidosis. JACC Cardiovasc Imaging. 2009;2:1369-77
 10. Carroll JD, Gaasch WH, McAdam KP. Amyloid cardiomyopathy: characterization by a distinctive voltage/mass relation. Am J Cardiol. 1982;49:9-13
 11. Maceira AM, Prasad SK, Hawkins PN, Roughton M, Pennell DJ. Cardiovascular magnetic resonance and prognosis in cardiac amyloidosis. J Cardiovasc Magn Reson. 2008;10:54 

Titel: Aanbevelingen Nucleaire Geneeskunde 2007

Eindredactie: Drs. P.C. Barneveld - Dr. P van Urk

ISBN: 978-90-78876-01-4

Uitgever: Kloosterhof acquisitie services - uitgeverij

Omvang 480 pagina's

Uitvoering garengenaaid

Prijs € 53,- (leden NVNG exclusief verzendkosten)
€ 74,20 (exclusief verzendkosten)

Stuur uw aanvraag naar info@kloosterhof.nl

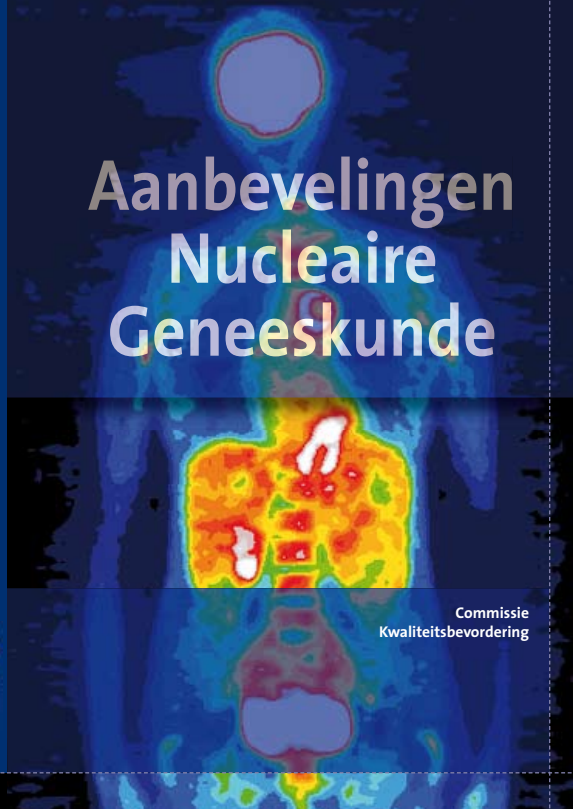
Deze Aanbevelingen beschrijven vrijwel alle gangbare patiëntonderzoeken en therapieën die op een afdeling Nucleaire Geneeskunde kunnen worden uitgevoerd. De nadruk ligt op de kwaliteit van de procedures en de daarvoor noodzakelijke apparatuur en radiofarmaca.

Het merendeel van de patiëntonderzoeken betreft diagnostische verrichtingen, maar ook therapeutische handelingen met behulp van radioactieve stoffen worden besproken. Verder komen in de Aanbevelingen fysische en farmaceutische aspecten aan de orde.

Het boek is vooral bedoeld als handboek en naslagwerk op een afdeling Nucleaire Geneeskunde en voor degenen die nog in opleiding zijn. Het is echter geen leerboek en het is niet gebaseerd op evidence based medicine methodiek omdat daarvoor te weinig tijd en onderzoek beschikbaar was.

De in deze Aanbevelingen opgenomen protocollen zijn onder regie van de Commissie Kwaliteitsbevordering van de Nederlandse Vereniging voor Nucleaire Geneeskunde (NVNG) opgesteld door leden van de NVNG met medewerking van de NVKF (Nederlandse Vereniging voor Klinische Fysica) en NVZA (Nederlandse Vereniging voor Ziekenhuisapothekers).

De Aanbevelingen werden vastgesteld op een algemene ledenvergadering van de NVNG. Met deze publicatie worden de huidige inzichten binnen de Nucleaire Geneeskunde met betrekking tot kwalitatief goede patiëntenzorg vastgelegd.



Aanbevelingen Nucleaire Geneeskunde 2007

Aanbevelingen Nucleaire Geneeskunde

Commissie Kwaliteitsbevordering

Nuclear imaging in cardiac amyloidosis: the role of ^{123}I -MIBG

W. Noordzij, MD¹
H.J. Verberne, MD, PhD²
R.H.J.A. Slart, MD, PhD¹

¹ Department of Nuclear Medicine & Molecular Imaging, University Medical Center Groningen, Groningen, The Netherlands.

² Department of Nuclear Medicine, Academic Medical Center, University of Amsterdam, Amsterdam, The Netherlands.

Abstract

Noordzij W, Verberne HJ, Slart RHJA. Nuclear imaging in cardiac amyloidosis: the role of ^{123}I -MIBG

Cardiac amyloidosis is a restrictive cardiomyopathy with potential fatal consequences due to amyloid depositions in the myocardial tissue, but also infiltration in the nerve conduction system. The prognosis is poor. Early detection of cardiac involvement has become of major clinical interest, because its occurrence and severity may influence the choice of treatment. Within nuclear medicine a technique was introduced to detect myocardial sympathetic denervation in patients with amyloidosis. The use of iodine-123 labelled meta-iodobenzylguanidine (^{123}I -MIBG), a result of chemical modification of an analogue of norepinephrine, is well established in patients with heart failure, and plays an important role in cardiac amyloidosis. It is stored in vesicles in the sympathetic nerve terminals and not catabolised like norepinephrine. Decreased heart-to-mediastinum ratios (HMR) on late planar images and increased wash-out rates indicate cardiac sympathetic denervation and are associated with poor prognosis. Single photon emission computed tomography (SPECT) provides additional information and has advantages for evaluating abnormalities in regional distribution in the myocardium. However, inferior wall defects should be interpreted with caution. Several studies point out the value of HMR and wash-out rate as parameters for sympathetic innervation abnormalities in cardiac amyloidosis. It is a highly reproducible and an easily accessible method, making it not easily substituted by other modalities. However, there is an increasing urge for standardisation of image acquisition, collimator choice and analysis of quantitative values, such as HMR and wash-out rate. The use of positron emission tomography in cardiac amyloidosis has not been reported.

Tijdschr Nucl Geneesk 2011; 33(4):799-805

Introduction

Cardiac amyloidosis is a rare disorder. Almost every type of amyloidosis can be complicated with cardiac involvement.

The prevalence of this cardiac involvement varies widely among the different types. About 50% of all amyloidosis patients experience some cardiac manifestations related to the disease. It is frequent in primary (immunoglobulin light chain, or AL type) and familial (transthyretin, or ATTR type, which leads to familial amyloidotic polyneuropathy (FAP)), but uncommon in secondary (serum amyloid A protein, or AA type) amyloidosis. Up to 90% of all AL amyloidosis patients have cardiac manifestation, however only 5% have clinically isolated cardiac disease. Cardiac involvement eventually leads to a type of cardiomyopathy that does not present with ventricular hypertrophy or dilatation. Instead, the ventricular filling is restricted, resulting in symptoms and signs of heart failure. Heart failure occurs in at least 25% of all patients (1). In ATTR type amyloidosis, however, cardiac involvement leads less frequently to systolic dysfunction and heart failure. Furthermore symptoms are milder and progression is slower, when compared to AL amyloidosis. Restrictions in ventricular filling result in persistently elevated venous pressures, liver enlargement, ascites and oedema. Consequently, patients usually suffer from dyspnoea and fatigue. Amyloidosis is the most common cause of this so-called 'restrictive cardiomyopathy'.

The diagnosis is based on histological finding from endomyocardial biopsy, especially when amyloidosis is limited to the heart. Four samples provide a sensitivity of nearly 100%, and a negative biopsy almost always rules out the disease. But, this gold standard is not performed in every patient. Amyloid deposition in blood vessels makes them fragile and gives patient an increased risk of bleeding. Different imaging modalities are used for haemodynamics and to determine prognosis. Correct and early recognition of cardiac amyloidosis and its various types remains a challenge. The prognosis of cardiac amyloidosis is worse than other forms of the disease. The disease can be rapidly progressive and, in patients with ventricular septum thickness >15 mm, left ventricular ejection fraction (LVEF) <40% and symptoms of heart failure, the median survival may be less than 6 months (2). No specific treatment exists for cardiac amyloidosis or restrictive cardiomyopathy. However, heart failure should be treated and cardiac transplantation should be considered in severe cases. Therefore early detection of cardiac involvement is essential as the occurrence and

severity of cardiac amyloidosis may influence the limited choice of treatment options and more importantly affects prognosis.

The role of non-scintigraphic imaging modalities

The role of non-scintigraphic imaging modalities to assess potential cardiac amyloidosis is discussed in detail elsewhere in this issue by Groenink et al. In short transthoracic echocardiography and cardiac magnetic resonance imaging with gadolinium enhancement are discussed.

Transthoracic echocardiography plays an important role in the evaluation of cardiac manifestation of amyloidosis. Nowadays it is the modality of choice for the evaluation of amyloid deposition in the heart (3). The most common finding is left ventricular wall thickening due to amyloid deposition in the myocardium. This is often associated with right ventricular wall thickening, diffuse valvular infiltration, dilated atria and pericardial effusion (4). Although echocardiography plays a major role, the diagnosis of cardiac amyloidosis is often only possible when the disease reaches a relatively advanced stage, where irreversible functional and structural myocardial changes have occurred. If echocardiography is inconclusive, cardiac magnetic resonance imaging with gadolinium enhancement might be useful. Gadolinium is an extracellular fluid tracer which accumulates in expanded interstitial place. Usually, in the intact myocardium, the distribution of gadolinium is very low and therefore gadolinium enhancement is absent. However, in case of myocardial interstitial space expansion, such as in amyloidosis due to extracellular amyloid infiltration, gadolinium concentration may increase within myocardial tissue. Global subendocardial late gadolinium enhancement can be found in approximately two-thirds of patients with systemic amyloidosis (5). But also for this modality, the utility in early cardiac involvement is unclear.

The role of scintigraphic imaging modalities

Scintigraphy, using labelled serum amyloid P component (SAP), provides not only information on different organ distributions, but serial scans can provide evidence of progression and regression of the disease (6). Unfortunately, these SAP-scans are unsuitable for detecting amyloid depositions in the myocardium, due to movement, blood-pool content and tracer uptake in the spleen.

Myocardial adrenergic denervation, using iodine-123 metaiodobenzylguanidine (¹²³I-MIBG) has been shown in patients with amyloidosis (7-9). Indirectly, MIBG visualises the effect of amyloid deposition in the myocardium. This technique might be able to detect early cardiac denervation before actual heart failure occurs. The purpose of this review is to discuss the role of ¹²³I-MIBG in the assessment of cardiac amyloidosis.

General cardiac innervation

The autonomous nerve system (ANS) consists of fibres that innervate involuntary (smooth) muscle, modified cardiac muscle (the intrinsic stimulating and conducting tissue of

the heart), and glands. The efferent nerve fibres and ganglia of the ANS are organized into two systems: sympathetic and parasympathetic system. The functional distinction between the two subdivisions of the ANS can be related to the differences in the neurotransmitters that are involved: norepinephrine by the sympathetic system and acetylcholine by the parasympathetic system.

Sympathetic nervous system

The cell bodies of the preganglionic neurons of the sympathetic system are located in a part of the gray matter expanding between the first thoracic and third lumbar segments of the spinal cord. The cell bodies of the postganglionic neurons occur in two locations: the paravertebral and prevertebral ganglia. Paravertebral ganglia are linked to form right and left sympathetic trunks on each side of the vertebral column. The prevertebral ganglia are in the plexus that surround the origins of the main branches of the abdominal aorta. Postganglionic sympathetic fibres destined for the viscera of the thoracic cavity (e.g. the heart) pass through the cardiopulmonary splanchnic nerves to enter the cardiac plexuses. These fibres end in the SA and AV nodes and in relation to the termination of parasympathetic fibres on the coronary arteries. They interact with postsynaptic β -adrenergic receptor on the cell membrane of myocytes through norepinephrine. Norepinephrine is produced in the presynaptic nerve terminals through multiple biochemical processes and ultimately stored at high concentrations in presynaptic vesicles. After a stimulus, these vesicles release norepinephrine into the synaptic cleft by exocytosis and subsequently norepinephrine binds to the β -adrenergic receptors, resulting in cardiac stimulatory effects. Postganglionic parasympathetic fibres, on the other hand, interact with muscarinic receptors in the cardiac cell membrane through acetylcholine. The onset of the cardiac response to sympathetic stimulation is slow for two main reasons. First, norepinephrine appears to be released from the cardiac sympathetic nerve terminals at a relatively slow rate. Second, the effects of the neurally released norepinephrine on the heart are mediated mainly via a relatively slow second messenger system, the adenylyl cyclase system. This system eventually varies calcium conductance of the cell membrane. Hence, sympathetic activity alters heart rate (and AV conduction) much more slowly than does parasympathetic activity.

Consequences of impaired sympathetic innervation in cardiac amyloidosis

Cardiac amyloidosis is a form of restrictive cardiomyopathy, due to the progressive deposition of amyloid fibrils in myocardium, and direct depression of diastolic function. Usually this occurs in both left and right ventricles, causing biventricular heart failure. But cardiac amyloidosis is often presented as severe right-sided heart failure only. Eventually, systolic dysfunction leads to congestive heart failure. This

occurs only in late stages because the LVEF is (nearly) normal until late in disease. Symptoms caused by heart failure are dyspnoea, orthopnoea, peripheral oedema and sometimes, in late stages of the disease, ascites. Amyloid depositions in the atria can cause atrial fibrillation (AF) with gives complaints of fast and irregular heart action. Also, AF is associated with the development of thromboembolisms. A poor LVEF and amyloid infiltration can contribute to the complications of embolisms (e.g. cerebral infarction). Furthermore, microvascular disease does not only give complaints of angina due to myocardial ischemia (10), it also often leads to syncope (11). The development of syncope is probably based on multiple factors. First, it may be a consequence of bradycardia due to amyloid infiltration in the conduction system. Second, a syncope can be a result of sustained ventricular tachycardia, hypotension due to autonomic neuropathy or sudden cardiac death due to electromechanical dissociation rather than ventricular dysrhythmia (12).

General dynamics and use of MIBG

Meta-iodobenzylguanidine (MIBG) is a result of chemical modification of the false neurotransmitter analogue guanethidine, and therefore analogue of norepinephrine. The uptake of MIBG occurs similar to uptake of norepinephrine: predominantly through a specific uptake system ("uptake-1") and to a much lesser extent by a non-specific uptake system (passive diffusion, "uptake-2"). Eventually, like norepinephrine, MIBG is stored in granules of presynaptic nerve terminals (figure 1). In a normal situation, unlike norepinephrine, MIBG is not bound to receptors on the myocyte membrane and thus

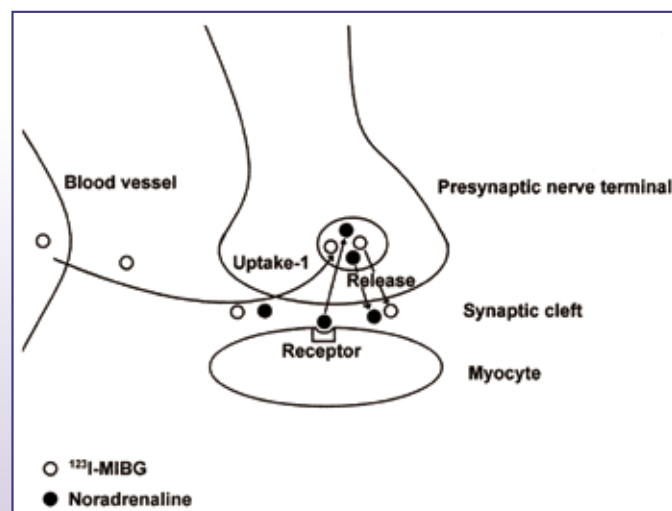


Figure 1. Schematic representation of the MIBG uptake mechanism. Adapted from Scott LA, Kench PL. Cardiac autonomic neuropathy in the diabetic patient: does ^{123}I -MIBG imaging have a role to play in early diagnosis? *J Nucl Med Technol.* 2004;32:66-71.

not catabolised by monoamine oxidase (MOA) Therefore, it is retained in these granules (13, 14).

At present, planar (anterior view, during 3-5 minutes) and sometimes single photon emission computed tomography (SPECT) images are made 15 minutes as well as 3 to 5 hours after administration using 111-300 (mean 185) MBq ^{123}I -MIBG. A semi-quantitative method of heart mediastinum ratio (HMR) is used to determine global uptake on the planar images. It is believed that the early images show interstitial uptake, and late images represent actual neuronal uptake. The wash-out rate between these images provides additional information and reflects the degree of sympathicotonia (15,16). Although normal values for HMR and wash-out rates seem to vary between age and image acquisition, HMR values less than 1.6 as well as was-out rate >20% seem to be an indication for cardiac denervation (figure 2 and 3) (17).



Figure 2. An example of normal MIBG uptake. HMR on early (left) image 2.50, HMR on late (right) image 2.50, wash-out 0%.



Figure 3. An example of abnormal MIBG uptake. HMR on early (left) image 1.89, HMR on late (right) image 1.37, wash-out 27%.

Use of planar images of MIBG in amyloidosis

The use of MIBG is studied most intensively in patients with familial amyloidotic polyneuropathy (FAP). The first reported case of severe peripheral neuropathy due to FAP in which 111 MBq ^{123}I -MIBG was used, showed no definite myocardial activity in all cardiac regions on neither early (30 minutes post injection (pi)) nor late images (4h pi) (7). In contrast, left ventricular ejection fraction was normal on radionuclide ventriculography, as well as myocardial perfusion using

thallium. But analysis of heart rate variability (HRV) suggested highly damaged vagal and sympathetic activities. Thus, the defects on the MIBG scan were considered to represent impaired cardiac sympathetic nerve endings due to amyloid depositions.

The lack of MIBG uptake in myocardial tissue was also seen in a second case-report (18). In this patient with FAP, a ^{123}I -MIBG scan was performed, which showed no uptake in the heart, indicating severe impairment of cardiac sympathetic function. Also several other investigations were performed, including technetium-99m labelled dimercaptosuccinic acid ($^{99\text{m}}\text{Tc}$ -DMSA), thallium-201 (^{201}Tl) and iodine-123 labelled 15-(p-iodophenyl)-3-(R,S)-methyl-pentadecanoic acid (^{123}I -BMIPP) studies. These studies showed myocardial involvement of amyloidosis ($^{99\text{m}}\text{Tc}$ -DMSA), normal myocardial perfusion (^{201}Tl) and normal fatty acid metabolism (^{123}I -BMIPP) respectively.

In the first clinical trial, 12 patients with FAP were prospectively followed, using ^{123}I -MIBG and comparing it to echocardiography, and ^{201}Tl and $^{99\text{m}}\text{Tc}$ -labeled pyrophosphate ($^{99\text{m}}\text{Tc}$ -PYP) imaging studies (8). All 12 patients suffered from biopsy-proven cardiac amyloidosis. Four mCi (148 MBq) ^{123}I -MIBG was administered and scans were performed 30 minutes and 3h pi. In 8 out of these 12 patients no myocardial localisation of MIBG was found on either the early or the late images. The remaining 4 patients showed only limited uptake in the anterior wall on both early and late images. Four patients had LV wall thickening on echocardiography, with otherwise normal results. There was no significant correlation found between the prevalence of decreased uptake of ^{123}I -MIBG and LV wall thickness and results of $^{99\text{m}}\text{Tc}$ -PYP scans. All 12 patients had normal myocardial perfusion on ^{201}Tl scan. So, in conclusion, patients with FAP were found to have a high incidence of myocardial adrenergic denervation with viable myocardium, which can be found early in cardiac amyloidosis in the absence of clinical apparent heart disease.

In the second clinical trial, 17 patients with FAP were analysed before liver transplantation (9). All patients had biopsy-proven FAP by either specimens from rectal mucosa or peripheral nerves. These patients underwent ^{123}I -MIBG (300 MBq) scanning at 20 minutes and 4h pi, heart rate variability analysis, coronary angiography, radionuclide ventriculography, rest ^{201}Tl scan, echocardiography and measurement of plasma catecholamine levels. MIBG scans were also performed in 12 age-matched control subjects. Planar MIBG images were analysed using HMR and wash-out rate, defined as percent change in activity from early to late images within the LV. All patients had no evidence of coronary artery disease, perfusion defects or diminished LVEF. However, cardiac MIBG uptake was dramatically decreased in FAP patients compared to the age-matched control population, on both early and late images (HMR at 4h: 1.36 ± 0.26 vs. 1.98 ± 0.35 , $p < 0.001$). The wash-out rate was not significantly different. On the other hand, cardiac MIBG uptake at 4h correlated with the severity of

polyneuropathy. In concordance to the results of the former mentioned trial, these patients with FAP had sympathetic denervation as assessed by MIBG imaging, despite normal LV systolic function and myocardial perfusion.

In continuation of these findings a subsequent trial in 31 patients with FAP was performed after liver transplantation (19). The purpose of this study was to evaluate the outcomes of cardiac sympathetic innervation and amyloid infiltration after liver transplantation. Cardiac sympathetic innervation was assessed in the same manner as the study published in 1999 by the same others: 300 MBq ^{123}I -MIBG, scans at 20 minutes and 4h pi, the use of HMR and wash-out rates. A same age-matched control population was used for normal values of HMR and wash-out rate. All patients also underwent rest ^{201}Tl scan, heart-rate variability analysis, echocardiography, and right heart catheterisation. Sympathetic denervation was found in patients before liver transplantation compared to the control population (HMR 1.45 ± 0.29 vs. 1.98 ± 0.35 , $p < 0.001$). After liver transplantation, there was no significant change in global MIBG HMR (1.46 ± 0.28). This may implicate that progression of cardiac sympathetic denervation stops after liver transplantation and that early reinnervation cannot be measured within 2 years after liver transplantation. There was no correlation between age and echocardiographic findings. However, conduction disturbances, ventricular arrhythmias and LV wall thickening were associated with low MIBG uptake and progressed after liver transplantation. This may implicate progression of cardiac amyloid infiltration. Also in this study, low cardiac MIBG uptake was associated with severity of polyneuropathy, which worsened after liver transplantation. The authors conclude that MIBG imaging can provide an objective measurement of cardiac sympathetic innervation, which could help to guide the indications for liver transplantation in patients with early stage of FAP.

Although symptoms and consequences of cardiac amyloid depositions in AL amyloidosis is often more frequent and severe than in FAP (causing more fatal dysfunction), the use MIBG in this type of disease is less intensively studied. In fact only one major study has been performed in which the presence of impaired myocardial sympathetic innervation was related to clinical autonomic abnormalities and congestive heart failure in AL amyloidosis (20). In this study 25 patients with biopsy-proven cardiac manifestation of AL amyloidosis, underwent autonomic function tests, echocardiography, heart rate variability analysis and ^{123}I -MIBG scanning. The MIBG scans were performed, using 111 MBq ^{123}I -MIBG, at 30 minutes and 3h pi. Myocardial uptake and wash-out rates were calculated using HMR. Furthermore, 20 of 25 patients underwent rest ^{201}Tl scan for myocardial perfusion. Of the 25 patients, 9 suffered from autonomic dysfunction and 16 did not. Five of 9 patients with autonomic dysfunction and 10 of 16 without had congestive heart failure. There was no significant difference in amyloid deposition in the right ventricle (RV) or LV wall thickness based on echocardiographic

results. None of the patients had myocardial perfusion defects. In patients with autonomic dysfunction, HMR (1.37 ± 0.05 vs. 1.66 ± 0.09 after 30 minutes, $p < 0.001$ and 1.29 ± 0.05 vs. 1.53 ± 0.06 after 3h, $p < 0.001$) and wash-out rates ($30.8 \pm 4.0\%$ vs. $41.5 \pm 4.8\%$) were significantly decreased compared to those without autonomic dysfunction. In both groups, HMR was significantly decreased and wash-out rate increased in patients with heart failure (10 of 16 without autonomic dysfunction, 5 of 9 with autonomic symptoms). Therefore, myocardial uptake and turnover of MIBG in patients with AL amyloidosis are heterogeneous and dependant on the presence of congestive heart failure and cardiac autonomic dysfunction.

To the best of our knowledge there have not been studies performed in which patients with AA amyloidosis were scanned using ^{123}I -MIBG for the detection of cardiac denervation.

Discussion

Amyloidosis is a systemic disease that can affect multiple organs and has a poor prognosis. The value of identification of cardiac involvement is very high, because the high rates of arrhythmia, rapid deterioration and sudden cardiac death. Diagnostic imaging is important for decision making concerning ICD implants and heart transplantation. This review focussed on the use of ^{123}I -MIBG, being the best literature based imaging modality for cardiac sympathetic denervation. Myocardial defects in MIBG activity correlate with impaired cardiac sympathetic function due to amyloid depositions. This can be identified early in the disease. Furthermore, lower HMR and higher was-out rates correspond to severity of the disease.

The use of HMR and wash-out rates is also used in patients with other forms of heart failure. These studies show that decreased HMR on late images and increased wash-out rates are related to an increase in systolic dysfunction. Lower MIBG uptake was even reported to indicate poorer prognosis in patients with heart failure. In the recently published ADMIRE-HF (AndreView Myocardial for Risk Evaluation in Heart Failure, AndreView = ^{123}I -MIBG) study, 961 patients with NYHA (New York Heart Association) functional class II/III and LVEF $\leq 35\%$ were followed during 2 years. All underwent ^{123}I -MIBG (early and late) and myocardial perfusion imaging. The primary goal was to relate HMR < 1.60 to a composite end point, including progression of NYHA functional class (worsening of heart failure), potentially life-threatening arrhythmic event or cardiac death. Cumulative 2-year event rate of the composite end point was significantly lower in patients with HMR ≥ 1.60 (15% vs. 38%, $p < 0.001$) (21). Imaging with ^{123}I -MIBG seemed to be of independent prognostic value in patients with heart failure. In a subsequent multivariate analysis HMR was reported to be an independent predictor of both cardiac and all-cause death (22).

As mentioned before, normal values for HMR and wash-out

rates seem to vary, not only between different ages but also between different image acquisitions protocols. Concerning the image acquisition, the most important factor seems to be the collimator used for MIBG imaging. In addition to the 159 keV peak which is used for imaging, ^{123}I -MIBG also has a 529 keV peak. Collimators exhibit different degree of scattering by gamma rays of 529 keV, so that these rays mix in with the data from 159 keV rays. The image quality is impaired by these scattered rays, when using low-energy collimators. A medium energy collimator seem be a solution for this problem, although not every institution will have access to such a collimator (23-25). Other factors causing differences in HMR and wash-out rates are the methods of setting ROI's (especially concerning site, size and form), the moment of late images, the duration of an acquisition and the correction for decay (26,27). On the other hand, according to blood activity, the slope of vascular clearance curves or estimate renal function (eGFR), variations in the quantity of vascular structures in the mediastinum and the rate of renal clearance of ^{123}I -MIBG from the blood pool do not seem to contribute to increased interindividual variation in uptake on either early or late images (28). In a recent proposal for standardization of ^{123}I -MIBG cardiac sympathetic imaging, evidence based recommendations for, among others, image acquisition, collimator choice and data analysis are enlisted for routine clinical application. Standardization of MIBG cardiac imaging should contribute to its clinical applicability and integration into current nuclear cardiology practice (27,29).

The focus of this review was the role of planar images of ^{123}I -MIBG in cardiac amyloidosis, and their place in the evaluation of cardiac sympathetic function. The acquisition of SPECT has also been reported, and has advantages for evaluating abnormalities in regional distribution in the myocardium (7-9,18-20). Usually, the reconstructed data are displayed in 3 planes (short axis, horizontal long axis and vertical long axis), which is similar to that used in myocardial perfusion SPECT. Various patterns of distribution of myocardial MIBG accumulation are reported. In 16 patients with AL amyloidosis who had no autonomic dysfunction, only 2 had a homogeneous distribution of MIBG (20). The reduced uptake in the other patients was mainly localised in inferior and inferoposterior wall segments. Of the 9 with patients with autonomic dysfunction, 5 had only MIBG accumulation in the anterior wall. The reduced uptake and focal defects in the inferior wall were also reported in the patients in pre liver transplantation setting (9). These inferior wall defects should be interpreted carefully, hence substantial MIBG uptake in the liver may overlap the myocardial inferoposterior wall. In addition, even in normal cases, MIBG uptake is relatively low in the inferior wall, especially in the elderly (30-32). Analogue to myocardial perfusion imaging, the use of polar maps can be used to calculate extent and severity scores for segmental defects. Comparing perfusion imaging to MIBG distribution gives extra information about the presence

or absence of mismatch patterns. Myocardial ischemia or infarction disrupts sympathetic transmission, which may lead to denervation of a region larger than affected by ischemia only. Furthermore, sympathetic nervous tissue is more sensitive to ischemia than myocytes. The presence of innervation/perfusion imaging mismatches correlates with electrophysiological abnormalities and increasing inducibility of potential lethal dysrhythmia (33,34).

Also various positron emission tomography (PET) analogues of norepinephrine are under investigation (35). These are even more similar to norepinephrine than MIBG and contain advantages for imaging. ^{11}C -meta-hydroxy-ephedrine (^{11}C -mHED) is the most commonly used PET tracer. It has a higher sensitivity for the uptake-1 mechanism than ^{123}I -MIBG, and is not linked to the uptake-2 mechanism, which might implicate a better differentiation between innervated and denervated myocardium. In a group of 21 patients with left ventricular dysfunction who underwent both ^{123}I -MIBG and ^{11}C -mHED imaging, the correlation between MIBG wash-out rate and mHED wash-out rate was poor ($r=0.57$). But the defect size on both early ($r=0.94$) and late images ($r=0.88$) was related more closely between these two modalities. Therefore ^{11}C -mHED seems to have advantages over ^{123}I -MIBG in regional abnormalities (36). Other ^{11}C labelled tracers like ^{11}C -phenethylguanidine are currently under investigation. Promising results from a study using rats show that ^{11}C -phenethylguanidine and its analogues are transporter slower than MIBG and mHED and therefore might provide more accurate measurement of cardiac nerve density (37). To the best of our knowledge no PET tracers have been used to visualise cardiac denervation in patients with cardiac manifestation of amyloidosis.

Conclusions

The use of ^{123}I -MIBG in cardiac sympathetic denervation is well established. Several studies point out the value of HMR and wash-out rate as parameters for sympathetic innervation abnormalities in cardiac amyloidosis. It is a highly reproducible and an easily accessible method, making it not easily substituted by other modalities. However, there is an increasing urge for standardisation of quantitative values, such as HMR and wash-out rate.

List of references

- Dubrey SW, Cha K, Anderson J et al. The clinical features of immunoglobulin light-chain (AL) amyloidosis with heart involvement. *QJM*. 1998;91:141–57
- Ronsyn M, Shivalkar B, Vrints CJM. Cardiac amyloidosis in full glory. *Heart*. 2011;97:720
- Falk RH, Plehn J, Deering T et al. Sensitivity and specificity of the echocardiographic features of cardiac amyloidosis. *Am J Cardiol*. 1987;59:418–22
- Klein AL, Hatle LK, Taliervo CP et al. Serial Doppler echocardiographic follow-up of left ventricular diastolic function in cardiac amyloidosis. *J Am Coll Cardiol*. 1990;16:1135–41
- Maceira AM, Joshi J, Prasad SK et al. Cardiovascular magnetic resonance in cardiac amyloidosis. *Circulation*. 2005;111:186–93
- Hawkins PN. Serum amyloid P component scintigraphy for diagnosis and monitoring amyloidosis. *Curr Opin Nephrol Hypertens*. 2002;11:649–55
- Nakata T, Shimamoto K, Yonekura S et al. Cardiac sympathetic denervation in transthyretin-related familial amyloidotic polyneuropathy: detection with iodine-123-MIBG. *J Nucl Med*. 1995;36:1040–2
- Tanaka M, Hongo M, Kinoshita O et al. Iodine-123 metaiodobenzylguanidine scintigraphic assessment of myocardial sympathetic innervation in patients with familial amyloid polyneuropathy. *J Am Coll Cardiol*. 1997;29:168–74
- Delahaye N, Dinanian S, Slama MS et al. Cardiac sympathetic denervation in familial amyloid polyneuropathy assessed by iodine-123 metaiodobenzylguanidine scintigraphy and heart rate variability. *Eur J Nucl Med*. 1999;26:416–24
- Mueller PS, Edwards WD, Gertz MA. Symptomatic ischemic heart disease resulting from obstructive intramural coronary amyloidosis. *Am J Med*. 2000;109:181–88
- Chamarthi B, Dubrey SW, Cha K et al. Features and prognosis of exertional syncope in light-chain associated AL cardiac amyloidosis. *Am J Cardiol*. 1997;80:1242–45
- Falk RH, Rubinow A, Cohen AS. Cardiac arrhythmias in systemic amyloidosis: correlation with echocardiographic abnormalities. *J Am Coll Cardiol*. 1984;3:107–13
- Kline RC, Swanson DP, Wieland DM et al. Myocardial imaging in man with I-123 Metaiodobenzylguanidine. *J Nucl Med*. 1981;22:129–32
- Wieland DM, Brown LE, Rogers WL et al. Myocardial imaging with a radioiodinated norepinephrine storage analog. *J Nucl Med*. 1981;22:22–31
- Somsen GA, Verberne HJ, Fleury E et al. Normal values and within-subject variability of cardiac I-123 MIBG scintigraphy in healthy individuals: Implications for clinical studies. *J Nucl Cardiol*. 2004;11:126–33
- Ogita H, Shimonagata T, Fukunami M et al. Prognostic significance of cardiac 123I metaiodobenzylguanidine imaging for mortality and morbidity in patients with chronic heart failure: A prospective study. *Heart*. 2001;86:656–60
- Jacobson AF, Lombard J, Banerjee G et al. 123I-MIBG scintigraphy to predict risk for adverse cardiac outcomes in heart failure patients: Design of two prospective multicenter international trials ADMIRE-HF study. *J Nucl Cardiol*. 2009;16:113–21
- Arbab AS, Koizumi K, Toyama K et al. Scan findings of various myocardial SPECT agents in a case of amyloid polyneuropathy with suspected myocardial involvement. *Ann Nucl Med*. 1997;11:139–41
- Delahaye N, Rouzet F, Sarda L et al. Impact of liver transplantation on cardiac autonomic denervation in familial amyloid polyneuropathy. *Medicine*. 2006;85:229–38
- Hongo M, Urushibata K, Kai R et al. Iodine-123 metaiodobenzylguanidine scintigraphic analysis of myocardial sympathetic innervation in patients with AL (primary) amyloidosis.

- Am Heart J. 2002;144:122-9
21. Jacobson AF, Senior R, Cerqueira MD et al. Myocardial iodine-123 meta-iodobenzylguanidine imaging and cardiac events in heart failure: Results of the prospective ADMIRE-HF (AdreView myocardial imaging for risk evaluation in heart failure) study. *J Am Coll Cardiol.* 2010;55:2212-21
 22. Travin M, Anathasubramaniam K, Henzlova MJ et al. Imaging of myocardial sympathetic innervation for prediction of cardiac and all-cause mortality in heart failure: Analysis from the ADMIRE-HF trial. *Circulation.* 2009;120:S350
 23. Verberne HJ, Feenstra C, de Jong WM et al. Influence of collimator choice and simulated clinical conditions on 123I-MIBG heart/mediastinum ratios: a phantom study. *Eur J Nucl Med Mol Imaging.* 2005;32:1100-7
 24. Dobbeleir AA, Hambye AS, Franken PR. Influence of high energy photons on the spectrum of iodine-123 with low- and medium-energy collimators: consequences for imaging with 123I labelled compounds in clinical practice. *Eur J Nucl Med.* 1999;26:655-8
 25. Inoue Y, Suzuki A, Shirouzu I et al. Effect of collimator choice on quantitative assessment of cardiac iodine 123 MIBG uptake. *J Nucl Cardiol.* 2003;10:623-32
 26. Yamashino S, Yamazaki J. Neuronal imaging using SPECT. *Eur J Nucl Med Mol Imaging.* 2007;34:S62-73
 27. Verberne HJ, Habraken JB, van Eck-Smit BL et al. Variations in 123I-metaiodobenzylguanidine (MIBG) late heart mediastinal ratios in chronic heart failure: a need for standardisation and validation. *Eur J Nucl Med Mol Imaging.* 2008;35:547-53
 28. Verberne HJ, Verschure DO, Somsen GA et al. Vascular time-activity variation in patients undergoing 123I-MIBG myocardial scintigraphy: implications for quantification of cardiac and mediastinal uptake. *Eur J Nucl Med Mol Imaging.* 2011;38:1132-8
 29. Flotats A, Carrió I, Agostini D et al. Proposal for standardization of 123I-metaiodobenzylguanidine (MIBG) cardiac sympathetic imaging by the EANM Cardiovascular Committee and the European Council of Nuclear Cardiology. *Eur J Nucl Med Mol Imaging.* 2010;37:1802-12
 30. Gill JS, Hunter GJ, Gane G et al. Heterogeneity of the human myocardial sympathetic innervation: in vivo demonstration by iodine 123-labeled meta-iodobenzylguanidine scintigraphy. *Am Heart J.* 1993;126:390-8
 31. Estorch M, Carrio I, Berna L et al. Myocardial iodine-labeled metaiodobenzylguanidine 123 uptake relates to age. *J Nucl Cardiol.* 1995;2:126-32
 32. Tsuchimochi S, Tamaki N, Tadamura E et al. Age and gender differences in normal myocardial adrenergic neuronal function evaluated by iodine-123-MIBG imaging. *J Nucl Med.* 1995;36:969-74
 33. Simões MV, Barthel P, Matsunari I et al. Presence of sympathetically denervated but viable myocardium and its electrophysiologic correlates after early revascularised, acute myocardial infarction. *Eur Heart J.* 2004;25:551-7
 34. Sasano T, Abraham R, Chang KC et al. Abnormal sympathetic innervation of viable myocardium and the substrate of ventricular tachycardia after myocardial infarction. *J Am Coll Cardiol.* 2008;51:2266-75
 35. Bengel FM, Schwaiger M. Assessment of cardiac sympathetic neuronal function using PET imaging. *J Nucl Cardiol.* 2004;11:603-16
 36. Matsunari I, Aoki H, Nomura Y et al. Iodine-123 metaiodobenzylguanidine imaging and carbon-11 hydroxyephedrine positron emission tomography compared in patients with left ventricular dysfunction. *Circ Cardiovasc Imaging.* 2010;3:595-603
 37. Raffel DM, Jung YW, Gildersleeve DL et al. Radiolabeled phenethylguanidines: novel imaging agents for cardiac sympathetic neurons and adrenergic tumors. *J Med Chem.* 2007;50:2078-88 

Oldelft Benelux Medical Solutions

...Het hele spectrum aan gamma camera's...



AnyScan



X-Ring-R



CardioDESK



Cardio-C



X-Ring 4R



Nucline TH

...van kleine enkelkops
tot geavanceerde
SPECT-PET-CT combinaties.

Met [Mediso](#) levert Oldelft Benelux het hele spectrum aan gamma camera's; van kleine enkelkops, tot geavanceerde SPECT-CT-PET combinaties.



Oldelft Benelux heeft reeds meer dan 80 jaar ervaring in de verkoop en service van diagnostische apparatuur en innovatieve healthcare ICT systemen. Zij heeft zich ontwikkeld van producent van apparatuur naar System Integrator en Service Provider voor ziekenhuizen en zorginstellingen.

Voor meer informatie omtrent de [Mediso](#) oplossingen kunt u contact opnemen met uw accountmanager, of stuur een e-mail naar info@oldelftbenelux.nl.

Development and evaluation of agents for targeting visceral amyloid

J.S. Wall, PhD^{1,2}
A. Solomon, MD²
S.J. Kennel, PhD^{1,2}

Departments of Radiology¹ and Medicine², University of Tennessee Graduate School of Medicine, 1924 Alcoa Highway, Knoxville, TN 37920, USA

Abstract

Wall JS, Solomon A, Kennel SJ. Development and evaluation of agents for targeting visceral amyloid

Visceral amyloidosis is a rare disease characterized by the deposition in organs and tissues of protein fibrils, heparan sulfate proteoglycans as well as serum amyloid P component and other serum proteins. Imaging these pathologic deposits aids in the clinical management of patients with amyloidosis. Whole body scintigraphic imaging of amyloid load as well as organ-specific anatomic imaging provides information that can inform prognosis and can be used to monitor disease progression or response to therapy. These capabilities are limited in the USA, which has led to our development and evaluation of two new reagents that specifically target amyloid *in vivo* and have been used to image visceral deposits in mice and patients with AL amyloidosis. The fibril-reactive mAb 11-1F4, when labeled with iodine-124 was shown to bind AL amyloid in patients by using PET/CT imaging. These studies were performed to support the evaluation of this reagent as a novel immunotherapy for AL patients. In addition, we have identified a heparin-binding peptide that co-localizes with murine AA amyloid *in vivo* and can be used to image the deposits. The interaction of this peptide, designated p5, with amyloid is dependent on the net positive charge and truncated forms that would be more desirable as clinical imaging agents were found to be significantly less efficient for amyloid imaging. The development and positive preclinical validation of these two reagents offers potential new therapeutic and diagnostic tools for patients with these devastating diseases.

Tijdschr Nucl Geneesk 2011; 33(4):807-814

Introduction

Amyloidosis is a fatal protein-folding disorder characterized by the formation of well-structured protein aggregates that deposit in organs and tissues in conjunction with serum amyloid P component (SAP) and heparan sulfate proteoglycans (HSPG) (1-7). The unrelenting accumulation of amyloid invariably leads to organ dysfunction and severe morbidity or death. Amyloid can affect any organ or tissue

but the kidneys, pancreas, liver, spleen, nervous tissue and heart constitute the major sites of deposition in patients with familial or sporadic forms of amyloid disease. Although varying in etiology and site of deposition, the amyloid deposits share remarkable structural homogeneity consisting of unbranched fibrils of ~ 10 nm in diameter and comprising proteins that adopt a cross- β pleated sheet secondary structure as evidenced by X-ray diffraction and nuclear magnetic resonance (NMR) (8, 9). The deposits can be cerebral, as in patients with Alzheimer's, Huntington's or prion diseases, or they can involve visceral organs as seen in patients with light chain (AL) amyloidosis, reactive (AA) amyloidosis and senile systemic amyloidosis (transthyretin amyloid; ATTR). Furthermore, deposits may be localized or systemic, in which the precursor protein is produced locally (at the site of deposition) or circulates in the blood stream, respectively (10). The peripheral amyloidoses are orphan disorders but account for more than 5,000 new patients annually in the USA alone.

Currently, in the USA, there are no reliable methods to document the extent, the progression, or the resolution of visceral amyloid deposits in patients. To this end, we have, over the last decade, developed amyloid-reactive antibody and peptide agents for imaging visceral amyloid deposits that we anticipate will provide a non-invasive, quantitative, objective method to assist in diagnosis and prognostication. These quantitative, non-invasive measurements can also provide valuable insights into the patient response to anti-amyloid therapies. Before discussing our progress in this field we will briefly describe the important role that imaging can play and many of the techniques that are currently employed to study patients with visceral amyloidosis.

Amyloidosis is an "anatomic" pathology that, unlike the solid tumors associated with cancer that can be detected by functional imaging such as positron emission tomography (PET), has no metabolic or "functional" features, other than expansion of the deposits. Thus, standard clinical anatomical imaging modalities, magnetic resonance imaging (MRI), X-ray, computed tomography (CT) and ultrasound (US), can be used to visualize relatively large amyloid deposits in organs and tissues (11, 12). However, more often than not, it is the malformation of organ architecture, caused by the amyloid mass, that is visualized e.g. thickening of the intraventricular septum of the heart, rather than the actual

amyloid deposits. Therefore, although anatomic imaging of patients with peripheral amyloidosis is generally not diagnostic, it can assist in guiding biopsies, visualizing rare tumor-like amyloid masses, and providing prognostic indicators in patients with cardiac amyloidosis. With the advent of dual-modality imaging capabilities such as PET/CT, SPECT/CT and now PET/MRI, radiolabelled, amyloid-specific imaging agents can provide molecular insights to complement the high resolution anatomical imaging thereby providing unparalleled visualization of the amyloid as well as its pathologic sequelae.

Whole body planar scintigraphy or single photon emission tomography (SPECT) using iodine-123 (^{123}I)-labelled SAP has been used for this purpose in Europe for more than two decades (13-16). SAP scintigraphy provides images of amyloid load that can be used to complement routine diagnosis by histochemical analysis of tissue biopsies, to aid in prognostication and diagnosis, and to document response to therapy (17, 18). Although ^{123}I -SAP imaging is the most common imaging technique for the detection of amyloid in the peripheral organs, radiotracers such as technetium-99m ($^{99\text{m}}\text{Tc}$)-aprotinin and $^{99\text{m}}\text{Tc}$ -3,3-diphosphono-1,2-propanodicarboxylic acid (DPD) have also been used and have proven particularly effective for imaging cardiac amyloid deposits (19-23). Radiolabelled SAP is the gold standard tracer for clinical imaging of visceral amyloidosis; however, it has not been approved by the US Food and Drug Administration due to the human plasma source of this protein. Therefore, alternative techniques are required to document, non-invasively and longitudinally, the whole body burden and organ distribution of peripheral amyloid.

The important role of imaging in the development of the therapeutic monoclonal antibody 11-1F4

The monoclonal antibody (mAb) 11-1F4 was generated using heat and acid denatured $\kappa 4$ immunoglobulin light chain protein LEN as an immunogen (24). This antibody bound to both AL κ and λ amyloid fibrils but did not react with free light chain proteins in solution as shown by enzyme-linked immunoassay. MAb 11-1F4 was later shown to react selectively with a neo-epitope formed at the N-terminus of immunoglobulin light chain proteins that adopt a non-native folding pattern when in amyloid fibrils (25-27). Light chains folded properly as in circulation or associated with heavy chains in the form of antibodies do not bind to mAb 11-1F4. Since 11-1F4 mAb binds to amyloid fibrils, and therefore may have opsonising activity, it presented potential as an immunotherapeutic agent for patients with AL κ or AL λ amyloidosis. Due to the lack of an experimental animal model of AL amyloidosis and the scant reports of this disease occurring naturally in non-laboratory animals, we developed a murine model of human "amyloidoma" in which to test the therapeutic potential of 11-1F4 (28, 29). In this model human AL amyloid, extracted from autopsy-derived liver or spleen tissues, is injected subcutaneously (sc) between the scapulae of Balb/c mice, where it becomes vascularised within 7 days

post injection (figure 1A-C). Remarkably, when these mice were administered with 11-1F4 mAb intravenously, the rate of dissolution of the "amyloidoma" was dramatically increased. Further data indicated that the removal of the amyloid was dependent on an antibody-mediated cellular process, involving opsonisation of the amyloid by the 11-1F4 mAb (28). To test whether the 11-1F4 mAb was indeed localizing with the sc amyloidoma, we used small animal imaging techniques

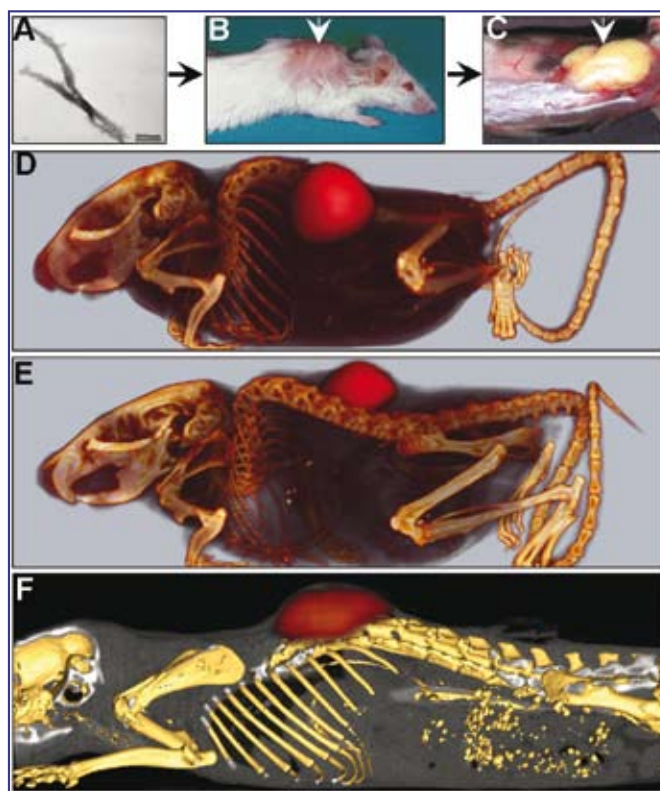


Figure 1. The 11-1F4 mAb localizes with human AL amyloid in a mouse model of amyloidoma. Human AL amyloid extract, shown by using electron microscopy to contain fibrillar material (A), was injected subcutaneously between the scapulae of Balb/c mice (B) and became vascularized within 7 days (C). ^{125}I -labelled 11-1F4 mAb, administered intravenously via the lateral tail vein, localized with both AL κ (D) and AL λ (E) in SPECT images. Similarly, GMP-grade ^{124}I -11-1F4 bound AL κ amyloid as evidenced in PET images (F).

to visualize the distribution of radiolabelled ^{125}I -11-1F4 in amyloidoma-bearing mice by using dual modality SPECT and X-ray computed tomographic (CT) imaging (30-32). The ^{125}I -11-1F4 mAb was readily observed associated with the human amyloid mass in SPECT images at 72 h post injection (figure 1D and E). This indicated that 11-1F4 mAb was indeed capable of binding to amyloid *in vivo* and, perhaps equally importantly, was shown not to bind to amyloid-free organs or tissues in the mouse – an important requirement for an immunotherapeutic

reagent. These findings were confirmed by quantifying the radioactivity associated with tissues and organs as well as by micro-autoradiography (30).

Although encouraging, preclinical imaging data could not predict whether the 11-1F4 mAb would bind amyloid efficiently in a patient with AL in whom there was significant (>1 mg/mL) circulating free light chain precursor protein. This could only effectively be addressed by performing imaging studies in human patients with AL. To translate the preclinical 11-1F4 mAb imaging procedure into humans, it was necessary to use a higher energy radioisotope than ^{125}I , which cannot be imaged in large subjects due to attenuation and scatter of the low energy photons emitted by this nuclide. Furthermore, to generate rapid, whole body, quantitative, high-resolution tomographic images of the mAb biodistribution *in vivo*, we chose to use PET/CT imaging. For this, we used ^{124}I to radiolabel 11-1F4 since ^{124}I is a positron emitter and has a convenient 4 day half-life. In preliminary mouse studies using ^{124}I -labelled 11-1F4 mAb prepared for human use, we again demonstrated, using small animal PET/CT imaging, the interaction of the mAb with human amyloidoma (30) (figure 1F).

Based upon our positive preclinical imaging findings that demonstrated the reactivity of mAb 11-1F4 with human AL amyloid xenografts in mice, we began an investigation into the biodistribution of this reagent in patients with AL by using PET/CT imaging of AL patients using the ^{124}I -11-1F4 (33).

These studies were performed to demonstrate the specific binding of 11-1F4 to tissue amyloid *in vivo* in the presence of circulating light chain proteins and thus, support the clinical evaluation of 11-1F4 as an immunotherapeutic reagent. Visual inspection of the PET images revealed specific co-localization of the antibody with AL amyloid in ~ 60% of the patients imaged to date (n = 38). Predominantly, amyloid in the liver and spleen imaged well, as did deposits in the adrenal glands, lymph nodes, and bone marrow (figure 2). However, the ^{124}I -11-1F4 failed to image amyloid in most patients. Notably, amyloid in heart and kidneys (2 organs most prone to fatal failure due to amyloid burden) was rarely discerned by visual inspection of the PET images.

Our demonstration of the specific uptake of 11-1F4 mAb in visceral amyloid deposits provides impetus for its evaluation as an immunotherapeutic agent in patients with AL. In this regard, PET/CT imaging of patients using ^{124}I -11-1F4 will be used to stratify the patient population and define those subjects most likely to benefit from the immunotherapy, based on specific organ uptake in PET images. Additionally, the ability to non-invasively and longitudinally image tissue amyloid load using ^{124}I -11-1F4 will provide an additional tool for monitoring response to the therapy in those patients enrolled in an 11-1F4 therapy trial.

Although using imaging to demonstrate the targeting of a fibril-specific mAb to amyloid in man is a significant achievement, this antibody will likely not be an effective first-line diagnostic and disease-monitoring imaging agent

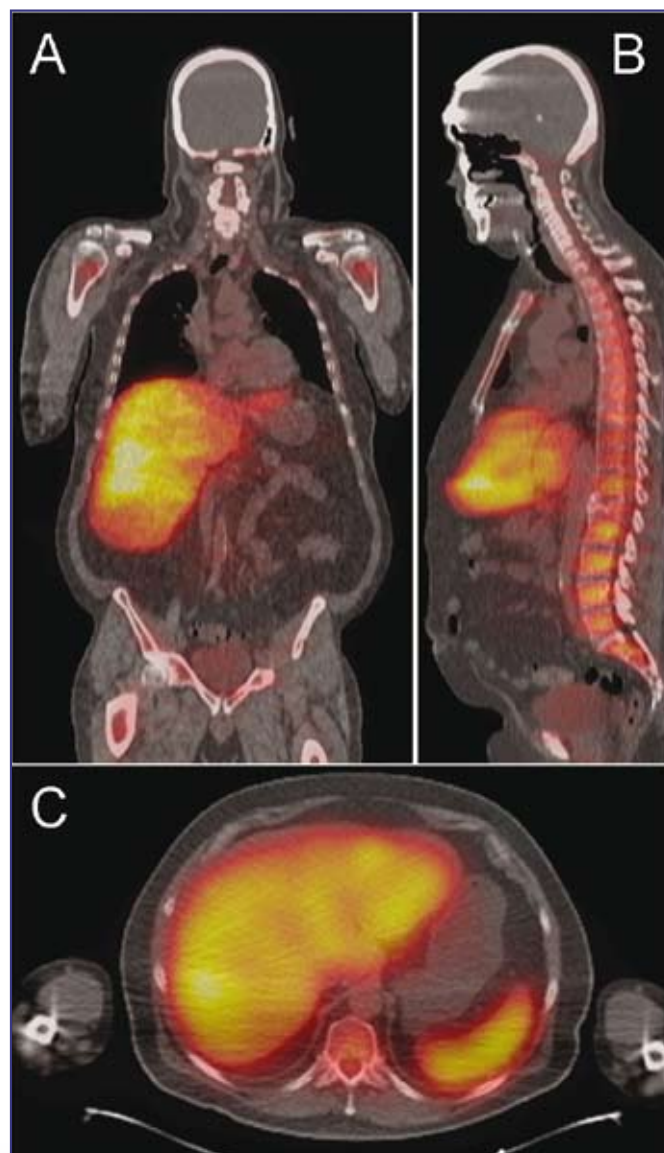


Figure 2. The ^{124}I -labelled 11-1F4 mAb specifically bound AL amyloid in patients. (A) Coronal, (B) sagittal, and (C) transaxial PET/CT images demonstrated the localization of the ^{124}I -11-1F4 mAb in the liver, spleen, and bone marrow of a patient with AL amyloidosis.

for all patients. Thus, with the continuing need to determine the presence and biodistribution of amyloid in the major target organs of patients and in those subjects entered in therapeutic clinical trials, we have evaluated the use of amyloid-associated HSPG as a target for imaging due to its ubiquitous presence in high concentrations of all amyloid deposits, irrespective of the nature of the fibril protein (34-36). We have used small peptide probes that bind amyloid-associated HSPG. These peptides can be chemically synthesized, have a better likelihood of extravasation (as compared to larger proteins such as SAP or mAb 11-1F4) and thus may provide superior imaging of extra-vascular amyloid deposits.

Amyloid imaging using heparin-binding peptide p5

The presence of HSPG in all amyloid deposits, regardless of the type of protein fibril, has been well established, and its importance in the etiology of the disease has been demonstrated *in vivo* and *in vitro* (34, 37, 38). Indeed, organs that over expressed the heparanase enzyme in a transgenic mouse model, and therefore lacked significant sulfated proteoglycans, did not support AA amyloidogenesis

(37). Furthermore, soluble HS mimetics, such as polyvinyl sulfonate, have been used successfully to inhibit AA amyloidosis in mice (39, 40). Amyloid-associated HSPG has been shown by chromatographic analyses (41-44) and by reaction with antibodies (45, 46) to be biochemically distinct from that found in the extra-cellular matrices and plasma membranes of healthy tissues. Notably, amyloid-associated HSPGs appear to be more heavily sulfated than those in

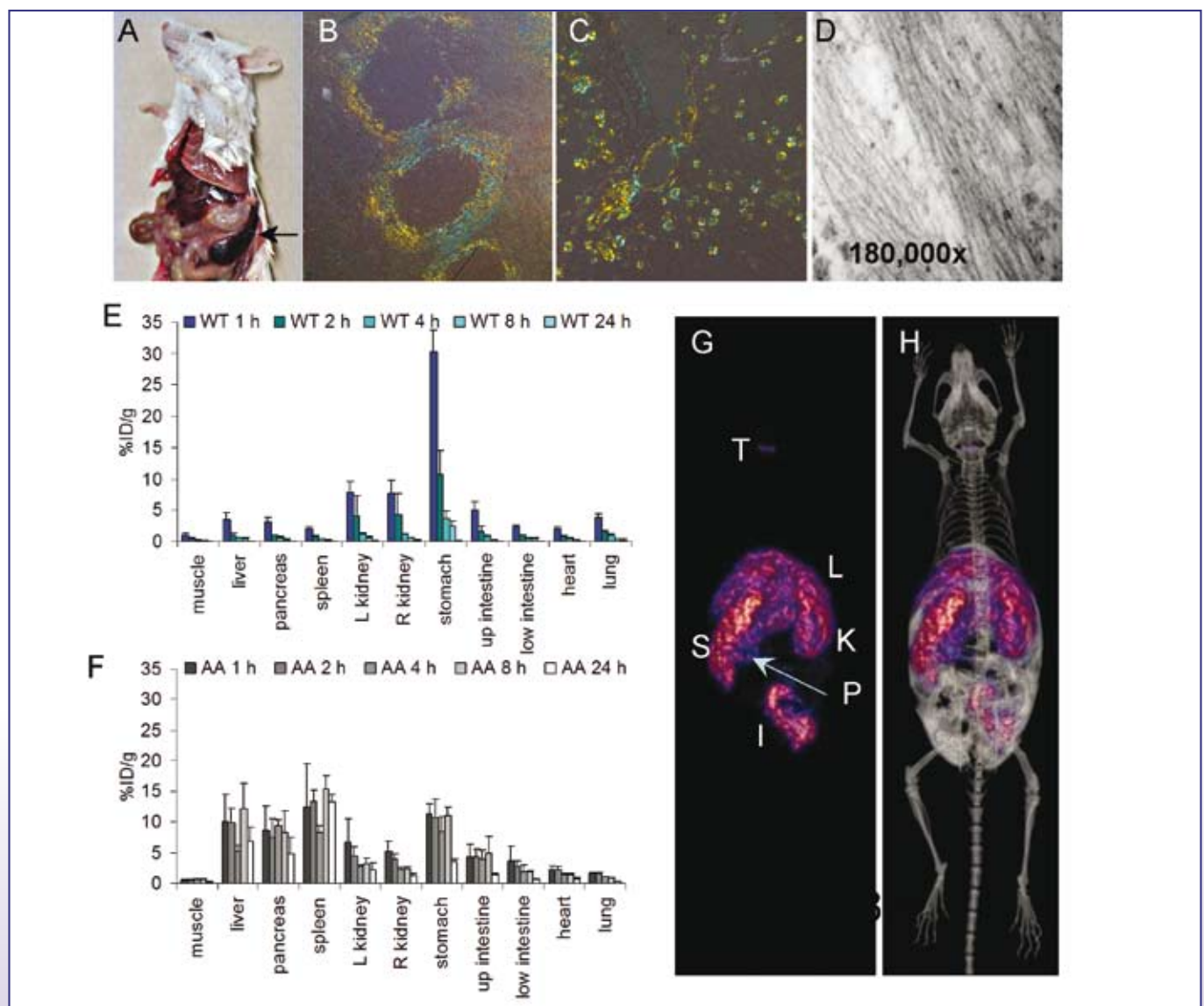


Figure 3. The heparin-binding peptide p5 binds to amyloid in a murine model of AA amyloidosis. (A) AA amyloid develops in the H2/IL-6 transgenic mouse resulting in splenomegaly (arrow) as well as hepatomegaly and ultimately renal failure due to amyloid burden in the papilla. Significant AA appears as perifollicular deposits in the spleen and within the hepatic sinusoids as evidence by blue-gold birefringence in Congo red-stained tissue sections (B and C). The amyloid contains characteristic fibrils when viewed by electron microscopy (D). ¹²⁵I-p5 peptide was cleared from the tissues of healthy wild type (WT) mice over 24 h (E), but was retained in amyloid-laden liver, spleen, pancreas, and intestines of mice with AA (F). SPECT (G) and SPECT fused with contrast-enhanced CT (H) imaging showed ¹²⁵I-p5 peptide uptake in the spleen (S), liver (L), kidney (K), pancreas (P), and intestines (I). Traces of free iodide, liberated during catabolism were seen in the thyroid (T).

normal tissue (41, 43, 44, 46). The high concentration and unique chemical structure makes it a potential biomarker that may be targeted with suitable imaging reagents for the purpose of diagnosis, prognostication, and monitoring response to therapy.

Our preliminary studies to test this hypothesis used HS-reactive single chain variable fragments (scFvs) that exhibited differential reactivity to glycosaminoglycans. We have demonstrated using small animal SPECT imaging, biodistribution studies and micro-autoradiography that the scFv NS4F5, that binds hyper-sulfated (heparin-like) HS, was singularly capable of specific amyloid binding *in vivo* in mice using these techniques (46). Based on these observations, made using our murine model of AA (46), we next evaluated a series of 7 heparin-binding peptides as potential imaging agents for amyloid *in vivo* by using small animal SPECT imaging, tissue biodistribution measurements, and micro-autoradiography. For these studies, we used a transgenic mouse, designated H2-L^d-huIL-6 Tg Balb/c (C) (H2/IL-6) that constitutively expresses human interleukin 6 protein resulting in the high circulating concentrations of acute phase proteins including serum amyloid protein A (sAA), the precursor of AA amyloid (47, 48). These mice develop spontaneous AA in the spleen, liver, kidney, heart, pancreas, and eventually all organs (figure 3A-D). This process can be initiated and expedited by intravenous injection of AA amyloid extract that acts as an amyloid enhancing factor (AEF) by seeding the pathology (47). From studies on the 7 candidate peptides, we identified one, designated p5 (a 31-amino acid, polybasic, heparin-binding peptide), that bound rapidly and specifically with amyloid *in vivo* and in sufficient concentrations as to be imaged by SPECT as early as 1 h and as late as 24 h post injection (pi) (49). The peptide was rapidly cleared from the circulation and amyloid free organs (figure 3E) but was retained in the H2/IL-6 mice for more than 24 h post injection in amyloid-laden organs, such as the liver, pancreas, and spleen (figure 3F). High resolution SPECT/CT imaging of ¹²⁵I-p5 peptide in H2/IL-6 mice with AA revealed uptake of the tracer in the liver, spleen, kidney, pancreas and intestines (figure 3G). These sites of uptake were more readily identified, particularly the pancreas, when contrast-enhanced CT image data were co-registered with the SPECT data (figure 3H). The specific binding of the p5 peptide with amyloid within these organs was confirmed by using micro-autoradiography (49). This technique provides a means to observe the microscopic distribution of the ¹²⁵I-labelled peptide within formalin-fixed paraffin embedded tissue sections that are exposed to photographic emulsion. The distribution of radiotracer, indicated by the black silver granules in amyloid laden tissues (figure 4), correlated precisely with the presence of amyloid based on Congo red staining of consecutive tissue sections and was consistently more easily visualized. The retention of this ¹²⁵I peptide in amyloid-laden organs *in vivo* was shown to increase linearly with the amyloid load as evidenced by a comparison with qualitative Congo red scoring

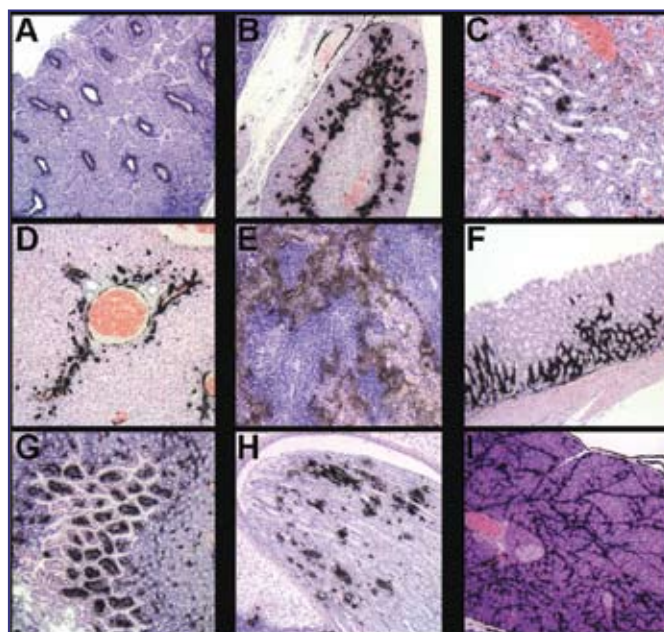


Figure 4. Peptide p5 specifically binds to AA amyloid when injected *iv* into AA mice as evidenced in micro-autoradiographs. Black deposits indicate the presence of ¹²⁵I-p5 at sites confirmed to contain amyloid by Congo red staining of consecutive tissue sections. (A) lymph node, (B) adrenal gland, (C) renal cortex, (D) liver, (E) spleen, (F) gastric wall, (G) small intestine, (H) renal papilla, and (I) pancreas.

of stained tissue sections (49). In addition, we have observed scant radioactivity within healthy organs. Finally, a biotinylated form of peptide p5 was shown to stain human AA, AL, ATTR and A β amyloid in formalin-fixed paraffin-embedded tissue sections (49). These data support the evaluation of this basic peptide as a novel agent for the clinical detection of peripheral organ amyloidosis in man by using molecular imaging. In considering the translation of peptide p5 into the clinic, we tested several variants of the original sequence to identify the optimal peptide. The costs of producing good manufacturing practice (GMP)-grade peptide p5 is based on the number of amino acids, therefore, we have evaluated the amyloid imaging efficacy of 2 truncated forms of the peptide, designated p5(1-24) and p5(1-17). To directly compare the efficacy of each peptide with the parental p5 reagent, we performed *in vivo* dual energy SPECT imaging studies in which the truncated p5 peptides were radiolabelled with ¹²⁵I, and the p5 was labelled with ^{99m}Tc. Both forms of the peptide were co-injected into the same mouse, and the biodistribution of each one simultaneously assessed by SPECT imaging using both high and low energy window acquisitions as well as dual isotope tissue biodistribution measurements (figure 5). Both p5(1-24) and p5(1-17) were found in lower concentrations in the liver, spleen, and pancreas of mice with AA as compared to ^{99m}Tc-p5 (figure 5A and B). This quantitative analysis was confirmed in the SPECT images. The ^{99m}Tc-p5 peptide was

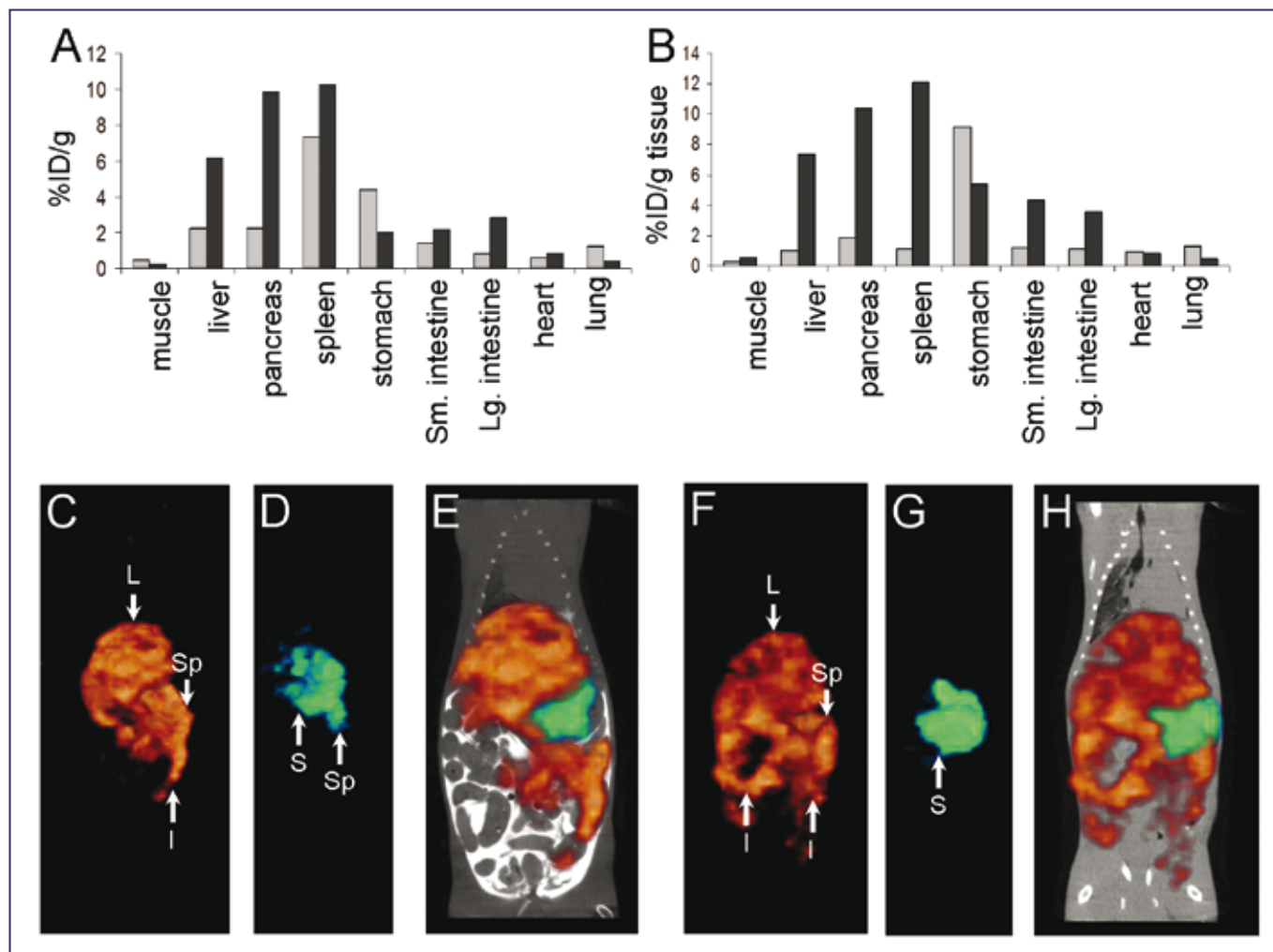


Figure 5. Truncated forms of peptide p5 do not effectively bind or image murine AA amyloid *in vivo*. Dual energy biodistribution of ^{125}I -p5(1-24) (A, grey) and $^{99\text{m}}\text{Tc}$ -p5(A, black), or ^{125}I -p5(1-17) (B, grey) and $^{99\text{m}}\text{Tc}$ -p5(B, black) demonstrated that truncation of p5 peptide decreased the reactivity with AA amyloid *in vivo*. This was confirmed in SPECT and CT contrast-enhanced SPECT/CT imaging. SPECT images of (C) $^{99\text{m}}\text{Tc}$ -p5, (D) ^{125}I -p5(1-24), and the fused image (E) as well as (F) $^{99\text{m}}\text{Tc}$ -p5, (G) ^{125}I -p5(1-17), and the fused image (H). L, liver; Sp, spleen; I, intestine, and S, stomach.

seen in the liver, spleen, and intestines (figure 5C and E) whereas the p5(1-24) was seen only in the spleen, with some free ^{125}I -iodide (liberated during catabolism) observed in the stomach (figure 5D and E). Similar results were observed with ^{125}I -p5(1-17) in that there was little binding to any amyloid deposits *in vivo*, and only ^{125}I -iodide was seen in the stomach (figure 5G and H), as compared to the dramatic uptake of ^{125}I -p5 in the amyloid in visceral organs (figure 5F). We had initially hypothesized that truncation of the p5 peptide, and therefore reduction in the net positive charge, would result in a slight decrease in the amyloid reactivity of the radiolabelled product *in vivo* but possibly result in a faster whole body clearance giving it an advantage over the full length p5 peptide. However, the reduction in peptide size and charge resulted in a dramatic decrease in amyloid

reactivity. The truncated peptides could not be used to detect amyloid deposits *in vivo* based on SPECT imaging. With the result that shorter peptides were inferior, we also tested if a longer peptide might actually bind amyloid better. A peptide with 14 more amino acids including three extra AOK motifs was tested. The longer peptide p5(+14) was able to bind to and image amyloid in the AA mice, but gave significant background binding in WT mice and thus was an inferior imaging agent (data not shown). Based on these findings, we continue to develop the full-length p5 peptide (31-mer) as the prime candidate for imaging visceral amyloid in patients.

Conclusion

Imaging visceral amyloid deposits either by ^{123}I -SAP scintigraphy, MRI, US or CT is common practice in these

patients and provides the physician with a more complete picture of the disease and a means to monitor progression or regression of the pathology in response to therapy. To further assist in the management of patients with visceral amyloidosis, we have developed a mAb that specifically targets both AL λ and AL κ amyloid deposits and may prove to be therapeutically efficacious. Furthermore, we have demonstrated that the mAb 11-1F4, when radiolabelled, can be used to image AL amyloid-laden organs and tissues. This will allow the physician to identify patients who may benefit from 11-1F4 treatment as well as non-invasively monitor response to therapy and change in amyloid burden in patients. However, due to certain limitations in 11-1F4 imaging we have also identified a novel polybasic heparin-binding peptide that, due to its structural properties, binds amyloid specifically and can be used to image amyloid *in vivo*. When radioiodinated, the p5 peptide can be used to visualize the presence of amyloid by using small animal SPECT or PET imaging up to 24 h post injection. The ability to bind many extracellular amyloid deposits, the rapid loss of signal from unbound ¹²⁵I-p5, and the lack of binding to healthy tissues support the evaluation of this peptide as a potential amyloid imaging agent for the non-invasive, quantitative detection and monitoring of disease in patients with amyloidosis.

List of references

1. Kahn SE, Andrikopoulos S, Verchere CB. Islet amyloid: a long-recognized but underappreciated pathological feature of type 2 diabetes. *Diabetes*. 1999;48:241-53
2. Kisilevsky R, Ancsin JB, Szarek WA, Petanceska S. Heparan sulfate as a therapeutic target in amyloidogenesis: prospects and possible complications. *Amyloid*. 2007;14:21-32
3. Ohashi K. Pathogenesis of beta2-microglobulin amyloidosis. *Pathology international*. 2001;51:1-10
4. Merlini G, Bellotti V. Molecular mechanisms of amyloidosis. *N Engl J Med*. 2003;349:583-96
5. Merlini G, Westermarck P. The systemic amyloidoses: clearer understanding of the molecular mechanisms offers hope for more effective therapies. *J Intern Med*. 2004;255:159-78
6. De Lorenzi E, Giorgetti S, Grossi S et al. Pharmaceutical strategies against amyloidosis: old and new drugs in targeting a "protein misfolding disease". *Curr Med Chem*. 2004;11:1065-84
7. Merlini G. Systemic amyloidosis: are we moving ahead? *Neth J Med*. 2004;62:104-5
8. Goldsbury C, Baxa U, Simon MN et al. Amyloid structure and assembly: insights from scanning transmission electron microscopy. *Journal of structural biology*. 2010;173:1-13
9. Nelson R, Eisenberg D. Recent atomic models of amyloid fibril structure. *Current opinion in structural biology*. 2006;16:260-5
10. Westermarck P, Benson MD, Buxbaum JN et al. A primer of amyloid nomenclature. *Amyloid*. 2007;14:179-83
11. Ketteler M, Koch KM, Floege J. Imaging techniques in the diagnosis of dialysis-related amyloidosis. *Semin Dial*. 2001;14:90-3
12. Sueyoshi E, Sakamoto I, Okimoto T et al. Cardiac amyloidosis: typical imaging findings and diffuse myocardial damage demonstrated by delayed contrast-enhanced MRI. *Cardiovasc Intervent Radiol*. 2006;29:710-2
13. Hawkins PN, Pepys MB. Imaging amyloidosis with radiolabelled SAP. *European journal of nuclear medicine*. 1995;22:595-9
14. Hazenberg BP, van Rijswijk MH, Piers DA et al. Diagnostic performance of ¹²³I-labeled serum amyloid P component scintigraphy in patients with amyloidosis. *The American journal of medicine*. 2006;119:355 e15-24
15. Jager PL, Hazenberg BP, Franssen EJ et al. Kinetic studies with iodine-123-labeled serum amyloid P component in patients with systemic AA and AL amyloidosis and assessment of clinical value. *J Nucl Med*. 1998;39:699-706
16. Hawkins PN, Myers MJ, Epenetos AA, Caspi D, Pepys MB. Specific localization and imaging of amyloid deposits *in vivo* using ¹²³I-labeled serum amyloid P component. *The Journal of experimental medicine*. 1988;167:903-13
17. Rydh A, Suhr O, Hietala SO et al. Serum amyloid P component scintigraphy in familial amyloid polyneuropathy: regression of visceral amyloid following liver transplantation. *European journal of nuclear medicine*. 1998;25:709-13
18. Tan SY, Irish A, Winearls CG et al. Long term effect of renal transplantation on dialysis-related amyloid deposits and symptomatology. *Kidney international*. 1996;50:282-9
19. Glaudemans AW, Slart RH, Zeebregts CJ et al. Nuclear imaging in cardiac amyloidosis. *European journal of nuclear medicine and molecular imaging*. 2009;36:702-14
20. Han S, Chong V, Murray T et al. Preliminary experience of ^{99m}Tc-Aprotinin scintigraphy in amyloidosis. *European journal of haematology*. 2007;79:494-500
21. Schaadt BK, Hendel HW, Gimsing P et al. ^{99m}Tc-aprotinin scintigraphy in amyloidosis. *J Nucl Med*. 2003;44:177-83
22. Puille M, Altland K, Linke RP et al. ^{99m}Tc-DPD scintigraphy in transthyretin-related familial amyloidotic polyneuropathy. *European journal of nuclear medicine and molecular imaging*. 2002;29:376-9
23. Rapezzi C, Guidalotti P, Salvi F, Riva L, Perugini E. Usefulness of ^{99m}Tc-DPD scintigraphy in cardiac amyloidosis. *Journal of the American College of Cardiology*. 2008;51:1509-10
24. Solomon A, Weiss DT, Macy SD, Antonucci RA. Immunocytochemical detection of kappa and lambda light chain V region subgroups in human B-cell malignancies. *Am J Pathol*. 1990;137:855-62
25. O'Nuallain B, Allen A, Ataman D et al. Phage display and peptide mapping of an immunoglobulin light chain fibril-related conformational epitope. *Biochemistry*. 2007;46:13049-58
26. O'Nuallain B, Allen A, Kennel SJ et al. Localization of a conformational epitope common to non-native and fibrillar immunoglobulin light chains. *Biochemistry*. 2007;46:1240-7
27. O'Nuallain B, Murphy CL, Wolfenbarger DA et al. The Amyloid-Reactive Monoclonal Antibody 11-1F4 Binds a Cryptic Epitope on Fibrils and Partially Denatured Immunoglobulin Light Chains and Inhibits Fibrillogenesis. *Amyloid and Amyloidosis: Proceedings of the Xth International Symposium on Amyloidosis; 2005; Tours, France: CRC Press*
28. Hrnčić R, Wall J, Wolfenbarger DA et al. Antibody-mediated

- resolution of light chain-associated amyloid deposits [In Process Citation]. *Am J Pathol.* 2000;157:1239-46
29. Hrnčić R, Wall JS, Murphy C, Solomon A. Dissolution of human amyloid extract in the mouse. International symposium on amyloidosis; Amyloid and amyloidosis; 1998; Rochester, MN: New York, N.Y.; London; Parthenon Pub. Group
 30. Wall JS, Kennel SJ, Paulus M et al. Radioimaging of Light Chain Amyloid with a Fibril-Reactive Monoclonal Antibody. *J Nucl Med.* 2006;47:2016-24
 31. Wall JS, Paulus MJ, Gleason S et al. Micro-Imaging of Amyloid in Mice. *Methods in Enzymology.* 2006;412:161-82
 32. Wall JS, Paulus MJ, Kennel SJ et al. Radioimaging of Primary (AL) Amyloidosis with an Amyloid-Reactive Monoclonal Antibody. *Amyloid and Amyloidosis: Proceedings of the Xth International Symposium on Amyloidosis; 2005; Tours, France: CRC Press.*
 33. Wall JS, Kennel SJ, Stuckey AC et al. Radioimmunodetection of amyloid deposits in patients with AL amyloidosis. *Blood.* 2010;116:2241-4
 34. Ancsin JB. Amyloidogenesis: historical and modern observations point to heparan sulfate proteoglycans as a major culprit. *Amyloid.* 2003;10:67-79
 35. Kisilevsky R. Review: amyloidogenesis-unquestioned answers and unanswered questions. *Journal of structural biology.* 2000;130:99-108
 36. O'Callaghan P, Sandwall E, Li JP et al. Heparan sulfate accumulation with Aβ deposits in Alzheimer's disease and Tg2576 mice is contributed by glial cells. *Brain pathology (Zurich, Switzerland).* 2008;18:548-61
 37. Li JP, Galvis ML, Gong F et al. In vivo fragmentation of heparan sulfate by heparanase overexpression renders mice resistant to amyloid protein A amyloidosis. *Proceedings of the National Academy of Sciences of the United States of America.* 2005;102:6473-7
 38. Snow AD, Bramson R, Mar H, Wight TN, Kisilevsky R. A temporal and ultrastructural relationship between heparan sulfate proteoglycans and AA amyloid in experimental amyloidosis. *J Histochem Cytochem.* 1991;39:1321-30
 39. Inoue S, Hultin PG, Szarek WA, Kisilevsky R. Effect of poly(vinylsulfonate) on murine AA amyloid: a high-resolution ultrastructural study. *Laboratory investigation; a journal of technical methods and pathology.* 1996;74:1081-90
 40. Dember LM, Hawkins PN, Hazenberg BP et al. Eprodisate for the treatment of renal disease in AA amyloidosis. *N Engl J Med.* 2007;356:2349-60
 41. Lindahl B, Lindahl U. Amyloid-specific heparan sulfate from human liver and spleen. *The Journal of biological chemistry.* 1997;272:26091-4
 42. Snow AD, Kisilevsky R, Stephens C, Anastassiades T. Characterization of tissue and plasma glycosaminoglycans during experimental AA amyloidosis and acute inflammation. Qualitative and quantitative analysis. *Laboratory investigation; a journal of technical methods and pathology.* 1987;56:665-75
 43. Stenstad T, Magnus JH, Husby G. Characterization of proteoglycans associated with mouse splenic AA amyloidosis. *The Biochemical journal.* 1994;303:663-70
 44. Sugumaran G, Elliott-Bryant R, Phung N et al. Characterization of splenic glycosaminoglycans accumulated in vivo in experimentally induced amyloid-susceptible and amyloid-resistant mice. *Scandinavian journal of immunology.* 2004;60:574-83
 45. Bruinsma IB, te Riet L, Gevers T et al. Sulfation of heparan sulfate associated with amyloid-beta plaques in patients with Alzheimer's disease. *Acta neuropathologica.* 2010;119:211-20
 46. Smits NC, Kurup S, Rops AL et al. The heparan sulfate motif (GlcNS6S-IdoA2S)₃, common in heparin, has a strict topography and is involved in cell behavior and disease. *The Journal of biological chemistry.* 2010;285:41143-51
 47. Solomon A, Weiss DT, Schell M et al. Transgenic mouse model of AA amyloidosis. *Am J Pathol.* 1999;154:1267-72
 48. Wall JS, Richey T, Allen A et al. Quantitative tomography of early-onset spontaneous AA amyloidosis in interleukin 6 transgenic mice. *Comparative medicine.* 2008;58:542-50
 49. Wall JS, Richey T, Stuckey A et al. In vivo molecular imaging of peripheral amyloidosis using heparin-binding peptides. *Proc Natl Acad Sci U S A.* 2011. 

SCAN

Een afdeling of organisatie doorlichten. Geen genoegen nemen met de oppervlakkige feiten. Je eigen mogelijkheden en verwachtingen analyseren. Kortom, een loopbaan in een ziekenhuis op wereldniveau.

Medisch diensthoofd nucleaire geneeskunde

Topreferent zijn in patiëntenzorg, opleiding en onderzoek, dat zijn de drie hoofdopdrachten van UZ Leuven. In België en Europa spelen we een toonaangevende rol die we willen behouden en verder uitbouwen. Daartoe bundelen meer dan 8 000 gedreven medewerkers elke dag hun expertise. UZ Leuven behaalde als eerste Belgische ziekenhuis het internationale JCI-label voor veilige en kwaliteitsvolle zorg.

Momenteel hebben we een interessante opportuniteit binnen **nucleaire geneeskunde** voor een (m/v):

Medisch diensthoofd

Situering: Binnen het kader van UZ Leuven als academisch medisch centrum streeft de dienst nucleaire geneeskunde naar excellentie op drie vlakken: klinische zorg, de productie van radiofarmaca (radiofarmacie) en beeldvorming (medische fysica). De dienst beoogt een optimale wisselwerking tussen deze drie aspecten waarbij de kwaliteit op elk niveau wordt geoptimaliseerd. De dagelijkse klinische activiteit wordt verder verfijnd op basis van doorgedreven klinisch onderzoek, waarbij zowel de uitvoering als de indicaties van nucleaire onderzoeken en therapieën worden geanalyseerd met als uiteindelijk doel een zorgverbetering voor de individuele patiënt. Deze onderzoeksactiviteiten zijn ingebed in een intense samenwerking met meerdere externe partners. De kwaliteit van de patiëntenzorg en de service naar de verwijzende arts worden verzekerd door een volledig uitgewerkt systeem van kwaliteitsmanagement. Voor de verdere uitbouw van de medische beeldvorming binnen UZ Leuven ligt er een grote opportuniteit in een intense samenwerking met de dienst radiologie.

Competentieprofiel: U onderlijnt het klinisch belang van de nucleaire geneeskunde in samenspraak met verwijzers en andere diagnostici. U neemt een actieve rol op in opleiding en onderwijs. U hebt een inspirerende en stimulerende rol bij het wetenschappelijk onderzoek, klinisch en preklinisch, op het vlak van zowel radiofarmacie, imaging als pathofysiologie. U bewaakt bovendien het evenwicht tussen de klinische en wetenschappelijke opdracht van de dienst. U staat garant voor continue optimalisering en innovatie binnen uw vakgebied. U bezit de nodige management-capaciteiten, vlotte communicatievaardigheden en u weet uw medewerkers te inspireren en/of bij te sturen. U hebt oog voor de praktische organisatie van de dienst en streeft naar een optimale multidisciplinaire samenwerking tussen medici, paramedici, apothekers en technologen.

Vereisten: U behaalde een in België of in de Europese Unie erkend diploma als arts en specialist in nucleaire geneeskunde. U hebt relevante klinische expertise. Ervaring in wetenschappelijk onderzoek en management is een pluspunt.

Wij bieden: Een boeiende, complexe, hoogtechnologische ziekenhuisorganisatie met continue uitdagingen op inhoudelijk vlak. Een degelijk personeelsstatuut met talrijke extralegale voordelen.



Amyloid Imaging in Alzheimer's Disease

N. Tolboom, MD, PhD¹

R. Ossenkuppele, MSc²

B.N.M. van Berckel, MD, PhD¹

Departments of Nuclear Medicine & PET Research¹,

Neurology and Alzheimer Centre²,

VU University Medical Centre, Amsterdam, the Netherlands

Abstract

Tolboom N, Ossenkuppele R, Van Berckel BNM.

Amyloid Imaging in Alzheimer's Disease

Over the past two decades, positron emission tomography (PET) tracers have been developed for *in vivo* visualisation and quantification of Alzheimer's disease (AD) pathology.

The current overview will focus on the performance of the most widely used ligand for *in vivo* imaging of AD pathology, ¹¹C-PIB and will also cover the amyloid and tau ligand ¹⁸F-FDDNP. The more recently developed ¹⁸F-labelled amyloid agents will be discussed briefly.

Tijdschr Nucl Geneesk 2011; 33(4):816-820

Introduction

Over the past two decades, positron emission tomography (PET) tracers have been developed for *in vivo* visualisation and quantification of Alzheimer's disease (AD) pathology. Previously, detection of AD pathology was only possible at post mortem examination of the brain or at brain biopsy. The possibility to image the amount and distribution of AD pathology during life has initiated a new research area. It shows promise to facilitate early and accurate diagnosis of AD, provides more insight in the time course and regional deposition of pathology during life and assists in the development and individual assessment of potential treatments. The current overview will focus on the performance of the most widely used ligand for *in vivo* imaging of AD pathology, ¹¹C-PIB (1) and will also cover the amyloid and tau ligand ¹⁸F-FDDNP (2). The more recently developed ¹⁸F-labelled amyloid agents will be discussed briefly.

Alzheimer's disease

AD is a progressive neurodegenerative disorder. The diagnosis of AD can be preceded by a prodromal phase, which is usually characterised by isolated episodic memory impairment, often referred to as mild cognitive impairment (MCI) (3,4). At present, a clinical diagnosis of AD is made when, in addition to progressive memory impairment, impairment in at least one other cognitive domain, e.g. aphasia, apraxia, agnosia or executive dysfunctioning is present (5).

Neuropathologically, AD is characterized by the accumulation of amyloid-beta (A β) in senile plaques and hyperphosphorylated tau in neurofibrillary tangles (NFT) (6). This hallmark pathology starts to accumulate many years before cognitive symptoms arise and especially NFT spread in a predictable manner throughout the brain. NFT are mainly present in the medial temporal (MTL)

and lateral temporal lobes and, to a lesser extent, in frontal, parietal, and occipital lobes (7). Amyloid plaques are more evenly distributed throughout the cortex with relatively mild involvement of the MTL. Although accumulation of amyloid is thought to play a key role in the pathogenesis of AD (8), it is the deposition of NFT that is more directly associated with degree of cognitive impairment and thus severity of disease (9).

In the past decades, the "amyloid cascade hypothesis" has been put forward in an effort to explain the biological basis of AD (8). The essence of this hypothesis is that increased production or decreased clearance of A β peptides cause AD. At present, disease modifying therapies are being developed, targeting the pathological accumulation of A β peptides. Together with development of therapies, earlier and more accurate diagnosis of AD is essential, as treatment potentially will have most effect in the early phases of the disease. For this purpose new criteria for preclinical and clinical stages of AD have been proposed recently (10-12).

Molecular imaging in the diagnosis of dementia

AD is a clinical diagnosis according to the recently proposed revised criteria by the National Institute of Aging-Alzheimer Association (NIA-AA) workgroup (10). The diagnostic process does not necessarily have to include supportive biomarkers. However, pathophysiological and topographical markers do strongly increase the likelihood of the clinical diagnosis AD. Also, MCI patients with abnormal biomarkers are now, according to these criteria, referred to as "MCI due to AD". Besides these new clinical criteria, new *research* criteria for early diagnosis of AD incorporating novel and established biomarkers have been proposed (12). For an individual to meet these criteria, a combination of episodic memory impairment together with at least one supportive biomarker is necessary. These supportive criteria consist of: presence of medial temporal lobe atrophy on MRI (13), abnormal cerebrospinal fluid biomarkers (CSF) (i.e. low A β -42 concentrations, increased total tau or hyperphosphorylated tau concentrations or a combination of the three) (14), a proven autosomal dominant mutation associated with AD within the immediate family, increased ¹¹C-PIB binding on PET scan, or reduced glucose metabolism in bilateral temporal parietal regions on ¹⁸F-fluorodeoxyglucose (¹⁸F-FDG) PET (15) (figure 1). It is currently not clear which of the aforementioned criteria will be used for the diagnosis of dementia in the Netherlands. New guidelines are under construction.

As mentioned above, ¹⁸F-FDG PET is a well validated PET tracer for differential diagnosis of dementia. In AD, this tracer typically reveals hypometabolism in bilateral temporal parietal

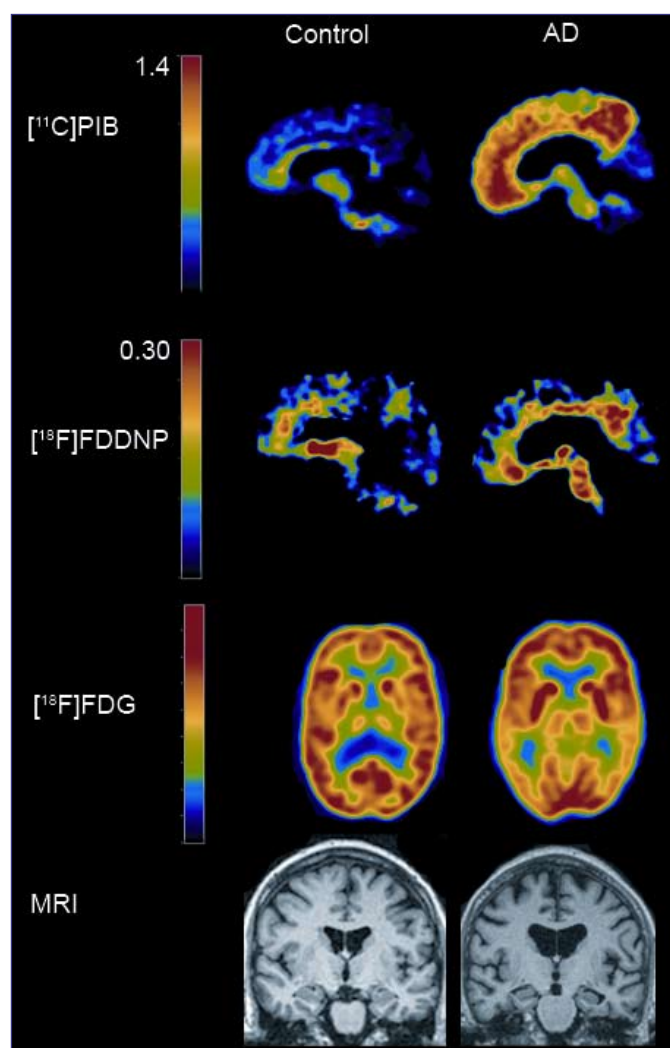


Figure 1. Examples of normal (left panel, healthy control) and AD-like (right panel, AD patient) images for ^{11}C -PIB, ^{18}F -FDDNP, ^{18}F -FDG and MTA on MRI. All scans were acquired in the same subjects. Uptake is represented by the colour scale for the PET images. Increased ^{11}C -PIB and ^{18}F -FDDNP uptake is seen mainly in frontal regions on sagittal images. Decreased ^{18}F -FDG is seen mainly in parietotemporal regions on the axial image. MTA is best seen on coronal images.

regions and posterior cingulate (15,16). ^{18}F -FDG PET has a high negative predictive value for the presence of neurodegenerative disease, but suffers from low specificity as many other causes of cognitive impairment can induce disturbances in glucose metabolism (17,18). Moreover, reading of ^{18}F -FDG PET images for the diagnosis of dementia is not straight forward and requires a well-trained eye. Although ^{18}F -FDG PET does not measure AD pathology directly and thus is an indirect measure of disease, the degree of hypometabolism is associated with the degree of cognitive impairment.

Imaging AD pathology using PET: ^{11}C -PIB and ^{18}F -FDDNP

Since 2004, it has become possible to image the hallmarks of AD pathology in vivo. The first PET study using a tracer

for this purpose in the living human brain was published with 2-(1-{6-[(2-[^{18}F]fluoroethyl) (methyl)amino]-2-naphthyl} ethylidene) malononitrile (^{18}F -FDDNP) (2) as pioneering ligand. This was shortly followed by the first clinical N-methyl- ^{11}C -2-(4'-methylaminophenyl)-6-hydroxybenzothiazole (^{11}C -PIB) PET study (1). ^{11}C -PIB was designed to measure the amount of fibrillary A β deposits (19,20), whilst ^{18}F -FDDNP labels not only amyloid plaques but also neurofibrillary tangles. Both tracers displayed increased retention in AD patients compared with controls (1-2,21-23), but magnitude and regional distribution of the signal obtained with ^{18}F -FDDNP differed from that obtained with ^{11}C -PIB. Tracer uptake was calculated using a reference tissue, pons or cerebellar grey matter, regions thought to be devoid of fibrillary amyloid plaques and thus specific binding. Following the early studies (1,2), several groups have replicated the initial results found with ^{11}C -PIB (24-28), but relatively limited new information has become available for ^{18}F -FDDNP (29-34).

^{18}F -FDDNP

In a recent study, the binding of ^{18}F -FDDNP and ^{11}C -PIB in AD, MCI and controls was assessed in a head-to-head comparison confirming marked differences between the two tracers (35). First, although both tracers were able to distinguish AD patients from controls at a group level, binding of ^{18}F -FDDNP in AD patients was 9-fold lower than that of ^{11}C -PIB. Binding of ^{18}F -FDDNP in AD patients was approximately 2-fold of that seen in controls. Second, regional binding patterns of both tracers differed substantially. For ^{18}F -FDDNP, although AD patients displayed an overall increase in binding compared to MCI patients and controls, in all three groups, the highest values were found in the MTL. For ^{11}C -PIB, AD patients showed increased binding in all cortical brain regions compared to healthy controls, with relatively the smallest increase in the MTL.

The low specific signal indicates that the accuracy of ^{18}F -FDDNP as a differential diagnostic tool for detection of AD pathology in individual subjects is substantially lower than that of ^{11}C -PIB. However, ^{18}F -FDDNP is the only PET ligand available to date with, besides binding to amyloid, also affinity for tangles (36). This suggests a potential ability to monitor progression of disease. Clearly, this potential application remains to be investigated thoroughly. Moreover, these characteristics are more likely to be useful in research settings for differentiation at group level than for use in individual subjects.

^{11}C -PIB

Increased ^{11}C -PIB binding is seen in a vast majority of AD patients, indicating high sensitivity for detection of AD. Compared to ^{18}F -FDDNP, high specific to non-specific binding ratio was found for ^{11}C -PIB with AD patients displaying 8-fold specific signal in cortical areas, with respect to controls (35). Initially, ^{11}C -PIB binding in MCI was reported to be similar to that of either controls or AD patients. Several longitudinal studies, however, have shown a subtle increase in already present amyloid burden in MCI patients over time, indicating that ^{11}C -PIB retention in MCI patients is somewhat more variable (37-39).

Approximately 40-60% of MCI patients show increased levels of ^{11}C -PIB retention when compared to controls with negligible binding (28,37-40). These so-called ^{11}C -PIB 'positive' (PIB+) MCI patients are thought to be the subset of patients that progress to AD. Recent studies have indeed demonstrated high conversion rates in PIB+ MCI (28,38;40). ^{11}C -PIB binding therefore has a prognostic value in MCI: patients with MCI and increased binding are thought to have 'MCI due to AD' and have a very high risk of progressing to AD with manifest dementia.

Although negligible global ^{11}C -PIB binding is seen in most healthy controls, approximately 10% of healthy controls younger than 70 and up to 50% in those over 85 years have been reported to display increased ^{11}C -PIB binding (25,41-43). ^{11}C -PIB load tended to vary, but in general it was lower than that seen in most AD patients (41,44). This is largely in line with post mortem studies reporting presence of AD pathology in around 30% of cognitively healthy elderly subjects (45). These subjects may be preclinical AD patients, as deposition of pathology is thought to start a decade before cognitive impairment arises (46). Amyloid in the brain as measured with ^{11}C -PIB has been associated with an increased likelihood for cognitive deterioration in healthy controls (42). However, to verify if amyloid positive subjects are indeed 'preclinical AD' cases, longitudinal follow up with periods of at least 10 years are necessary. In the differential diagnosis of AD, ^{11}C -PIB binding is mainly of use in distinguishing between AD from neurodegenerative disorders that are caused by tauopathies such as frontotemporal dementia (FTD). FTD is a cause of dementia associated with behavioural problems and frequently misdiagnosed as AD. Amyloid accumulation in the brain and therefore ^{11}C -PIB binding is negligible in FTD and other tau induced dementias (47). ^{11}C -PIB binding is of little use in the differentiation between AD and dementia with Lewy bodies (DLB), another type of dementia frequently misdiagnosed as AD. Increased ^{11}C -PIB binding is seen in up to 92% of DLB patients (48), in keeping with the high amounts of amyloid plaques that are found in the brains of neuropathologically confirmed DLB patients.

Analysis and assessment of amyloid images

For both ^{11}C -PIB and ^{18}F -FDDNP, RPM2, a parametric implementation of the simplified reference tissue model, was identified as the most optimal tracer kinetic model for data analysis (49,50). Cerebellar grey matter was used as reference region. This parametric model requires the data to be acquired as a dynamic scan, following tracer uptake, retention and clearance over time. Dynamic scanning enables full quantification, as it takes into account differences in plasma clearance and changes in other parameters that affect tracer uptake, such as blood flow. The latter is especially important, as regional blood flow may change with the progression of AD. This is essential for accurately monitoring deposition of pathology (progression of disease/ longitudinal imaging) and for assessing therapeutic efficacy. However, if scans are performed solely for diagnostic purposes, e.g. visual assessment of PIB + versus PIB -, simple tissue ratios provide sufficient information, despite the fact that

they overestimate specific binding (51). This allows for short imaging protocols that are most comfortable for patients and enhance cost-effectiveness of amyloid imaging.

Visual interpretation of the amyloid imaging ligands ^{11}C -PIB and ^{18}F -FDDNP as supportive diagnostic markers for AD has been evaluated and compared with ^{18}F -FDG PET and medial temporal lobe atrophy (MTA) on MRI (52) (Figure 1). Visual interpretation of ^{11}C -PIB images showed high diagnostic accuracy (0.93) combined with a high inter-observer agreement ($\kappa = 0.85$). Furthermore, the agreement of the visual ^{11}C -PIB PET interpretation with quantitative assessment of ^{11}C -PIB was high ($\kappa = 0.85$). Moreover, visual rating of ^{11}C -PIB for identification of AD performed equally well as the combination of ^{18}F -FDG (high sensitivity, low specificity) and MTA (high specificity, low sensitivity (53)). Visual rating of ^{18}F -FDDNP images for identification of AD had lowest sensitivity, specificity and accuracy. Additionally, agreement with quantitative assessment was only fair. Visual rating of ^{18}F -FDG had lowest inter-observer agreement ($\kappa = 0.56$) illustrating the complexity of reading ^{18}F -FDG for AD diagnostics.

Amyloid imaging in development of potential treatments

Several disease modifying therapies are being developed, targeting the pathological accumulation of A β peptides. Stratification of participants based on presence of underlying AD pathology, thereby identifying subjects who will potentially benefit from therapies targeting that pathology, will greatly improve the power of therapeutic trials. Furthermore, imaging of AD pathology can also be used as a tool to measure treatment efficacy. In a recent study, anti-A β monoclonal antibody Bapineuzumab reduced fibrillar plaque load in AD patients as measured with ^{11}C -PIB PET (54). It remains to be verified, however, whether an actual decrease in pathological load as induced by medication can be measured accurately using ^{11}C -PIB. At present, little is known about how conformational changes of amyloid (and tangles) will affect PET measurements.

New amyloid imaging ligands

This overview focused on the two most widely used amyloid imaging tracers, but currently new tracers are being developed. These new tracers are specifically designed to have a longer half life or higher specific binding, aiming to increase their clinical applicability (55-60). The first clinical study with a ^{18}F -labeled derivative of ^{11}C -PIB, renamed as ^{18}F -flutemetamol, has recently been published (59). Although this ligand seems to be promising, time to equilibrium is long (>80 min). Moreover, non-specific binding in white matter of ^{18}F -flutemetamol is considerably higher than with ^{11}C -PIB, which can complicate quantification of especially subtle amyloid deposition. This also seems to be the case with other new amyloid imaging agents, like ^{18}F -florbetapir (61), ^{18}F -flutemetamol (62) or ^{18}F -florbetaben (55), of which clinical trials are currently ongoing. An ^{18}F -amyloid imaging agent that does not appear to have this problem is ^{18}F -AZD4694 (58). However, human studies with this ligand have not yet been performed.

Towards an early and accurate diagnosis

Amyloid imaging has had a major impact on the field of dementia research and it is likely to do so also with respect to clinical diagnosis of AD in the near future. To date, the best documented tracer for early and differential diagnostics of AD still is ^{11}C -PIB. The data on MCI patients and cognitively healthy controls strongly suggest that ^{11}C -PIB is indeed able to detect early accumulation of AD related pathology. However, ^{18}F -labelled amyloid binding agents are currently being evaluated and improved and it is only a matter of time before they will be widely available. The major drawback of amyloid imaging using ^{11}C -PIB, being confined to centers with an on site cyclotron, will be eliminated. This will lead to early and accurate diagnosis in more and more patients with (prodromal) AD and hopefully treatment with disease modifying therapies before irreversible damage has occurred.

List of references

1. Klunk WE, Engler H, Nordberg A et al. Imaging brain amyloid in Alzheimer's disease with Pittsburgh Compound-B. *Ann Neurol*. 2004;55:306-19
2. Small GW, Kepe V, Ercoli LM et al. PET of brain amyloid and tau in mild cognitive impairment. *N Engl J Med*. 2006;355:2652-63
3. Small BJ, Fratiglioni L, Viitanen M, Winblad B, Backman L. The course of cognitive impairment in preclinical Alzheimer disease: three- and 6-year follow-up of a population-based sample. *Arch Neurol*. 2000;57:839-44
4. Petersen RC, Smith GE, Waring SC et al. Mild cognitive impairment: clinical characterization and outcome. *Arch Neurol*. 1999;56:303-8
5. McKhann G, Drachman D, Folstein M et al. Clinical diagnosis of Alzheimer's disease: report of the NINCDS-ADRDA Work Group under the auspices of Department of Health and Human Services Task Force on Alzheimer's Disease. *Neurology*. 1984;34:939-44
6. Braak H, Braak E. Neuropathological staging of Alzheimer-related changes. *Acta Neuropathol (Berl)*. 1991;82:239-59
7. Braak H, Braak E. Staging of Alzheimer's disease-related neurofibrillary changes. *Neurobiol Aging*. 1995;16:271-8
8. Hardy JA, Higgins GA. Alzheimer's disease: the amyloid cascade hypothesis. *Science*. 1992;256:184-5
9. Bierer LM, Hof PR, Purohit DP et al. Neocortical neurofibrillary tangles correlate with dementia severity in Alzheimer's disease. *Arch Neurol*. 1995;52:81-8
10. McKhann G, Knopman D, Chertkow H et al. The diagnosis of dementia due to Alzheimer's disease: Recommendations from the National Institute on Aging-Alzheimer's Association workgroups on diagnostic guidelines for Alzheimer's disease. *Alzheimer's & Dementia*. 2011;7:263-9
11. Albert MS, DeKosky ST, Dickson DW et al. The diagnosis of mild cognitive impairment due to Alzheimer's disease: Recommendations from the National Institute on Aging-Alzheimer's Association workgroups on diagnostic guidelines for Alzheimer's disease. *Alzheimer's & Dementia*. 2011;7:270-9
12. Dubois B, Feldman HH, Jacova C et al. Research criteria for the diagnosis of Alzheimer's disease: revising the NINCDS-ADRDA criteria. *Lancet Neurol*. 2007;6:734-46
13. Scheltens P, Leys D, Barkhof F et al. Atrophy of medial temporal lobes on MRI in "probable" Alzheimer's disease and normal ageing: diagnostic value and neuropsychological correlates. *J Neurol Neurosurg Psychiatry*. 1992;55:967-72
14. Schoonenboom NS, Pijnenburg YA, Mulder C et al. Amyloid beta(1-42) and phosphorylated tau in CSF as markers for early-onset Alzheimer disease. *Neurology*. 2004;62:1580-4
15. Silverman DH, Gambhir SS, Huang HW et al. Evaluating early dementia with and without assessment of regional cerebral metabolism by PET: a comparison of predicted costs and benefits. *J Nucl Med*. 2002;43:253-66
16. Minoshima S, Giordani B, Berent S et al. Metabolic reduction in the posterior cingulate cortex in very early Alzheimer's disease. *Ann Neurol*. 1997;42:85-94
17. Ishii K, Sakamoto S, Sasaki M et al. Cerebral glucose metabolism in patients with frontotemporal dementia. *J Nucl Med*. 1998;39:1875-8
18. Ishii K, Imamura T, Sasaki M et al. Regional cerebral glucose metabolism in dementia with Lewy bodies and Alzheimer's disease. *Neurology*. 1998;51:125-30
19. Klunk WE, Lopresti BJ, Ikonovic MD et al. Binding of the positron emission tomography tracer Pittsburgh compound-B reflects the amount of amyloid-beta in Alzheimer's disease brain but not in transgenic mouse brain. *J Neurosci*. 2005;25:10598-606
20. Klunk WE, Wang Y, Huang GF et al. The binding of 2-(4'-methylaminophenyl)benzothiazole to postmortem brain homogenates is dominated by the amyloid component. *J Neurosci*. 2003;23:2086-92
21. Shoghi-Jadid K, Small GW, Agdeppa ED et al. Localization of neurofibrillary tangles and beta-amyloid plaques in the brains of living patients with Alzheimer disease. *Am J Geriatr Psychiatry*. 2002;10:24-35
22. Price JC, Klunk WE, Lopresti BJ et al. Kinetic modeling of amyloid binding in humans using PET imaging and Pittsburgh Compound-B. *J Cereb Blood Flow Metab*. 2005;25:1528-47
23. Lopresti BJ, Klunk WE, Mathis CA et al. Simplified quantification of Pittsburgh Compound B amyloid imaging PET studies: a comparative analysis. *J Nucl Med*. 2005;46:1959-72
24. Verhoeff NP, Wilson AA, Takeshita S et al. In-vivo imaging of Alzheimer disease beta-amyloid with ^{11}C -SB-13 PET. *Am J Geriatr Psychiatry*. 2004;12:584-95
25. Rowe CC, Ng S, Ackermann U et al. Imaging beta-amyloid burden in aging and dementia. *Neurology*. 2007;68:1718-25
26. Archer HA, Edison P, Brooks DJ et al. Amyloid load and cerebral atrophy in Alzheimer's disease: an ^{11}C -PIB positron emission tomography study. *Ann Neurol*. 2006;60:145-7
27. Edison P, Archer HA, Hinz R et al. Amyloid, hypometabolism, and cognition in Alzheimer disease: an ^{11}C -PIB and ^{18}F -FDG PET study. *Neurology*. 2007;68:501-8
28. Forsberg A, Engler H, Almkvist O et al. PET imaging of amyloid deposition in patients with mild cognitive impairment. *Neurobiol Aging*. 2008;29:1456-65
29. Ercoli LM, Siddarth P, Kepe V et al. Differential FDDNP PET patterns in nondemented middle-aged and older adults. *Am J Geriatr Psychiatry*. 2009;17:397-406
30. Boxer AL, Rabinovici GD, Kepe V et al. Amyloid imaging in

- distinguishing atypical prion disease from Alzheimer disease. *Neurology*. 2007;69:283-90
31. Small GW, Kepe V, Huang GF. In vivo brain imaging of tau aggregation in frontotemporal dementia using 18F-FDDNP PET. International Conference on Alzheimer and Related Disorders (ICAD). 2004 (Abstract)
 32. Braskie MN, Klunder AD, Hayashi KM et al. Plaque and tangle imaging and cognition in normal aging and Alzheimer's disease. *Neurobiol Aging*. 2010;31:1669-78
 33. Shin J, Lee SY, Kim SH, Kim YB, Cho SJ. Multitracer PET imaging of amyloid plaques and neurofibrillary tangles in Alzheimer's disease. *Neuroimage*. 2008;43:236-344.
 34. Lavretsky H, Siddarth P, Kepe V et al. Depression and anxiety symptoms are associated with cerebral FDDNP-PET binding in middle-aged and older nondemented adults. *Am J Geriatr Psychiatry*. 2009;17:493-502
 35. Tolboom N, Yaqub M, van der Flier WM et al. Detection of Alzheimer Pathology In Vivo Using Both 11C-PIB and 18F-FDDNP PET. *J Nucl Med*. 2009;50:191-7
 36. Agdeppa ED, Kepe V, Liu J et al. Binding characteristics of radiofluorinated 6-dialkylamino-2-naphthylethylidene derivatives as positron emission tomography imaging probes for beta-amyloid plaques in Alzheimer's disease. *J Neurosci*. 2001;21:RC189
 37. Villemagne VL, Pike K, Chetelat G et al. Longitudinal assessment of A β and cognition in aging and Alzheimer disease. *Ann Neurol*. 2011;69:181-92
 38. Koivunen J, Scheinin M, Virta JR et al. Amyloid PET imaging in patients with mild cognitive impairment: a 2-year follow-up study. *Neurology*. 2011;76:1085-90
 39. Jack CR, Jr., Lowe VJ, Weigand SD et al. Serial PIB and MRI in normal, mild cognitive impairment and Alzheimer's disease: implications for sequence of pathological events in Alzheimer's disease. *Brain*. 2009;132:1355-65
 40. Okello A, Koivunen J, Edison P et al. Conversion of amyloid positive and negative MCI to AD over 3 years: An 11C-PIB PET study. *Neurology*. 2009;73:754-60
 41. Mintun MA, LaRossa GN, Sheline YI et al. 11C-PIB in a nondemented population: potential antecedent marker of Alzheimer disease. *Neurology*. 2006;67:446-52
 42. Morris JC, Roe CM, Grant EA et al. Pittsburgh Compound B Imaging and Prediction of Progression From Cognitive Normality to Symptomatic Alzheimer Disease. *Arch Neurol*. 2009;66:1469-75
 43. Rowe CC, Ellis KA, Rimajova M et al. Amyloid imaging results from the Australian Imaging, Biomarkers and Lifestyle (AIBL) study of aging. *Neurobiol Aging*. 2010;31:1275-83
 44. Reiman EM, Chen K, Liu X et al. Fibrillar amyloid-beta burden in cognitively normal people at 3 levels of genetic risk for Alzheimer's disease. *Proc Natl Acad Sci U S A*. 2009;106:6820-5
 45. Price JL, Morris JC. Tangles and plaques in nondemented aging and "preclinical" Alzheimer's disease. *Ann Neurol*. 1999;45:358-68
 46. Morris JC, Price AL. Pathologic correlates of nondemented aging, mild cognitive impairment, and early-stage Alzheimer's disease. *J Mol Neurosci*. 2001;17:101-18
 47. Rabinovici GD, Furst AJ, O'Neill JP et al. 11C-PIB PET imaging in Alzheimer disease and frontotemporal lobar degeneration. *Neurology*. 2007;68:1205-12
 48. Edison P, Rowe CC, Rinne JO et al. Amyloid Load in Parkinson's Disease Dementia and Lewy Body Dementia Measured with 11C-PIB Positron Emission Tomography. *J Neurol Neurosurg Psychiatry*. 2008;79:1331-8
 49. Yaqub M, Tolboom N, Boellaard R et al. Simplified parametric methods for 11C-PIB studies. *Neuroimage*. 2008;42:76-86
 50. Yaqub M, Tolboom N, van Berckel BNM et al. Simplified parametric methods for 18F-FDDNP studies. *Neuroimage*. 2010;49:433-41
 51. McNamee RL, Yee SH, Price JC et al. Consideration of optimal time window for Pittsburgh compound B PET summed uptake measurements. *J Nucl Med*. 2009;50:348-55
 52. Tolboom N, Flier WM, Boverhoff J et al. Molecular imaging in the diagnosis of Alzheimer's disease: visual interpretation of 11C-PIB and 18F-FDDNP PET images. *J Neurol Neurosurg Psychiatry*. 2010;81:882-4
 53. Ng S, Villemagne VL, Berlangieri S et al. Visual Assessment Versus Quantitative Assessment of 11C-PIB PET and 18F-FDG PET for Detection of Alzheimer's Disease. *J Nucl Med*. 2007;48:547-52
 54. Rinne JO, Brooks DJ, Rossor MN et al. 11C-PiB PET assessment of change in fibrillar amyloid-[beta] load in patients with Alzheimer's disease treated with bapineuzumab: a phase 2, double-blind, placebo-controlled, ascending-dose study. *The Lancet Neurology*. 2010;9:363-72
 55. Rowe CC, Ackerman U, Browne W et al. Imaging of amyloid beta in Alzheimer's disease with 18F-BAY94-9172, a novel PET tracer: proof of mechanism. *Lancet Neurol*. 2008;7:129-35
 56. Lee JH, Byeon SR, Kim Y et al. 18F-labeled isoindol-1-one and isoindol-1,3-dione derivatives as potential PET imaging agents for detection of beta-amyloid fibrils. *Bioorg Med Chem Lett*. 2008;18:5701-4
 57. Nyberg S, Jonhagen ME, Cselenyi Z et al. Detection of amyloid in Alzheimer's disease with positron emission tomography using 11C-AZD2184. *Eur J Nucl Med Mol Imaging*. 2009;36:1859-63
 58. Sundgren-Andersson AK, Svensson S, Swahn BM et al. AZD4694: Fluorinated PET radioligand for detection of beta-amyloid deposits. International Conference on Alzheimer and Related Disorders (ICAD). 2009 (Abstract)
 59. Nelissen N, van Laere K, Thurfjell L et al. Phase 1 Study of the Pittsburgh Compound B Derivative 18F-Flutemetamol in Healthy Volunteers and Patients with Probable Alzheimer Disease. *J Nucl Med*. 2009;50:1251-9
 60. Sperling RA, Johnson KA, Pontecorvo MJ et al. PET Imaging of beta-amyloid with florpiramine F18 (F18-AV45): preliminary results from a phase II study of cognitively normal elderly subjects, individuals with MCI, and patients with a clinical diagnosis of AD. International Conference on Alzheimer and Related Disorders (ICAD). 2009 (Abstract)
 61. Clark C, Schneider JA, Bedell BJ et al. Use of Florbetapir-PET for imaging B-amyloid pathology. *JAMA: The Journal of the American Medical Association*. 2011;305:275-83
 62. Vandenberghe R, Van Laere K, Ivanoiu A et al. 18F-Flutemetamol amyloid imaging in Alzheimer disease and mild cognitive impairment - A phase 2 trial. *Ann Neurol*. 2010;68:319-29 

SIEMENS



PET en MR geïntegreerd in één systeem

De Biograph mMR, 's werelds eerste en enige whole-body moleculaire MR

De Biograph mMR brengt een revolutie in diagnostische beeldvorming tot leven. Voor het eerst zijn state-of-the-art 3T MRI en cutting-edge moleculaire beeldvorming volledig geïntegreerd in één systeem. Alleen Siemens maakt het mogelijk om gelijktijdig beelden te genereren van de morfologie, functie en het metabolisme van het hele lichaam. Whole-body PET en MR volledig geïntegreerd.

Precies uitgelijnd. Voor adembenemende, accurate beelden die leiden tot nieuwe inzichten in ziekteprocessen en de ontwikkeling van nieuwe behandelmethoden. Voor nieuwe onderzoeksmogelijkheden om tot een beter begrip van het leven te kunnen komen.

Biograph mMR – PET en MR zijn vanaf nu één.

www.siemens.nl/healthcare

Amyloid imaging with PET: what will be next?

J. Booij, MD, PhD

Department of Nuclear Medicine, Academic Medical Center,
University of Amsterdam, the Netherlands

Abstract

Booij, J. Amyloid imaging with PET: what will be next? In the near future, PET tracers will be commercially available to image extracellular fibrillar β -amyloid in the brain. This important development will be of interest not only for research purposes, but also in the diagnostic work-up of demented (or possibly demented) patients. Apart from this development, efforts are going on to image amyloid in the brain with imaging techniques other than PET, to image other relevant neuropathological features of dementia, and to image other protein aggregates than β -amyloid which may be relevant for neurodegenerative disorders. The highlights of these developments will be described in this short review. *Tijdschr Nucl Geneesk* 2011; 33(4):822-825

Introduction

In another article of this issue, the concept of amyloid imaging with PET was described extensively (1). In the near future, brain amyloid imaging will be of interest not only for research purposes (e.g., to test the clinically relevant hypothesis that amyloid depositions may be present in the brain years before the onset of dementia), but also in the diagnostic work-up of demented (or possibly demented) patients (2). In the forthcoming years, ^{18}F -labelled tracers (named flutemetamol, florbetapir, or florbetaben; 3-5) will be produced commercially at central cyclotron sites and delivered to clinical PET centres to image amyloid (2).

Although the importance of this development for the society of nuclear medicine, and the society at large, can not be emphasized sufficiently, efforts are going on to image amyloid in the brain with imaging techniques other than PET, to image other relevant neuropathological features of dementia, and to image other protein aggregates than β -amyloid which may be relevant for the neurodegenerative disorders. This short review will describe the highlights of these developments.

Brain amyloid imaging with SPECT and MR techniques

In 2004, the first successful human brain amyloid PET study in Alzheimer's patients was published (6). In that study, a tracer called Pittsburgh Compound-B (PiB) was used. This ^{11}C -labelled compound is a derivate of the amyloid dye Thioflavin-T. Likewise, the ^{18}F -labelled tracers are derivatives from Thioflavin. Compared to PET, SPECT offers several advantages. For that reason, several attempts have been made to develop SPECT tracers for imaging of amyloid plaques. However, as compared to PET, this progress is lagging far

behind (7). The development of iodinated tracers derived from the amyloid dye Congo red has been rather disappointing. Since Thioflavin-T has a lower molecular weight than Congo red, the development of SPECT tracers derived from Thioflavin has been more successful. The Thioflavin derivate ^{123}I -IMPY has been evaluated clinically (8,9). Although its brain distribution was comparable to that of amyloid PiB PET tracers, the signal to noise ratios were too low to be useful as a diagnostic tool (9). With the intention to increase these uptake ratios, by reducing the lipophilicity of IMPY, new iodinated Thioflavine derivatives have been synthesized and characterized recently (10). One of the novel compounds (BZMZ) showed high affinity for amyloid aggregates in vitro. In addition, the radioiodinated derivative displayed excellent uptake into, and rapid washout from, the brain of normal mice. Specific labeling of amyloid plaques was demonstrated by autoradiography with human AD brain sections in vitro and by autoradiograms in a mouse model of Alzheimer's disease ex vivo. These findings suggest that this is a promising SPECT probe for the imaging of amyloid plaques in the brain.

Additionally, also other potential tracers not derived from Congo red or Thioflavin-T have been synthesized (e.g., flavones; 7) and evaluated in-vitro and ex-vivo in small laboratory animals (11). Preliminary findings suggest that these new tracers bind to a binding site on amyloid aggregates different from that of Thioflavin-T and Congo red, and that some of them also label another neuropathological hallmark of Alzheimer's disease, namely intracellular neurofibrillary tangles (NFTs) (7). Finally, several $^{99\text{m}}\text{Tc}$ -labelled tracers have been synthesized with the intention to image amyloid. Although these radiotracers bind to amyloid in-vitro, the in-vivo brain uptake is too low to start clinical studies (12). All together, although there is progress in the development and characterization of SPECT tracers to image amyloid in the brain, it is not realistic that such a tracer will be (commercially) available in the forthcoming years.

Several groups have tried to image amyloid plaques in the brain with MRI techniques (13). Amyloid plaques contain iron (14). Since iron is paramagnetic, it can be used as an intrinsic MR contrast (i.e., without administration of an exogenous labelled contrast). Until now, successful ex-vivo MR studies have been performed in human tissue of patients suffering from Alzheimer's disease and in tissue obtained from a transgenic mice model of Alzheimer's disease (13, 15). Indeed, in human Alzheimer's tissue, amyloid plaques with high iron accumulation are clearly visualized ex-vivo, on T_2^* -weighted images, while others with less iron are not as discernable (15). So, although MR imaging of individual

plaques in mouse models of Alzheimer's disease and ex-vivo in human Alzheimer's tissue has been proven, there are many challenges in moving from mouse to human imaging (16). For example, movement artefact will be larger in human studies, imaging time should be reduced, as well as the field of view (16), which held back the initiation of clinical studies.

Another approach is to use exogenous plaque labelling contrast agents. A multifunctional molecule was tested, in which one part enhances blood-brain barrier permeability, another part MRI relaxation, and a third part affected binding to amyloid (17). Finally, in-vivo labelling in mouse models of Alzheimer's disease has been successful with a ^{19}F -labelled Congo red derivative (18). Compared to traditional proton MRI, the advantage of ^{19}F -MRI is the lack of background signal. Until now, particularly lack of sensitivity prevents the initiation of clinical studies.

Oligomeric forms of β -amyloid

β -amyloid is a peptide naturally occurring in the brain (19). Amyloid fibrils are composed of protofibrils forming a crossed β -pleated sheet structure. The assembly of these fibrils is the most obvious pathological feature of Alzheimer's disease, but it is not likely that these fibrils trigger neuronal degeneration. A hypothesis proposed several mechanistic pathways of fibril formation with monomeric amyloid self-aggregating to form soluble dimers and trimers and larger oligomers; prior to their formation of protofibrils and finally the fibrils found in plaques (19).

The PiB PET tracer preferentially binds to extracellular insoluble fibrillar β -amyloid plaques (6, 20) and with much lower affinity to the oligomeric forms of β -amyloid (21). The same may be true for the abovementioned ^{18}F -labelled PiB derivatives. However, the oligomeric forms of β -amyloid are believed to be more toxic than fibrillar amyloid (22-24), and correlate better with the degree of neurodegeneration (25) and cognitive deficits (26). Importantly, soluble oligomeric only comprise approximately 1% of total measurable β -amyloid in the frontal cortex of patients suffering from Alzheimer's disease (25). In addition, different types of oligomers have been reported (for a review, see 26), and it is not clear which of these types are toxic for neurons. This uncertainty, as well as the low amounts of oligomers, hampers the development of diagnostic markers to image these oligomers.

Amyloid imaging and correlations with cognitive deficits

The most direct pathological substrate of clinical symptoms in dementia is neurodegeneration, and most specifically loss of synapses (27). Indeed, recent autopsy data have confirmed that cerebral atrophy (indicating the loss of synapses and neurons), and not amyloid burden, is the most proximate pathological substrate of cognitive impairment in Alzheimer's disease (28). In this context, it is of interest that amyloid imaging with PET did not show correlations with clinical measures. First, approximately 10-20% of cognitively normal elderly subjects have evidence of significant amyloid burden, as shown by amyloid PET studies (29,30) and is associated

with APOE epsilon4 gene dose (31), a well known risk factor to develop Alzheimer's disease. Consequently, amyloid imaging may be a sensitive imaging tool to predict conversion to clinical Alzheimer's disease (32). Second, a study showed stable amyloid burden after 2 years of follow-up in patients with mild Alzheimer's disease (33). Third, a recent study showed that administration of humanised anti-amyloid-beta monoclonal antibody in patients with Alzheimer's disease resulted in a 9% decrease of amyloid binding (while the control group increased 15%), but this decrease had no beneficial impact on clinical symptoms (34).

Another neuropathological protein deposit that characterizes Alzheimer's disease (and other neurodegenerative diseases like Pick's disease and progressive supranuclear palsy) are intracellular NFT, which are formed by hyperphosphorylated tau. Neurodegeneration and NFT deposition are both neuronal processes and occur roughly in the same topographical distribution (35). So, tau pathology is associated with neuronal injury. Consequently, clinical symptoms may be more closely related to NFTs than to plaque formation (36). In this regard, it is of interest that the development of tau-imaging is on its way. A recent study by Fodero-Tavoletti and co-workers showed that a novel ^{18}F -labelled tracer (called THK523) binds with high affinity and selectivity to tau (37). Moreover, autoradiography/histofluorescence studies showed that it labels tau, but not amyloid, in brain tissue of patients suffering from Alzheimer's disease. Finally, micro-PET studies showed higher brain uptake in mouse models expressing tau than in control mice. It is therefore likely that human imaging trials will start in the near future. Tau imaging may be of interest particularly to monitor the therapeutic efficacy of newly developed drugs aimed at modifying tau pathology. Moreover, it may also be of value to monitor decline of cognitive functions. In this regard, however, its possible role has to be defined since glucose hypometabolism as measured by ^{18}F -FDG PET correlates also closely with cognitive signs (and disease progression) in Alzheimer's disease (38).

Synuclein imaging

Misfolded α -synuclein proteins comprise the principal component of Lewy bodies, which are pathological hallmarks of Lewy body disorders like Parkinson's disease and dementia with Lewy bodies. Although the abovementioned amyloid imaging tracers were developed to bind to β -amyloid fibrils, their precise molecular target might be not the β -amyloid peptide sequence *per se* but rather the generic β -pleated sheet structure that forms the amyloid folds (39). Amyloid structures are therefore not restricted to β -amyloid containing lesions but can also be formed by a range of other proteins, including α -synuclein (40). In this regard, it is not surprising that novel tracers aimed to image β -amyloid, are also tested whether they bind to synuclein as well. For example, PiB binds with lower affinity to α -synuclein fibrils than to β -amyloid fibrils (41). A novel ^{18}F -labelled tracer (BF227) labelled both β -amyloid plaques and Lewy bodies in immunohistochemical/

fluorescence analysis of human Alzheimer's disease and Parkinson's disease brain sections, respectively (42).

Nevertheless, it is likely that in the future attempts will be made to synthesize selective radiotracers for α -synuclein.

Conclusion

^{18}F -labelled amyloid PET tracers will be commercially available in the near future, and these tracers will find their way into research (to test the amyloid hypothesis; whether amyloid plaques kill brain tissue or are a side effect of the disease process) and routine diagnostic studies (43). These novel techniques will not only enhance our diagnostic armamentarium in nuclear medicine, but will also stimulate the development of other imaging techniques to image amyloid and other proteins relevant for the neuropathology of neurodegenerative disorders.

List of references

1. Tolboom N, Ossenkuppele R, van Berckel BNM. Amyloid Imaging in Alzheimer's disease. *Tijdsch Nucl Gen.* 2011;33:816-20
2. Herholz K, Ebmeier K. Clinical amyloid imaging in Alzheimer's disease. *Lancet Neurol.* 2011;10:667-70
3. Barthel H, Gertz HJ, Dresel S et al. Cerebral amyloid- β PET with florbetaben 18F in patients with Alzheimer's disease and healthy controls: a multicentre phase 2 diagnostic study. *Lancet Neurol.* 2011;10:424-35
4. Clark CM, Schneider JA, Bedell BJ et al. Use of florbetapir-PET for imaging beta-amyloid pathology. *JAMA.* 2011;305:275-83
Erratum in: *JAMA.* 2011;305:1096
5. Vandenberghe R, Van Laere K, Ivanoiu A et al. 18F-flutemetamol amyloid imaging in Alzheimer disease and mild cognitive impairment: a phase 2 trial. *Ann Neurol.* 2010;68:319-29
6. Klunk WE, Engler H, Nordberg A et al. Imaging brain amyloid in Alzheimer's disease with Pittsburgh Compound-B. *Ann Neurol.* 2004;55:306-19
7. Ono M, Saji H. SPECT Imaging Agents for Detecting Cerebral β -Amyloid Plaques. *Int J Mol Imaging.* 2011: in press
8. Newberg AB, Wintering NA, Plössl K et al. Safety, biodistribution, and dosimetry of 123I-IMPY: a novel amyloid plaque-imaging agent for the diagnosis of Alzheimer's disease. *J Nucl Med.* 2006;47:748-54
9. Newberg AB, Wintering NA, Clark CM et al. Use of 123I-IMPY SPECT to differentiate Alzheimer's disease from controls. *J Nucl Med* 2006;47 (suppl):78
10. Cui M, Ono M, Kimura H et al. Radioiodinated benzimidazole derivatives as single photon emission computed tomography probes for imaging of β -amyloid plaques in Alzheimer's disease. *Nucl Med Biol.* 2011;38:313-20
11. Ono M, Yoshida N, Ishibashi K et al. Radioiodinated flavones for in vivo imaging of beta-amyloid plaques in the brain. *J Med Chem.* 2005;48:7253-60
12. Ono M, Ikeoka R, Watanabe H et al. 99mTc/Re complexes based on flavone and aurone as SPECT probes for imaging cerebral β -amyloid plaques. *Bioorg Med Chem Lett.* 2010;20:5743-8
13. Jack CR Jr, Marjanska M, Wengenack TM et al. Magnetic resonance imaging of Alzheimer's pathology in the brains of living transgenic mice: a new tool in Alzheimer's disease research. *Neuroscientist.* 2007;13:38-48
14. Lovell MA, Robertson JD, Teesdale WJ, Campbell JL, Markesbery WR. Copper, iron and zinc in Alzheimer's disease senile plaques. *J Neurol Sci.* 1998;158:47-52
15. Meadowcroft MD, Connor JR, Smith MB, Yang QX. MRI and histological analysis of beta-amyloid plaques in both human Alzheimer's disease and APP/PS1 transgenic mice. *J Magn Reson Imaging.* 2009;29:997-1007
16. Chamberlain R, Wengenack TM, Poduslo JF, Garwood M, Jack CR Jr. Magnetic resonance imaging of amyloid plaques in transgenic mouse models of Alzheimer's disease. *Curr Med Imaging Rev.* 2011;7:3-7
17. Poduslo JF, Wengenack TM, Curran GL et al. Molecular targeting of Alzheimer's amyloid plaques for contrast-enhanced magnetic resonance imaging. *Neurobiol Dis.* 2002;11:315-29
18. Higuchi M, Iwata N, Matsuba Y et al. 19F and 1H MRI detection of amyloid beta plaques in vivo. *Nat Neurosci.* 2005;8:527-33
19. Fodero-Tavoletti MT, Villemagne VL, Rowe CC et al. Amyloid- β : The seeds of darkness. *Int J Biochem Cell Biol.* 2011: in press
20. Ikonomic MD, Klunk WE, Abrahamson EE et al. Post-mortem correlates of in vivo PiB-PET amyloid imaging in a typical case of Alzheimer's disease. *Brain.* 2008;131:1630-45
21. Maezawa I, Hong HS, Liu R et al. Congo red and thioflavin-T analogs detect Abeta oligomers. *J Neurochem.* 2008;104:457-68
22. Lambert MP, Viola KL, Chromy BA et al. Vaccination with soluble Abeta oligomers generates toxicity-neutralizing antibodies. *J Neurochem.* 2001;79:595-605
23. Walsh DM, Klyubin I, Fadeeva JV et al. Naturally secreted oligomers of amyloid beta protein potently inhibit hippocampal long-term potentiation in vivo. *Nature.* 2002;416:535-9
24. Ferreira ST, Vieira MN, De Felice FG. Soluble protein oligomers as emerging toxins in Alzheimer's and other amyloid diseases. *IUBMB Life.* 2007;59:332-45
25. McLean CA, Cherny RA, Fraser FW et al. Soluble pool of Abeta amyloid as a determinant of severity of neurodegeneration in Alzheimer's disease. *Ann Neurol.* 1999;46:860-6
26. Haass C, Selkoe DJ. Soluble protein oligomers in neurodegeneration: lessons from the Alzheimer's amyloid beta-peptide. *Nat Rev Mol Cell Biol.* 2007;8:101-12
27. Terry RD, Masliah E, Salmon DP et al. Physical basis of cognitive alterations in Alzheimer's disease: synapse loss is the major correlate of cognitive impairment. *Ann Neurol.* 1991;30:572-80
28. Savva GM, Wharton SB, Ince PG, Forster G, Matthews FE, Brayne C. Age, neuropathology, and dementia. *N Engl J Med.* 2009;360:2302-9
29. Mintun MA, Larossa GN, Sheline YI et al. 11C-PIB in a nondemented population: potential antecedent marker of Alzheimer disease. *Neurology.* 2006;67:446-52
30. Aizenstein HJ, Nebes RD, Saxton JA et al. Frequent amyloid deposition without significant cognitive impairment among the elderly. *Arch Neurol.* 2008;65:1509-17
31. Reiman EM, Chen K, Liu X et al. Fibrillar amyloid-beta burden in cognitively normal people at 3 levels of genetic risk for

- Alzheimer's disease. Proc Natl Acad Sci U S A. 2009; 21:6820-5
32. Koivunen J, Scheinin N, Virta JR et al. Amyloid PET imaging in patients with mild cognitive impairment: a 2-year follow-up study. Neurology. 2011;76:1085-90
 33. Engler H, Forsberg A, Almkvist O et al. Two-year follow-up of amyloid deposition in patients with Alzheimer's disease. Brain. 2006;129:2856-66
 34. Rinne JO, Brooks DJ, Rossor MN et al. 11C-PiB PET assessment of change in fibrillar amyloid-beta load in patients with Alzheimer's disease treated with bapineuzumab: a phase 2, double-blind, placebo-controlled, ascending-dose study. Lancet Neurol. 2010;9:363-72
 35. Jack CR Jr, Knopman DS, Jagust WJ et al. Hypothetical model of dynamic biomarkers of the Alzheimer's pathological cascade. Lancet Neurol. 2010;9:119-28
 36. Bennett DA, Schneider JA, Wilson RS, Bienias JL, Arnold SE. Neurofibrillary tangles mediate the association of amyloid load with clinical Alzheimer disease and level of cognitive function, Arch Neurol. 2004;61:378-84
 37. Fodero-Tavoletti MT, Okamura N, Furumoto S et al. 18F-THK523: a novel in vivo tau imaging ligand for Alzheimer's disease. Brain. 2011;134:1089-100
 38. Herholz K, Carter SF, Jones M. Positron emission tomography imaging in dementia. Br J Radiol. 2007;80:S160-7
 39. Fowler DM, Koulov AV, Balch WE, Kelly JW. Functional amyloid—from bacteria to humans. Trends Biochem Sci. 2007;32:217-24
 40. Ye L, Velasco A, Fraser G et al. In vitro high affinity alpha-synuclein binding sites for the amyloid imaging agent PIB are not matched by binding to Lewy bodies in postmortem human brain. J Neurochem. 2008;105:1428-37
 41. Fodero-Tavoletti MT, Smith DP, McLean CA et al. In vitro characterization of Pittsburgh compound-B binding to Lewy bodies. J Neurosci. 2007;27:10365-71
 42. Fodero-Tavoletti MT, Mulligan RS, Okamura N et al. In vitro characterisation of BF227 binding to alpha-synuclein/Lewy bodies. Eur J Pharmacol. 2009;617:54-8
 43. Ledford H. Alzheimer's-disease probe nears approval. Nature. 2011;469:458 

Quadramet® Summary of Product Characteristics

PRESCRIBING INFORMATION : QUADRAMET, solution for injection. Please refer to the full Summary of Product Characteristics (SPC) before prescribing. Detailed information on this medicinal product is available on the website of the European Medicines Agency (EMA) <http://www.ema.europa.eu>. **PRESENTATION** : Each ml of solution contains 1.3 GBq Samarium (¹⁵³Sm) lexidronam pentasodium at the reference date (corresponding to 20 to 46 µg/ml of samarium per vial). Samarium specific activity is approximately 28 – 65 MBq/µg of samarium. Each vial contains 2.4 GBq at the reference date. **THERAPEUTIC INDICATIONS** : QUADRAMET is indicated for the relief of bone pain in patients with multiple painful osteoblastic metastases which take up technetium (^{99m}Tc)-labelled biphosphonates on bone scan. The presence of osteoblastic metastases which take up technetium (^{99m}Tc)-labelled biphosphonates should be confirmed prior to therapy. **POSIOLOGY AND METHOD OF ADMINISTRATION** : QUADRAMET should only be administered by physicians experienced in the use of radiopharmaceuticals and after full oncological evaluation of the patient by qualified physicians. The recommended dose of QUADRAMET is 37 MBq per kg body weight and is to be administered by slow intravenous route through an established intravenous line over a period of one minute. QUADRAMET should not be diluted before use. Patients who respond to QUADRAMET generally experience the onset of pain relief within 1 week after treatment. Relief of pain may persist for 4 weeks up to 4 months. Patients who experience a reduction in pain may be encouraged to decrease their use of opioid analgesics. Repeat administration of QUADRAMET should be based on an individual patient's response to prior treatment and on clinical symptoms. A minimum interval of 8 weeks should be respected, subject to recovery of adequate bone marrow function. The data on the safety of repeated dosing are limited and based on compassionate use of the product. QUADRAMET is not recommended for use in children below the age of 18 years due to a lack of data on safety and efficacy. **CONTRAINDICATIONS** : QUADRAMET is contra-indicated in case of hypersensitivity to the active substance (ethylenediaminetetra(methylene)phosphonate (EDTMP) or similar phosphonates) or to any of the excipients, in pregnant women, in patients having received chemotherapy or radiotherapy or external radiation therapy in a preceding period of 5 weeks. QUADRAMET is used only as a palliative agent and should not be used concurrently with myelotoxic chemotherapy as this may enhance myelotoxicity. It should not be used concurrently with other biphosphonates if an interference is shown on the technetium (^{99m}Tc)-labelled biphosphonate bone scans. **SPECIAL WARNINGS AND PRECAUTIONS FOR USE** : In absence of clinical data, the injected activity should be adapted to the renal function. Use of QUADRAMET in patients with evidence of compromised bone marrow reserve from previous therapy or disease involvement is not recommended unless the potential benefit of the treatment outweighs its risks. Because of potential bone marrow suppression after administration, blood counts should be monitored weekly for at least 8 weeks, beginning 2 weeks after administration of QUADRAMET, or until recovery of adequate bone marrow function. The patient should be encouraged to ingest (or receive by intravenous administration) a minimum of 500 ml of fluids prior to injection and should be encouraged to void as often as possible after injection to minimise radiation exposure to the bladder. The clearance of QUADRAMET being rapid, the precautions relating to the excreted urinary radioactivity need not be taken after 6-12 hours following administration. Special precautions, such as bladder catheterisation, should be taken during six hours following administration to incontinent patients to minimise the risk of radioactive contamination of clothing, bed linen, and the patient's environment. For the other patients the urine should be collected for at least six (6) hours. Bladder catheterisation should be undertaken in patients with urinary obstruction. Radiopharmaceuticals may be received, used and administered only by authorised persons in designated clinical settings. Its receipt, storage, use, transfer and disposal are subject to the regulations and the appropriate licences of the local competent official organisations. Radiopharmaceuticals should be prepared by the user in a manner which satisfies both radiation safety and pharmaceutical quality requirements. Appropriate aseptic precautions should be taken, complying with the requirements of Good Manufacturing Practice for pharmaceuticals. **INTERACTIONS** : Because of the potential for additive effects on bone marrow, the treatment should not be given concurrently with chemotherapy or external beam radiation therapy. QUADRAMET may be given subsequent to either of these treatments after allowing for adequate marrow recovery. **PREGNANCY AND LACTATION** : QUADRAMET is contra-indicated in pregnancy. The possibility of pregnancy must strictly be ruled out. Women of childbearing potential have to use effective contraception during the treatment and the whole period of follow-up. There are no available clinical data relating to the excretion of QUADRAMET in human milk. If therefore QUADRAMET administration is deemed necessary, formula feeding should be substituted for breast-feeding and the expressed feeds discarded. **UNDESIRABLE EFFECTS** : Decreases in white blood cell and platelet counts and anaemia were observed in patients receiving QUADRAMET. In clinical trials white blood cell and platelet counts decreased to a nadir of approximately 40 % to 50 % of baseline 3 to 5 weeks after a dose, and generally returned to pre-treatment levels by 8 weeks post treatment. The few patients who experienced Grade 3 or 4 hematopoietic toxicity usually either had a history of recent external beam radiation therapy or chemotherapy or had rapidly progressive disease with probable bone marrow involvement. Postmarketing reports of thrombocytopenia have included isolated reports of intracranial haemorrhage, and cases in which the outcome was fatal. A small number of patients have reported a transient increase in bone pain shortly after injection (flare reaction). This is usually mild and self-limiting and occurs within 72 hours of injection. Such reactions are usually responsive to analgesics. Adverse drug reactions such as nausea, vomiting, diarrhoea and sweating were reported. Hypersensitivity reactions including rare cases of anaphylactic reaction have been reported after QUADRAMET administration. A few patients experienced cord/tongue compressions, disseminated intravascular coagulation and cerebrovascular accidents. The occurrence of these events may be linked to the patients' disease evolution. When there are spinal metastases at the cervico-dorsal level, an increased risk of spinal cord compression cannot be excluded. The radiation dose resulting from therapeutic exposure may result in higher incidence of cancer and mutations. In all cases, it is necessary to ensure that the risks of the radiation are less than from the disease itself. **DOSEMETRY** : the effective dose resulting from an injected activity of 2 590 MBq is 790 mSv. For an administered activity of 2 590 MBq, the typical radiation dose to the target organ, skeletal metastases, is 80.5 Gy and the typical radiation doses to the critical organs are: normal bone surfaces 17.5 Gy, red marrow 4.0 Gy, urinary bladder wall 2.5 Gy, kidneys 0.047 Gy and ovaries 0.021 Gy. **OVERDOSE** : The product should only be administered by qualified personnel in authorised settings. The possibility of pharmacological overdose is therefore remote. The risks to be expected are associated with the inadvertent administration of excess radioactivity. Radiation dose to the body can be limited by promoting a diuresis and frequent voiding of urine. **MARKETING AUTHORISATION HOLDER** : CIS bio international, BP 32, 91192 Gif sur Yvette Cedex France. **CLASSIFICATION FOR SUPPLY** : Subject to restricted medical prescription. **MARKETING AUTHORISATION NUMBER** : EU/19705/001. **DATE OF REVISION OF TEXT** : April 2011. **PLEASE REPORT ANY ADVERSE EVENTS TO HEALTH AUTHORITIES AND/OR CIS BIO INTERNATIONAL.**

Voorrang voor darmkankerpatiënten

Wil je weten hoe?



DarmkankerNederland.nl
zet darmkanker op de kaart

Ga naar
DarmkankerNederland.nl

Tijdschrift voor Nucleaire Geneeskunde
ISSN 1381-4842, nr. 4, december 2011
Uitgever



KLOOSTERHOF
ACQUISITIE SERVICES - UITGEVERIJ

Kloosterhof acquisitie services - uitgeverij
Napoleonsweg 128a
6086 AJ Neer
T 0475 59 71 51
F 0475 59 71 53
E info@kloosterhof.nl
I www.kloosterhof.nl

Hoofredacteuren van dit themanummer:

Drs. A.W.J.M. Glaudemans, a.w.j.m.glaudemans@umcg.nl
Dr. H.J. Verberne, h.j.verberne@amc.uva.nl

Hoofredacteur

prof. dr. J. Booiij
j.booiij@amc.uva.nl

Redactie

mw. drs. B. Bosveld
mw. drs. F. Celik
dr. J. van Dalen
dr. E.M.W. van de Garde
drs. A.W.J.M. Glaudemans
mw. prof. dr. I. Goethals
mw. dr. C.J. Hoekstra
dr. P. Laverant
J. de Swart
dr. H.J. Verberne

Bureau redactie

Yvonne van Pol-Houben
T 0475 60 09 44
E nucleaire@kloosterhof.nl

Advertentie-exploitatie

Kloosterhof Neer B.V.
acquisitie services - uitgeverij
Sandra Geraedts
T 0475 59 74 21
E. sandra@kloosterhof.nl

Vormgeving

Kloosterhof Vormgeving
Marie-José Verstappen
Sandra Geraedts

Abonnementen

Leden en donateurs van de aangesloten beroepsverenigingen ontvangen het Tijdschrift voor Nucleaire Geneeskunde kosteloos. Voor anderen geldt een abonnementsprijs van € 45,00 per jaar; studenten betalen € 29,00 per jaar (incl. BTW en verzendkosten). Opgave en informatie over abonnementen en losse nummers (€ 13,50) bij Kloosterhof acquisitie services - uitgeverij, telefoon 0475 59 71 51.

Verschijningsdata, jaargang 33

Nummer 4 23 december 2011

Verschijningsdata, jaargang 34

Nummer 1 24 maart 2012
Nummer 2 22 juni 2012
Nummer 3 22 september 2012
Nummer 4 28 december 2012

Aanleveren kopij, jaargang 34

Nummer 1 1 januari 2012
Nummer 2 1 april 2012
Nummer 3 1 juli 2012
Nummer 4 1 oktober 2012

Kloosterhof acquisitie services - uitgeverij

Het verlenen van toestemming tot publicatie in dit tijdschrift houdt in dat de auteur aan de uitgever onvoorwaardelijk de aanspraak overdraagt op de door derden verschuldigde vergoeding voor kopiëren, als bedoeld in Artikel 17, lid 2, der Auteurswet 1912 en in het KB van 20-71974 (stb. 351) en artikel 16b der Auteurswet 1912, teneinde deze te doen exploiteren door en overeenkomstig de Reglementen van de Stichting Reprorecht te Hoofddorp, een en ander behoudend uitdrukkelijk voorbehoud van de kant van de auteur.

Cursus- en Congresagenda

High Country Nuclear Medicine Conference

2 - 7 March, 2012. Steamboat Springs, USA. www.snm.org

30e NVvO Basiscursus Oncologie 2012

12 - 16 March, 2012. Ellecom, The Netherlands. www.nvvoncologie.nl

MIRO 2012

29 - 31 March, 2012. Vienna, Austria. www.miro-online.org

1st Balkan Congress of Nuclear Medicine

4 - 8 April, 2012. Antalya, Turkey. www.bcnm2012.org

Cursus Fluor-18 chemie

12-13 April, 2012. Amsterdam, The Netherlands. bwindhorst@rnc.vu.nl

TOPIM 2012 - ESMI midwinter conference

15 - 20 April, 2012. Les Houches, France. www.e-smi.eu

50th Annual Meeting of the German Society of Nuclear Medicine

25 - 28 April, 2012. Bremen, Germany. www.nuklearmedizin2012.de

ESSR'12 - 16th European Symposium on Radiopharmacy and Radiopharmaceuticals

26 - 29 April, 2012. Nantes, France. essr12.eanm.org

18de Symposium NKI-AVL - Ontwikkelingen in de oncologische zorg

7 June, 2012. Amsterdam, The Netherlands. www.nki.nl/symposium7juni2012

SNM Annual Meeting

9 - 13 June, 2012. Miami, FL, USA. www.snm.org/am2012

ESGAR 2012

12 - 15 June, 2012. Edinburgh, Great Britain. www.esgar.org

WMIC 2012

5 - 8 September, 2012. Dublin, Ireland. www.wmicmeeting.org

ASNC 2012

6 - 9 September, 2012. Baltimore, USA. www.asnc.org

EANM'12

27 - 31 October, 2012. Milan, Italy. www.eanm.org

Adreswijzigingen

Regelmatig komt het voor dat wijziging in het bezorgadres voor het Tijdschrift voor Nucleaire Geneeskunde op de verkeerde plaats worden doorgegeven. Adreswijzigingen moeten altijd aan de betreffende verenigingssecretariaten worden doorgegeven. Dus voor de medisch nucleair werkers bij de NVMBR, en voor de leden van de NVNG en het Belgisch Genootschap voor Nucleaire Geneeskunde aan hun respectievelijke secretariaten. De verenigingssecretariaten zorgen voor het doorgeven van de wijzigingen aan de Tijdschrift adresadministratie. Alleen adreswijzigingen van betaalde abonnementen moeten met ingang van 1 januari 2011 rechtstreeks aan de abonnementenadministratie van Kloosterhof Neer B.V. worden doorgegeven: Kloosterhof Neer B.V., t.a.v. administratie TvNG, Napoleonsweg 128a | 6086 AJ Neer of per E-mail: nucleaire@kloosterhof.nl

IMPAX Nuclear Medicine

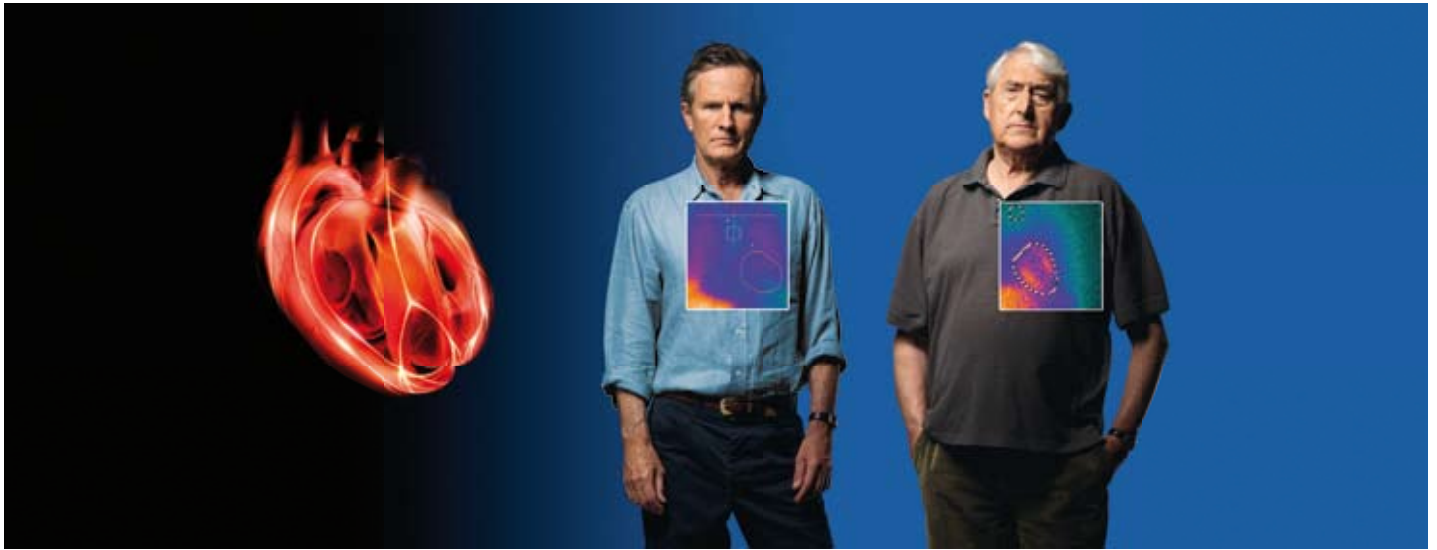
1 Solution Workstation Vendor

for all your **Nuclear Medicine** needs

With IMPAX Nuclear Medicine, Agfa HealthCare offers clinicians a unique solution which fully automates the Nuclear Medicine department's workflow and optimizes the communication between Nuclear Medicine specialists and other departments by making the relevant information available throughout the enterprise. IMPAX allows users to schedule a patient's entire examination flow, from arrival and process management through reporting and distribution of all nuclear medicine studies and reports. IMPAX Nuclear Medicine Information System supports complex scheduling requirements, including comprehensive resource planning, and can be integrated with the department's hot lab management solution to digitize and automate preparation of radiopharmaceuticals and registration of radiation dose. Oasis for IMPAX allows clinicians to further improve their workflow through its integrated and fully featured image processing and analysis software package. With IMPAX Nuclear Medicine, we help you transform the way you manage your department's workflow. **Healthcare transformation. We'll take you there.**

To learn more about our solutions, visit www.agfahealthcare.com.

Improving Heart Failure Risk Assessment



AdreView is a diagnostic agent providing a powerful prognostic insight into heart failure¹

- Assesses cardiac sympathetic innervation¹
- Helps predict patients who are at greater or lower risk of heart failure progression, arrhythmias & cardiac death¹
- Provides a Negative Predictive Value (NPV) of 96% for arrhythmia likelihood & an NPV of 98% for cardiac death likelihood over 2 years¹
- Provides superior prognostic information in combination with LVEF or BNP compared to LVEF or BNP alone¹
- Improves heart failure patients' risk assessment and may help clinicians' management decisions¹



GE imagination at work

AdreView™
Iobenguane I 123 Injection

AdreView is authorised for marketing in the following European countries: Germany, France, Spain, Italy, the United Kingdom, Denmark, Norway, The Netherlands and Belgium.

PRESCRIBING INFORMATION AdreView, Iobenguane (¹²³I) Injection 74 MBq/ml solution for injection

Please refer to full national Summary of Product Characteristics (SPC) before prescribing. Indications and approvals may vary in different countries. Further information available on request.

PRESENTATION Vials containing 74 MBq/ml [¹²³I]Iobenguane at calibration date and hour. Available pack size: 37 to 740 MBq. **DIAGNOSTIC INDICATIONS** • Assessment of sympathetic innervation of the myocardium as a prognostic indicator of risk for progression of symptomatic heart failure, potentially fatal arrhythmic events, or cardiac death in patients with NYHA class II or class III heart failure and LV dysfunction. • Diagnostic scintigraphic localisation of tumours originating in tissue that embryologically stems from the neural crest. These are pheochromocytomas, paragangliomas, chemodectomas and ganglioneuromas. • Detection, staging and follow-up on therapy of neuroblastomas. • Evaluation of the uptake of Iobenguane. The sensitivity to diagnostic visualisation is different for the listed pathological entities. The sensitivity is approximately 90% for the detection of pheochromocytoma and neuroblastoma, 70% in case of carcinoid and only 35% in case of medullary thyroid carcinoma (MTC). • Functional studies of the adrenal medulla (hyperplasia). **DOSAGE AND METHOD OF ADMINISTRATION** Cardiology: For adults the recommended dosage is 370MBq. Children under 6 months: 4 MBq per kg body weight (max. 40 MBq), the product must not be given to premature babies or neonates. Children between 6 months and 2 years: 4 MBq per kg body weight (min. 40 MBq). Children over 2 years: a fraction of the adult dosage should be chosen, dependent on body weight (see SPC for scheme). No special dosage scheme required for elderly patients. Oncology: For adults the recommended dosage is 80-200 MBq, higher activities may be justifiable. For children see cardiology. No special dosage scheme required for elderly patients. Administer dose by slow intravenous injection or infusion over several minutes. **CONTRAINDICATIONS** Hypersensitivity to the active substance or to any of the excipients. The product contains benzyl alcohol 10.4 mg/ml and must not be given to premature

babies or neonates **WARNINGS AND PRECAUTIONS** Drugs known or expected to reduce the Iobenguane(¹²³I) uptake should be stopped before administration of AdreView (usually 4 biological half-lives). At least 1 hour before the AdreView dose administer a thyroid blocking agent (Potassium Iodide Oral Solution or Lugol's Solution equivalent to 100 mg iodine or potassium perchlorate 400 mg). Ensure emergency cardiac and anti-hypertensive treatments are readily available. In theory, Iobenguane uptake in the chromaffin granules may induce a hypertensive crisis due to noradrenaline secretion; the likelihood of such an occurrence is believed to be extremely low. Consider assessing pulse and blood pressure before and shortly after AdreView administration and initiate appropriate anti-hypertensive treatment if needed. This medicinal product contains benzyl alcohol. Benzyl alcohol may cause toxic reactions and anaphylactoid reactions in infants and children up to 3 years old. **INTERACTIONS** Nifedipine (a Ca-channel blocker) is reported to prolong retention of Iobenguane. Decreased uptake was observed under therapeutic regimens involving the administration of antihypertensives that deplete norepinephrine stores or reuptake (reserpine, labetalol), calcium-channel blockers (diltiazem, nifedipine, verapamil), tricyclic antidepressives that inhibit norepinephrine transporter function (amityptiline and derivatives, imipramine and derivatives), sympathomimetic agents (present in nasal decongestants, such as phenylephrine, ephedrine, pseudoephedrine or phenylpropranolamine), cocaine and phenothiazine. These drugs should be stopped before administration of [¹²³I]Iobenguane (usually for four biological half-lives to allow complete washout). **PREGNANCY AND LACTATION** Only imperative investigation should be carried out during pregnancy when likely benefit exceeds the risk to mother and foetus. Radionuclide procedures carried out on pregnant women also involve radiation doses to the foetus. Any woman who has missed a period should be assumed to be pregnant until proven otherwise. If uncertain, radiation exposure should be kept to the minimum needed for clinical information. Consider alternative techniques. If administration to a breast feeding woman is necessary, breast-feeding should be interrupted for three days and the expressed feeds discarded. Breast-feeding can be restarted when the level in the milk will not result in a radiation dose to a child greater than 1 mSv. **UNDESIRABLE EFFECTS** In rare cases the following undesirable effects have occurred: blushes, urticaria, nausea,

cold chills and other symptoms of anaphylactoid reactions. When the drug is administered too fast palpitations, dyspnoea, heat sensations, transient hypertension and abdominal cramps may occur during or immediately after administration. Within one hour these symptoms disappear. Exposure to ionising radiation is linked with cancer induction and a potential for development of hereditary defects. For diagnostic nuclear medicine investigations the current evidence suggests that these adverse effects will occur with low frequency because of the low radiation doses incurred. **DOSIMETRY** The effective dose equivalent resulting from an administered activity amount of 200 MBq is 2.6 mSv in adults. The effective dose equivalent resulting from an administered activity amount of 370 MBq is 4.8 mSv in adults. **OVERDOSE** The effect of an overdose of Iobenguane is due to the release of adrenaline. This effect is of short duration and requires supportive measures aimed at lowering the blood pressure. Prompt injection of phentolamine followed by propranolol is needed. Maintain a high urine flow to reduce the influence of radiation. **CLASSIFICATION FOR SUPPLY** Subject to medical prescription (POM). **MARKETING AUTHORISATION HOLDERS.** DE: GE Healthcare Buchler GmbH & Co. KG, 18974.00.00. DK: GE Healthcare B.V., DK R. 1013. FR: GE Healthcare SA, NL 18599. NL: GE Healthcare B.V., RVG 57689. NO: GE Healthcare B.V., MTNr. 94-191. **DATE OF REVISION OF TEXT** 9 August 2010 .

GE Healthcare Limited, Amersham Place, Little Chalfont, Buckinghamshire, England HP7 9NA
www.gehealthcare.com

© 2010 General Electric Company – All rights reserved.
GE and GE Monogram are trademarks of General Electric Company.
GE Healthcare, a division of General Electric Company.

AdreView is a trademark of GE Healthcare Limited.

References: 1. Jacobson AF et al. Myocardial Iodine-123 Meta-Iodo-benzylguanidine Imaging and Cardiac Events in Heart Failure. Results of the Prospective ADMIRE-HF (AdreView Myocardial Imaging for Risk Evaluation in Heart Failure) Study. J Am Coll Cardiol 2010;55.

10-2010 JB4260/OS INT'L ENGLISH